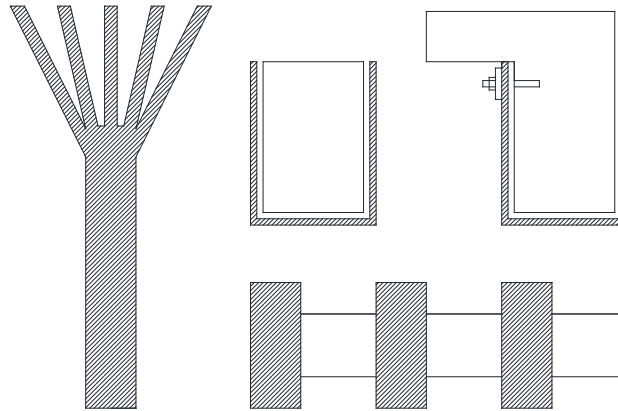


# Design and Detailing of Anchorages for Externally Bonded CFRP

Deliverable 4 – Final Report  
Contract No. BEA90  
April 2022



*Prepared by:*



**Nakin Suksawang, Ph.D., P.E.**

Associate Professor of Civil Engineering

Florida Institute of Technology

Phone: (321) 674-7504

E-mail: [nsuksawang@fit.edu](mailto:nsuksawang@fit.edu)

**Paul Ryan**

Florida Institute of Technology

E-mail : [pryan2017@my.fit.edu](mailto:pryan2017@my.fit.edu)



**Dan Su, Ph.D., P.E.**

Assistant Professor of Civil Engineering

Embry-Riddle Aeronautical University

Phone: 386-323-8298

E-mail: [dan.su@erau.edu](mailto:dan.su@erau.edu)



*For FDOT Project Manager:*

**William Potter, P.E.**

Assistant State Structures Design Engineer

State Structures Design Office

605 Suwannee Street

Tallahassee, FL 32399-0450

## Disclaimer

The opinions, findings, and conclusions expressed in this publication are those of the authors and not necessarily those of the State of Florida Department of Transportation.

## Approximate Conversions to SI Units

SYMBOL	WHEN YOU KNOW	MULTIPLY BY	TO FIND	SYMBOL
<b>LENGTH</b>				
<b>in</b>	inches	25.4	millimeters	mm
<b>ft</b>	feet	0.305	meters	m
<b>yd</b>	yards	0.914	meters	m
<b>mi</b>	miles	1.61	kilometers	km
<b>AREA</b>				
<b>in<sup>2</sup></b>	square inches	645.2	square millimeters	mm <sup>2</sup>
<b>ft<sup>2</sup></b>	square feet	0.093	square meters	m <sup>2</sup>
<b>yd<sup>2</sup></b>	square yard	0.836	square meters	m <sup>2</sup>
<b>ac</b>	acres	0.405	hectares	ha
<b>mi<sup>2</sup></b>	square miles	2.59	square kilometers	km <sup>2</sup>
<b>VOLUME</b>				
<b>fl oz</b>	fluid ounces	29.57	milliliters	mL
<b>gal</b>	gallons	3.785	liters	L
<b>ft<sup>3</sup></b>	cubic feet	0.028	cubic meters	m <sup>3</sup>
<b>yd<sup>3</sup></b>	cubic yards	0.765	cubic meters	m <sup>3</sup>
NOTE: volumes greater than 1000 L shall be shown in m <sup>3</sup>				
<b>MASS</b>				
<b>oz</b>	ounces	28.35	grams	g
<b>lb</b>	pounds	0.454	kilograms	kg
<b>T</b>	short tons (2000 lb)	0.907	megagrams (or "metric ton")	Mg (or "t")
<b>TEMPERATURE (exact degrees)</b>				
<b>°F</b>	Fahrenheit	5 (F-32)/9 or (F-32)/1.8	Celsius	°C
<b>ILLUMINATION</b>				
<b>fc</b>	foot-candles	10.76	lux	lx
<b>fl</b>	foot-Lamberts	3.426	candela/m <sup>2</sup>	cd/m <sup>2</sup>
<b>FORCE and PRESSURE or STRESS</b>				
<b>lbf</b>	poundforce	4.45	newtons	N
<b>lbf/in<sup>2</sup></b>	poundforce per square inch	6.89	kilopascals	kPa

## Technical Report Documentation Page

1. Report No.	2. Government Accession No.	3. Recipient's Catalog No.	
4. Title and Subtitle Design and Detailing of Anchorages for Externally Bonded CFRP		5. Report Date April 2022	
		6. Performing Organization Code	
7. Author(s) Nakin Suksawang, Paul Ryan, and Dan Su		8. Performing Organization Report No.	
9. Performing Organization Name and Address Florida Institute of Technology 150 W. University Blvd Melbourne, FL 32901		10. Work Unit No. (TRAIS)	
		11. Contract or Grant No. BEA90	
12. Sponsoring Agency Name and Address Research Center State of Florida Department of Transportation 605 Suwannee Street, M.S. 30, Tallahassee, Florida 32399-0450		13. Type of Report and Period Covered Final Report May 2021 – Nov 2021	
		14. Sponsoring Agency Code	
15. Supplementary Notes The FDOT Project Manager was William Potter, P.E.			
16. Abstract Recently, an increased number of CFRP repairs have been applied to strengthen concrete bridges' shear capacity. This poses many challenges as the bridge girder cannot be fully wrapped to ensure that the failure mode is governed by shear fracture combined with or followed by the CFRP fracture. Therefore, instead of fully wrapping the beam with CFRP, the FDOT Structural Design Manual does allow for a three-sided U-wrap, but it needs to be anchored to prevent debonding when considering shear strengthening. The primary method that has been utilized in Florida is the use of spike anchors. Although FDOT has promising results with them, they are invasive and impractical. Therefore, there is a need to explore other anchoring methods. The primary objective of this research is two fold: (1) to perform a synthesis of existing research on the topic of CFRP anchorage design and detailing with interest in externally bonded shear strengthening and other externally bonded end anchorage applications and (2) to provide modifications to current design and detailing guidance of CFRP anchorage. Based on the synthesis, it can be concluded that more tests are needed to better understand the failure mechanism of various anchors for prestressed concrete applications. Given the limited test data, the three most promising CFRP anchors details are proposed. These details include spike anchors, mechanical anchors, and CFRP strip details. However, they should be experimentally validated for their performance.			
17. Key Word CFRP Anchors, CFRP Strips, Mechanical Anchors, Prestressed Girder Retrofits, Shear Strengthening, Spike Anchors		18. Distribution Statement No Restriction	
19. Security Classif. (of this report) Unclassified	20. Security Classif. (of this page) Unclassified	21. No. of Pages 121	22. Price



## Acknowledgements

The authors would like to thank the direction and support provided by the FDOT project manager, Mr. William Potter. Additionally, the authors would like to recognize Mr. Serge Roux and Mr. Scott Arnold from Fyfe Co. for providing literatures and expertise on spike and mechanical anchors. The authors also acknowledge the help of Mr. Tarek Alkhrdaji from Structural Technologies with his expertise on spike anchors.

## Executive Summary

The use of externally bonded carbon fiber-reinforced polymer (CFRP) sheet to repair and strengthen existing concrete structures presents many advantages instead of traditional methods such as external prestressing, steel jacketing, and complete replacement. However, there are some challenges with the shear strengthening of girders as the girders cannot be fully wrapped with CFRP. One solution is to only wrap the beam on three sides (i.e., U-wrap) and anchor the CFRP ends so that the CFRP would not debond before shear fracture. Among the various CFRP anchorage systems, spike anchor is the most widely accepted anchorage method in the industry, with design and detail standards currently being developed by multiple agencies. It is also the current state of the practice in Florida. Although the Florida Department of Transportation (FDOT) has promising results with spike anchors, they are invasive to the concrete structures as their use requires drilling holes in the concrete section for embedding the spike anchors. These required holes can be impractical or structurally compromise the concrete section depending on the location. Furthermore, there are no standard details for the anchoring system. Therefore, there is a need to investigate other CFRP anchoring systems and develop design standards that could be referenced for shear strengthening of various bridge girders used in Florida.

The primary objective of this research is two fold: (1) to perform a synthesis of existing research on the topic of CFRP anchorage design and detailing for externally bonded shear strengthening applications and (2) to develop detailing guidance along with construction specification guidance for installation and quality control.

There are very little data to support the use of any CFRP anchor effectiveness in preventing delamination of the CFRP sheets, particularly for shear strengthening of prestressed concrete girders. Most of the data are for spike anchors, but they focus on reinforced concrete beams with no shear contribution of the prestressing force. Only four tests that utilized spike anchors were performed on AASHTO, Type IV prestressed girders, and six tests were performed on Tx48 I-beams, all of which were conducted by the University of Texas for the Texas Department of Transportation (TxDOT). These tests did not provide conclusive evidence on spike anchors increasing the shear performance of the beam but rather the importance of a bidirectional CFRP layout that could potentially increase the ultimate shear capacity of the beam by 40%. Nevertheless, the spike anchor system is the only system that has been utilized in the field and is the most widely adopted.

Another system applicable to prestressed concrete beams was the CFRP strip, which the University of North Florida studied for FDOT. However, the focus of the study was on anchoring the longitudinal CFRP laminate with transverse U-wrap CFRP strips to prevent delamination in predominantly flexural applications. Results of this study did indicate a load-carrying capacity increase of 68% or more when the U-wrap CFRP strip was applied. Their results would also support the finding on the spike anchor that showed the importance of bidirectional CFRP layout. Unfortunately, the study did not provide anchorage details for shear applications. Other anchoring systems reported also showed effectiveness, but the results were based on the laboratory's reinforced concrete beam or

component level testing. Their effectiveness cannot be validated using a prestressed concrete beam.

From this initial literature review, it can be concluded that more experimental research is needed, even with spike anchors, for prestressed concrete applications. CFRP strip and bidirectional CFRP layout have been shown to be more effective in increasing beam load-carrying capacity than utilizing the spike anchor alone. Therefore, more research is needed to compare the contribution of the spike anchor with and without the CFRP strip.

Although there is limited information to quantify and directly compare different CFRP anchor systems, qualitative criteria were developed and used in evaluating and recommending the top three potential CFRP anchoring systems. These criteria consist of proprietary system, invasiveness to the existing concrete structure, level of installation complexity, installation tolerances, and design guidance. The structural effectiveness of each system was not considered because of the limited information available for a direct comparison because only the spike anchor system was tested in shear using full-scale specimens. The CFRP strips, U-anchor, and spike anchors received the highest marks based on these criteria. However, the mechanical anchor system was selected instead because of the limited test information of the U-anchor and the fact that the CFRP supplier no longer recommends the U-anchor system in the United States.

Design drawings and details of the three anchoring systems were developed for prestressed and reinforced concrete sections typically used in Florida. These sections include AASHTO girders, Florida I-beam, bulb-T girder, inverted T-beam, reinforced concrete T-beam, and slab beam (including cast-in-place slab). The details are based on recommendations from the literature and the authors' engineering judgment, as there are limited standards, particularly for the CFRP strips and mechanical anchors. It is recommended that the proposed design drawings and details be further evaluated experimentally. The CFRP strips details could significantly reduce the cost of repairs using externally bonded CFRP.

## Table of Contents

Disclaimer .....	ii
Approximate Conversions to SI Units .....	iii
Technical Report Documentation Page .....	iv
Acknowledgements .....	v
Executive Summary .....	vi
List of Figures .....	xi
List of Tables .....	xiii
1. Introduction.....	1
2. Anchorage Types .....	3
2.1 Spike Anchor .....	3
2.1.1.1 Introduction.....	3
2.1.1.2 Installation Procedure .....	4
2.1.1.3 Schematics .....	4
2.1.1.4 Results.....	6
2.1.1.5 Design Guidance.....	10
2.1.1.6 Implementation .....	12
2.2 Near-Surface Anchor .....	13
2.2.1 U-Wrap .....	14
2.2.1.1 Introduction.....	14
2.2.1.2 Installation Procedure .....	14
2.2.1.3 Schematics .....	15
2.2.1.4 Results.....	16
2.2.1.5 Design Guidance.....	17
2.2.1.6 Implementation .....	18
2.2.2 U-Anchor .....	18
2.2.2.1 Introduction.....	18
2.2.2.2 Installation Procedure .....	18
2.2.2.3 Schematics .....	19
2.2.2.4 Results.....	19
2.2.2.5 Design Guidance.....	20
2.2.2.6 Implementation .....	20
2.2.3 Staple Anchor.....	21
2.2.3.1 Introduction.....	21

2.2.3.2	Installation Procedure .....	21
2.2.3.3	Schematics .....	21
2.2.3.4	Results.....	22
2.2.3.5	Design Guidance.....	23
2.2.3.6	Implementation .....	23
2.3	FRP Strip and Sheet .....	23
2.3.1.1	Introduction.....	23
2.3.1.2	Installation Procedure .....	24
2.3.1.3	Figures.....	24
2.3.1.4	Results.....	24
2.3.1.5	Implementation .....	28
2.4	Mechanical & Metallic Anchor (Bolted or Nailed) .....	28
2.4.1.1	Introduction.....	28
2.4.1.2	Installation Procedure .....	29
2.4.1.3	Figures.....	29
2.4.1.4	Results.....	30
2.4.1.5	Design Guidance.....	31
2.4.1.6	Implementation .....	31
2.4.2	Longitudinal Chase .....	31
2.4.2.1	Introduction.....	31
2.4.2.2	Installation Procedure .....	31
2.4.2.3	Figures.....	32
2.4.2.4	Results.....	32
2.4.2.5	Design Guidance.....	33
2.4.2.6	Implementation .....	34
2.5	Summary and Comparison.....	34
3.	Design Standards .....	37
3.1	American Concrete Institute (ACI 440.2R-17).....	39
3.2	Japan Society of Civil Engineers (JSCE).....	47
3.3	Fédération Internationale du Béton (FIB 14).....	53
3.4	Florida Department of Transportation (FDOT SDM Volume 4).....	62
3.5	Canadian Standards Association (CSA S806-12).....	65
3.6	Comparison of Design Guidance .....	67
4.	Anchor System Evaluation .....	71

4.1	Explanation of Properties by Anchor Type .....	77
4.1.1	Spike Anchor .....	77
4.1.2	U-Wrap .....	77
4.1.3	Staple Anchor.....	77
4.1.4	FRP Strip/Sheet.....	77
4.1.5	Mechanical/Metallic Anchors.....	77
4.1.6	Longitudinal Anchors .....	78
4.2	Anchor System Recommendation.....	78
4.3	Anchor System Details .....	80
4.3.1	Spike Anchor Details .....	81
4.3.2	FRP Strip Details .....	82
4.3.3	Mechanical Anchors .....	83
5.	Proposed Testing Program.....	84
5.1	Testing Procedure .....	84
5.2	Instrumentation .....	85
5.3	Test Matrices.....	86
5.4	Fabrication of Test Beams .....	87
6.	Conclusion .....	88
7.	References.....	90
	Appendix A: Design Details of Top Three Ranked Anchoring Systems .....	94

## List of Figures

Figure 1: Spike anchor schematic (Castillo et al., 2019) .....	5
Figure 2: Spike anchor cross-section (Castillo and Kanitkar, 2021) .....	5
Figure 3: PGA Blvd over FL Turnpike (SDR Engineering Consultants, Inc., 2018).....	6
Figure 4: Normalized shear capacity of 14 x 24 in. reinforced concrete beams strengthened with different configurations of CFRP laminates and spike anchors (Jirsa et al., 2017).....	7
Figure 5: Test configurations (Jirsa et al., 2017) .....	7
Figure 6: Spike anchors in Girder I-2 (Kim et al., 2012).....	8
Figure 7: Spike anchors in Girder I-3 (Kim et al., 2012).....	9
Figure 8: Spike anchors in Girder I-4 (Kim et al., 2012).....	9
Figure 9: Ultimate loads of reinforced girders (Kim et al., 2012) .....	9
Figure 10: Cracking and ultimate shear loads increase in percentage (Kim et al., 2012)	10
Figure 11: Spike anchor design procedure (Castillo et al., 2019).....	12
Figure 12: PGA Blvd girder anchorage details (SDR Eng., Inc., 2018).....	13
Figure 13: FRP wrapping schemes (ACI 440.2R-08, 2008).....	15
Figure 14: County Road 514 over I-75 bridge repair (SDR Eng. Consultants, Inc. 2017)	15
Figure 15: Girder test results (Kim and Bhiri, 2020).....	16
Figure 16: FRP stress limits (ACI Committee 440, 2008).....	17
Figure 17: Type II and III anchorage (Grelle and Sneed, 2013).....	19
Figure 18: Example of near-surface mounted laminate (McGuirk, G., 2011).....	19
Figure 19: Types of anchors tested (Khalifa et al., 1999).....	20
Figure 20: Strength increase from U-anchors (Khalifa et al., 1999) .....	20
Figure 21: Staple anchor testing apparatus (University of Miami, 2016).....	22
Figure 22: Staple anchor test results (University of Miami, 2016).....	22
Figure 23: FRP strip anchor (Grelle and Sneed, 2013).....	24
Figure 24: Beam reinforcement configurations (ElSafty & Graeff, 2012).....	25
Figure 25: Maximum load and strain of reinforced beams (ElSafty & Graeff, 2012).....	25
Figure 26: Strip and sheet nomenclature .....	28
Figure 27: Mechanical plate anchors for girder (Aljaafreh, Performance of Precast Concrete Bridge Girders with Externally Bonded Anchored CFRP, 2019) .....	29
Figure 28: Plate anchorage system (Grelle & Sneed, Review of Anchorage Systems for Externally Bonded FRP Laminates, 2013) .....	29
Figure 29: Load & deflection – girder with plate anchors (Aljaafreh, Performance of Precast Concrete Bridge Girders with Externally Bonded Anchored CFRP, 2019).	30

Figure 30: Ultimate strengths – girder with various anchor types (Aljaafreh, Performance of Precast Concrete Bridge Girders with Externally Bonded Anchored CFRP, 2019)	30
Figure 31: Tested girder designations (Aljaafreh, T., 2019)	30
Figure 32: Longitudinal chase cross-section (Grelle, S., Sneed, L., 2011)	32
Figure 33: Longitudinal chase test configuration (Kalfat and Al-Mahaidi, 2010)	32
Figure 34: Longitudinal chase test results (Kalfat and Al-Mahaidi, 2010)	33
Figure 35: ACI 440.2R-17 Fig. 10.2.5-Beam schematic	41
Figure 36: ACI 440.2R-17-Sustained plus cyclic load limits	42
Figure 37: ACI 440.2R-17-Elastic stress and strain distribution	44
Figure 38: ACI 440.2R-17 wrapping schemes	45
Figure 39: JSCE S6.2.1(a) Flowchart for structures without samples	48
Figure 40: JSCE S6.2.1(b) Flowchart for structures with samples	48
Figure 41: CFRP wrap shear capacity (JSCE, 2001)	52
Figure 42: JSCE Fig. C6.4.6-Failure mode and shear capacity	53
Figure 43: FIB-14 Beam nomenclature	53
Figure 44: Debonding interfaces (FIB-14, 2001)	55
Figure 45: FIB-14 Fig. 4-11 Cross-sectional analysis of beam under bending	56
Figure 46: FIB-14 Fig. 4-15 Linear elastic analysis of cracked section	57
Figure 47: FIB-14 - Failure mode based on load and displacement	60
Figure 48: FIB-14 FRP shear reinforcement nomenclature	60
Figure 49: FIB-14 FRP Material Safety Factors	61
Figure 50: Total shear resistance of a reinforced concrete beam (stirrup spacing = 9 in.) (Eamon 2014)	68
Figure 51: FRP shear resistance of a reinforced concrete beam (stirrup spacing = 9 in.) (Eamon 2014)	68
Figure 52: ISIS maximum stress level against creep rupture (Eamon, 2014)	69
Figure 53: Reduction factors for CFRP interface bond strength (Michigan-specific) (Eamon, 2014)	70
Figure 54: AASHTO Type IV beam schematic	83
Figure 55: Full-scale shear load test of the AASHTO IV beam repaired with externally bonded CFRP - Test Location 1	85
Figure 56: Full-scale shear load test of the AASHTO IV beam repaired with externally bonded CFRP - Test Location 2	85
Figure 57: Preliminary foil strain gauge locations	86



## List of Tables

Table 1: Summary of anchor details .....	35
Table 2: ACI effective strain (ACI Committee 440, 2017) .....	46
Table 3: JSCE material factor for CFRP sheets.....	49
Table 4: JSCE material factor for CFRP strands .....	49
Table 5: FDOT SDM vol. 4 modifications to ACI 4040.2R-17 .....	62
Table 6: Design guide comparison .....	72
Table 7: Effectiveness of anchors .....	74
Table 8: Anchor properties summary .....	76
Table 9: Ranking of anchors by detail .....	79
Table 10: List of reports detailing the size and spacings of FRP transverse laminate.....	80
Table 11: Existing spike anchor details .....	81
Table 12: Test matrix for AASHTO type VI beam .....	87

## 1. Introduction

For the past 20+ years, the Florida Department of Transportation (FDOT) has utilized externally bonded carbon fiber-reinforced polymer (CFRP) to repair and retrofit members of concrete bridges that have been damaged by over-height vehicles or suffered from corrosion damage and required load strengthening. The majority of the load strengthening applications have focused on increasing flexural capacity. Recently, many CFRP repairs have been applied to increase the shear capacity of concrete bridges; doing so poses many design challenges. Unlike flexural strengthening, where CFRP sheets are laminated to only the tensioned face of a beam, shear strengthening preferred installation method requires completely wrapping the beam. The advantage of having CFRP bonded to all faces of a member is that it forces a desirable failure mode to govern (i.e., shear fracture combined with or followed by CFRP fracture). Full wraps require access to all faces of a member, which is often not possible (i.e., bridge girders). Less favorable methods, such as the two-sided wrap and three-sided wrap (also known as a U-wrap), are often used when geometric or spatial constraints are present.

The most common failure mode observed among two-sided wraps and three-sided U-wraps is the less favorable bond failure mode, which is often combined with shear fracture. Since the bond failure, also known as debonding, occurs before the failure of the concrete member and before material failure of the CFRP, only a fraction of the ultimate strength of the CFRP laminate contributes to the shear capacity. Thus, additional anchorage must be used to prevent debonding. Mechanical fasteners, U-anchors, and fiber anchors (also known as spike anchors) are commonly used anchorage systems.

Volume 4 of the FDOT Structures Design Manual (SDM) allows for completely wrapped or three-sided U-wrap when considering shear strengthening. But because of the installation's impracticality, the completely wrapped bridge girders are seldom used, making the three-sided U-wrap the most utilized method. However, for the three-sided U-wrap to be utilized, FDOT requires CFRP anchorage details to prevent debonding and ensure that strain values comparable to complete wrapping are achieved in the CFRP. Furthermore, the FDOT SDM also requires that testing be performed to ensure the proper behavior of the three-sided U-wrap. As a result, Florida's most popular anchorage system is the spike anchor, which requires drilling the substrate upon installation.

Although FDOT has promising results with spike anchors, they are invasive to the concrete structures as their use requires drilling holes in the concrete section for embedding the spike anchors. Depending on the location, these required holes can be impractical or structurally compromise the concrete section. The TxDOT study (Kim, et al., 2012) also recommended an anchor depth of 6 inches. The absolute minimum anchor depth should be no shallower than 4 inches when a 6-inch depth is not possible. If spike anchors need to be installed on the web, the large embedment depth could be a problem for prestressed I-shaped (e.g., AASHTO and Florida I-beam) and U-shaped (e.g., Florida U-beam) girders as their web thickness ranges from 5.5 in. to 7 in.. Although the spike anchor could be installed at an incline, only one reinforced T-beam was evaluated with spike anchors installed at 20 degrees from the perpendicular plane, which resulted in a slight decrease in shear strength.

Consequently, the TxDOT study recommended a deviation of anchor holes from the perpendicular plane of up to 10 degrees in Project 0-6306. In the last project, 0-6783, a Tx46 shaped I-beam was strengthened using CFRP spike anchors installed 45 degrees from the perpendicular plane. Unfortunately, unexpected anchorage failures were encountered in some of the tests, so the results were inconclusive as some did show an increase in shear strength. As a result, the TxDOT study also recommended that further research be conducted for prestressed sections and details related to spike anchors. Therefore, there is a need to synthesize and evaluate various anchorage methods for CFRP shear strengthening and end anchorages.

The goal of this research project is to identify existing anchorage systems and provide recommendations to design guides and industry professionals based on the following criteria:

- Proprietary of the system
- Invasiveness to the concrete section
- Level of complexity during installation
- Installation tolerances
- Design guidance

Although the structural effectiveness of each system is a critical criterion, it is not considered in this project as there is insufficient data to compare directly.

## 2. Anchorage Types

Project restraints are unique and often require the adaptation of existing methods to succeed. For example, the repair of a bridge girder does not permit the full wrapping of a member with CFRP; therefore, additional anchorage must be applied. The invasiveness and complexity of anchors often dictate their use in projects. As the number of anchorage systems increases, the industry's design criteria must be clarified and published. The following anchor types were investigated, and their applications in the as-built environment were documented:

- Spike Anchor
- U-wrap/anchor
- Staple Anchor
- CFRP Strip and Sheet
- Mechanical and Metallic
- Longitudinal Chase

### 2.1 Spike Anchor

#### 2.1.1.1 Introduction

In addition to epoxy-based bonding substances, CFRP systems are fixed to concrete using anchors of varying sizes, shape, and materials. Spike anchors (also known as CFRP anchors) are a commonly researched anchorage type for CFRP reinforcement due to their known effectiveness. The Shimizu Corporation first developed spikes anchors in Japan to provide continuity for CFRP wraps of columns (Kobayashi, Fujil, Yabe, Tsukagoshi, & Sugiyama, 2001) by using a spike-shaped nail made of CFRP material to drive through the laminate and concrete, creating a strong, unified system consisting of concrete, epoxy, CFRP laminate, and anchor. The CFRP spike anchors exhibit failure modes similar to post-installed anchors. (del rey Castillo, Kanitkar, Smith, Griffith, & Ingham, 2019)

The use for shear strengthening in the beam was first reported by (Jinno, Tsukagoshi, & Yabe, 2001). They evaluated T-beams strengthened with U-shaped CFRP sheets combined with spike anchors placed vertically inside the slab, which yielded promising results. The University of Texas at Austin later studied this method, who researched shear strengthening using CFRP laminates sponsored by the Texas Department of Transportation (TxDOT), namely, projects 0-6306 (Kim, et al., 2012) and 0-6783 (Jirsa, et al., 2017). They placed spike anchors horizontally inside the web, resulting in a 40–45% increase in shear strength compared to traditional three-sided U-wrap with no anchorage. As a result, the method was implemented on an actual bridge located at the intersection of Loop 1604 and O'Connor Road in the San Antonio District. Garcia (Garcia, Sun, Kim, Ghannoum, & Jirsa, 2014) later developed a report detailing spike anchors' installation and quality control procedure. The final project 0-6783 (Pudleiner, Ghannoum, & Jirsa, 2019) further investigates the impact of the bi-directional layout of CFRP and anchors on the bridge element subjected to large shear forces. Final design recommendations and quality control procedures for CFRP anchors were also developed as part of this project.

The spike anchor is the primary method that has been utilized in Florida for shear strengthening. Although FDOT has promising results with spike anchors, they are invasive to the concrete structures as their use requires drilling holes in the concrete section for embedding the spike

anchors. Depending on the location, these required holes can be impractical or could structurally compromise the concrete section.

#### 2.1.1.2 Installation Procedure

CFRP spike anchors are typically constructed of bundles of fibers soaked in epoxy. After drilling a hole of adequate diameter and depth, the “spiked” end is inserted into the concrete structure. The TxDOT Project 0-6306 recommended at least a 4 in. hole depth with a 6 in. hole depth preferred. The anchor should be installed within the concrete core within the volume of concrete enclosed by the transverse stirrups. The opposite end of the anchor is flattened into a fan shape with 60 degrees fan angle to increase its surface area and bonded to the CFRP sheet. A 0.5 in. hole chamfer radius is recommended to avoid crimping of fiber.

The skill of the installer plays a crucial role in the effectiveness of CFRP sheets and anchors; however, the effects of poor installation of spike anchors in regard to shear strengthening is not thoroughly understood.

#### 2.1.1.3 Schematics

Figure 1 shows different spike anchor configurations. The “fan” (exposed) portion of a spike anchor can be mounted to substrates at various angles. However, only angles up to 10 degrees of inclination from perpendicular have been investigated (Garcia, Sun, Kim, Ghannoum, & Jirsa, 2014). A straight anchor remains in alignment (180 degrees) with the surface in which it is embedded, while a bent anchor changes direction beyond the embedment surface. The solid, embedded portion of a spike anchor can be seen in Figure 2.

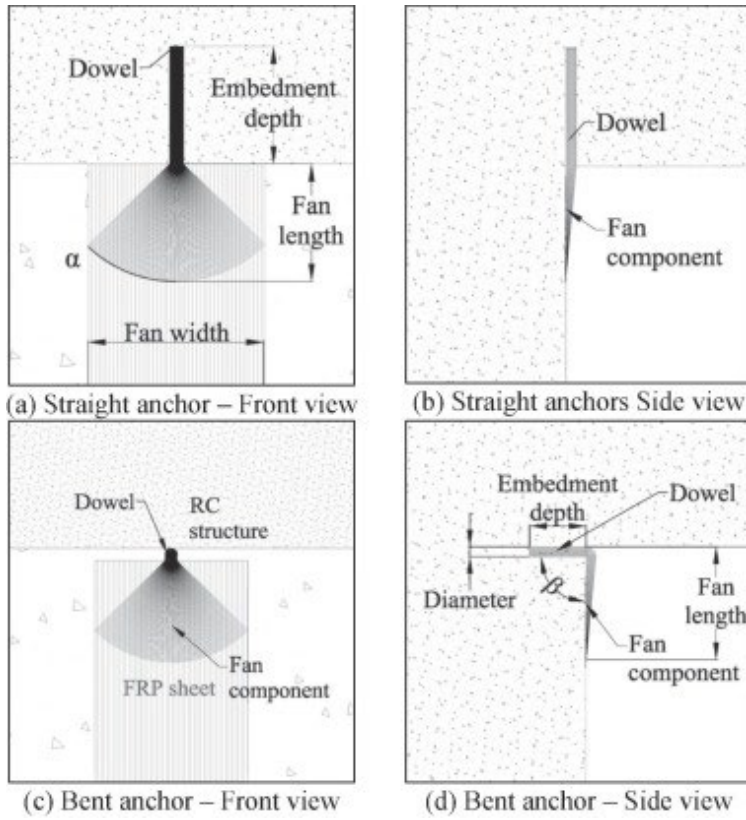


Figure 1: Spike anchor schematic (Castillo et al., 2019)



Figure 2: Spike anchor cross-section (Castillo and Kanitkar, 2021)

Figure 3 illustrates a construction drawing of an AASHTO girder developed by FDOT. Details A and B of the excerpt show the construction dimensions of the spike anchors.

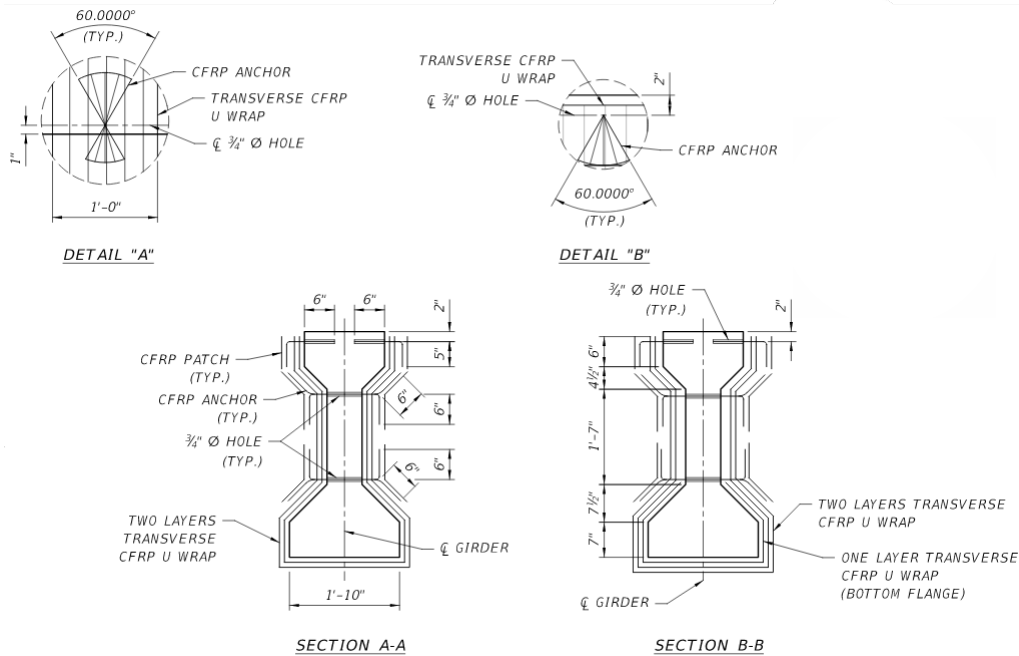


Figure 3: PGA Blvd over FL Turnpike (SDR Engineering Consultants, Inc., 2018)

#### 2.1.1.4 Results

Several test results are available for spike anchors, but most of these are for typical reinforced concrete beams, which are also reported in the 0-6306 and 0-6783 TxDOT projects. From the two projects, it could be concluded that spike anchors significantly contribute to the increase in the shear capacity to the CFRP sheets for a reinforced concrete beam. Figure 4 illustrates results that compare various shear strengthening configurations with spike anchors used on a 14 x 24 in. reinforced concrete beam. The shear strengthening configurations are shown in Figure 5. It is clear from the results that the use of bidirectional (vertical and horizontal) CFRP strips could impact the beam shear capacity in terms of strength increase and stiffness. What is not clear is the number of spike anchors as both single and double layers spike anchors have similar performance. Nevertheless, Jirsa (Jirsa, et al., 2017) proposed the number of spike anchors as a function of the width of the CFRP strips. Furthermore, the increase in shear capacity using spike anchor for prestressed concrete is inconclusive. The shear stress field of prestressed concrete differs from reinforced concrete, where the prestressed forces also contribute to the shear capacity.

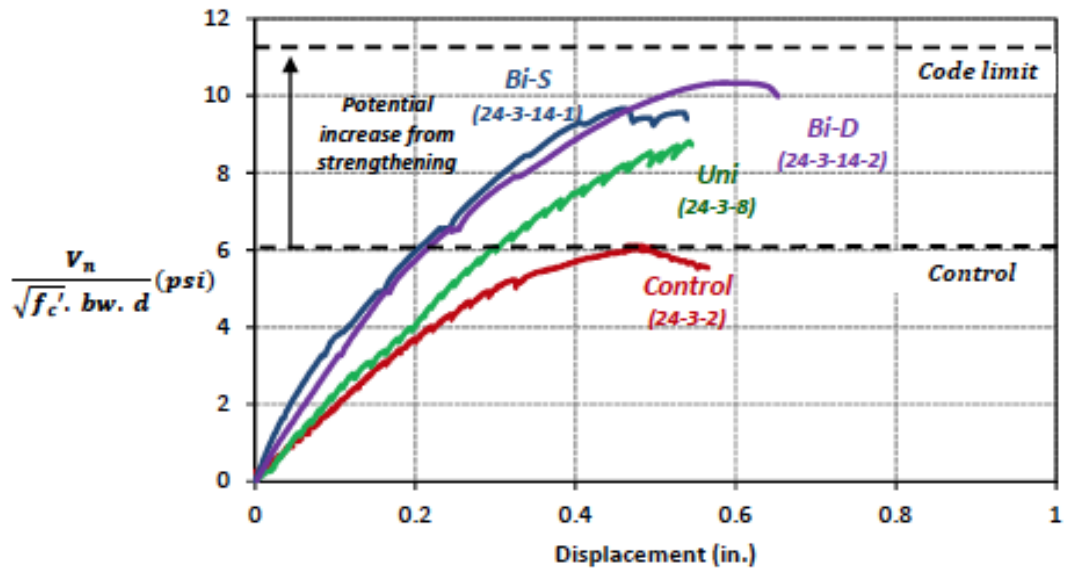


Figure 4: Normalized shear capacity of 14 x 24 in. reinforced concrete beams strengthened with different configurations of CFRP laminates and spike anchors (Jirsa et al., 2017)

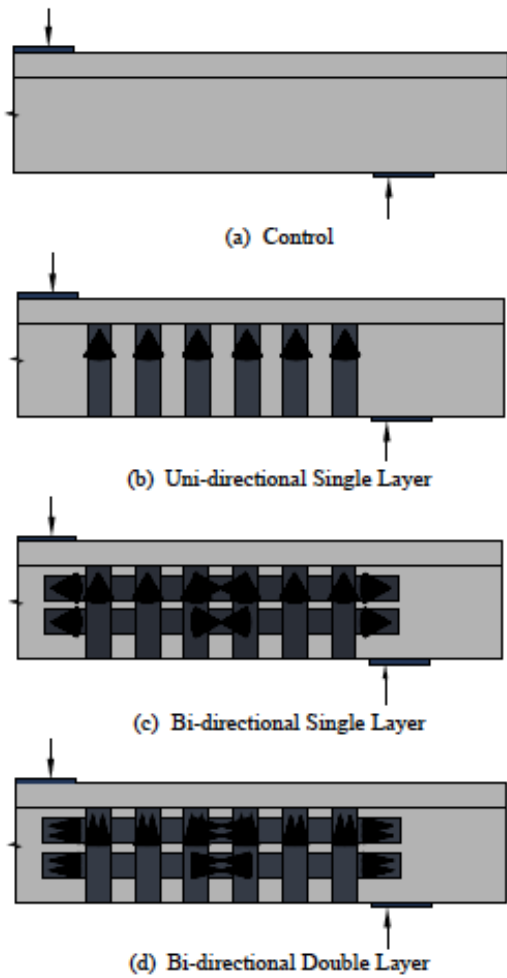


Figure 5: Test configurations (Jirsa et al., 2017)



A full-scale test using AASHTO Type IV girders was conducted at the University of Texas for TxDOT as part of the 0-6306 project (Kim, et al., 2012) and (Fyfe, 2019). The load was applied to the girders monotonically until failure. To ensure shear failure, the beam was strengthened using a post-tensioning system to increase flexural capacity. A total of four full-scale tests were conducted consisting of a control beam with no CFRP reinforcement labeled Girder I-1 and three shear strengthened beams using CFRP. Girder I-2 was strengthened with only six vertical CFRP sheets at 20 in. on center. The vertical sheets were anchored with twelve 2-way spike anchors and twelve 1-way spike anchors (see Figure 6). Girder I-3 was a fully wrapped beam with vertical and horizontal CFRP sheets anchored with thirty-eight 1-way spike anchors and forty-eight 2-way spike anchors (see Figure 7). The last beam, Girder I-4, had similar shear strengthening details as Girder I-2, but with additional horizontal CFRP sheets anchored with twenty-six 2-way anchors and twenty-two 1-way spike anchors (see Figure 8). Furthermore, while vertical strips were used for Girders I-2 and I-4, the strips in I-2 extended only to the top of the web, whereas, in Girder I-4, the vertical strips extended to the top of the beam.

Figure 9 and Figure 10 illustrate the cracking and ultimate shear capacities of the four beams. From these plots, it is not clear if the spike anchor effectively increases the ultimate shear capacity of the CFRP laminated sheets. Although there is an increase in ultimate shear capacity in all girders, the percent increase is minimal (2%) when only vertical CFRP strips are anchored (i.e., Girder I-2). Unlike previous tests that were performed on reinforced concrete beams, there was also no direct comparison between anchored and unanchored CFRP sheets. Thus, the effectiveness of the spike anchor could not be directly quantified. The shear strength is also not proportional to the amount of CFRP material. There is not much difference between the percent increase in cracking and ultimate shear when almost doubled amount of CFRP sheets and spike anchors are used, such as in Girder I-3 and I-4. Furthermore, the utilization of both vertical and horizontal CFRP sheets, such as in Girder I-3 and I-4, played much more prominent roles in improving the shear performance of the girders. The top flange anchorage may also contribute to the shear performance of Girders I-3 and I-4. However, the stress redistribution between the horizontal and vertical CFRP sheets is unclear.

Another full-scale test using Tx46 I-beam was later conducted as part of the 0-6783 project (Jirsa, et al., 2017). Unlike the AASHTO Type IV, the CFRP sheets were only applied to the web. The six tests performed on the modified I-beam (Control-18, Uni-18R, etc.) were inconclusive as the beam had premature anchorage failure.

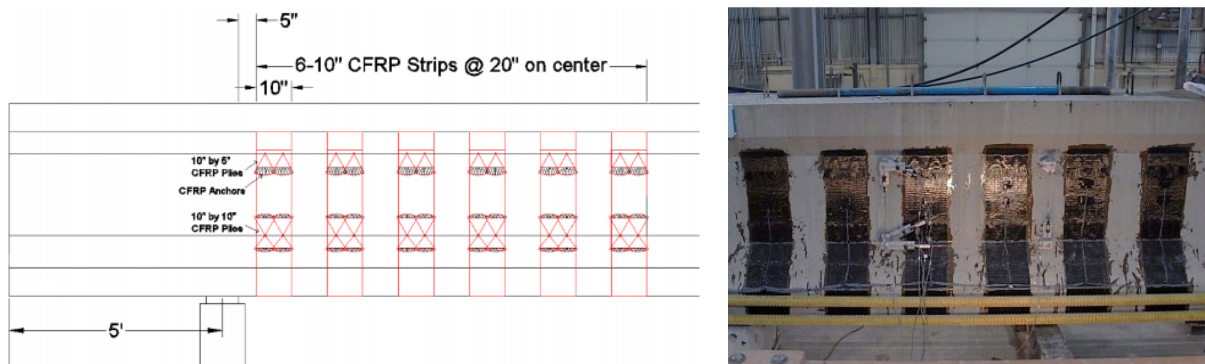


Figure 6: Spike anchors in Girder I-2 (Kim et al., 2012)

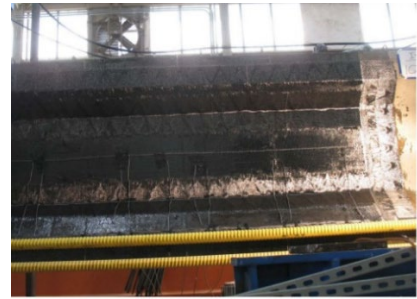
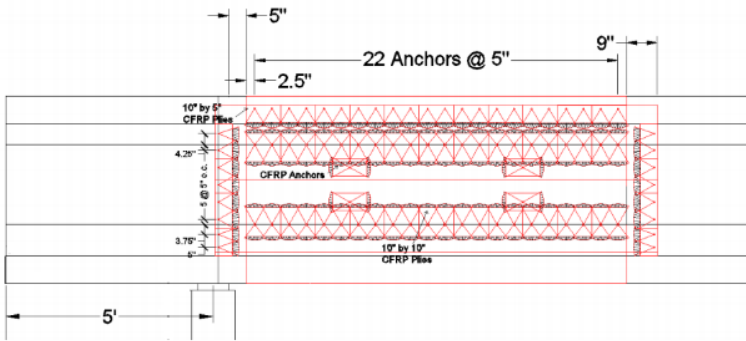


Figure 7: Spike anchors in Girder I-3 (Kim et al., 2012)

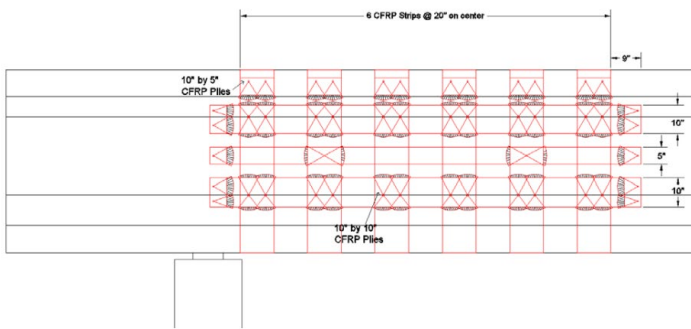


Figure 26 - Elevation View of I-4

Figure 8: Spike anchors in Girder I-4 (Kim et al., 2012)

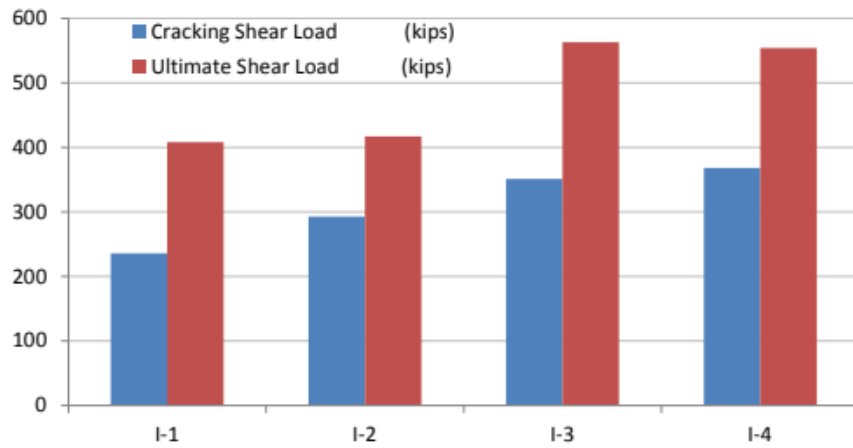


Figure 9: Ultimate loads of reinforced girders (Kim et al., 2012)

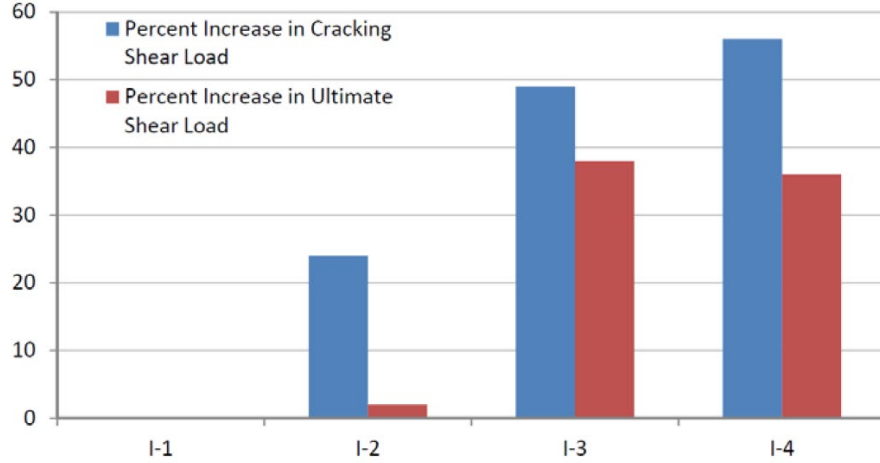


Figure 10: Cracking and ultimate shear loads increase in percentage (Kim et al., 2012)

### 2.1.1.5 Design Guidance

The following list outlines the steps necessary in the design of spike anchors according to del Rey Castillo (del rey Castillo, Kanitkar, Smith, Griffith, & Ingham, 2019):

1. Confirm the need to anchor the FRP using ACI 440.2R. If the required strength cannot be achieved with FRP laminate alone, anchors should be used.
2. Calculate the design/required strain of the anchored FRP sheets using ACI 440.2R.
3. Calculate the tensile force in the FRP sheets using the design strain and the modulus of elasticity of the FRP.
4. Assume a number of anchors to be installed and calculate the tensile force per anchor.
5. Assume reasonable fan and insertion angles.
6. Calculate dowel cross-sectional area ( $A_{dowel}^{dry}$  and  $A_{dowel}^{cured}$ ) and diameter ( $d_{dowel}^{dry}$  and  $d_{dowel}^{cured}$ ) using the following equations:

$$\text{Straight Anchors:} \quad \bar{N}_{fr} = 4.9E_a\varepsilon_a 10^{-3} A_{dowel}^{0.56} \left( \frac{90 - \alpha}{90} \right) \quad \text{Eq. 2.1}$$

$$\text{Angle Anchors} \quad \bar{N}_{fr} = 3.0E_a\varepsilon_a 10^{-3} A_{dowel}^{0.56} \left( \frac{90 - \alpha}{90} \right) \quad \text{Eq. 2.2}$$

(45°-135°):

$\bar{N}_{fr}$  = Average fiber rupture load capacity for a given lap joint (kN)

$E_a$  = Modulus of elasticity of anchor (MPa)

$A_{dowel}$  = cross-sectional area of anchor (mm<sup>2</sup>)

$\alpha$  = half of fan angle (deg.)

7. Calculate dimensions of the drilled hole using the following equations:

$$\bar{N}_{cc} = 12.04h_{ef}^{1.5} \sqrt{f'_c} \quad \text{Eq. 2.3}$$

$$f'_c \geq 20 \text{ MPa:} \quad \bar{N}_{cb} = 5.65\pi d_o h_{ef} \quad \text{Eq. 2.4}$$

$$f'_c < 20 \text{ MPa:} \quad \bar{N}_{cb} = 10.86\pi d_o h_{ef} \quad \text{Eq. 2.5}$$

$N_{cc}$  and  $N_{cb}$  = tensile force in anchor in the case of concrete cone and combined failure modes (respectively)

$h_{ef}$  and  $d_o$  = embedment depth and drilled hole diameter (respectively)

8. Check that anchor diameter and embedment depth are acceptable in terms of constructability. If either parameter is deemed unacceptable, insertion angle or the fan angle may be revised.
9. Calculate the fan area using the following equation: Using the tensile force in the anchor,

$$N_{sd} = 0.35V_{sb}A_{fan} \quad \text{Eq. 2.6}$$

$V_{sb}$  = Shear bond strength of the epoxy resin (MPa)

$N_{sd}$  = Anchor fan debonding capacity (N)

$A_{fan}$  = area of surface of fan bonded to the FRP sheet (mm<sup>2</sup>)

10. Assume the anchor fan width  $w_{fan}$  to calculate the fan length  $l_{fan}$
11. Verify fan is appropriately sized. If the fan is larger than the structural member onto which it is to be bonded, the number of anchors, the fan angle, and/or the insertion angle should be revised.

Dry or cured values can be used in the equations for  $\bar{N}_{fr}$ , as long as the values are consistent between cross-sectional area and modulus of elasticity (i.e., either dry modulus of elasticity and dry cross-sectional area are used, or cured modulus of elasticity and cured cross-sectional area are used).

Inadequately saturated anchors achieve the rupture capacity calculated using published design procedures but fail in a brittle manner. Proper design guidance must be followed; quality control and assurance are vital when applying spike anchors.

Figure 11 illustrates the design procedure developed by (del Rey Castillo et al., 2019) and utilizes existing design guides, such as ACI 440.2R.

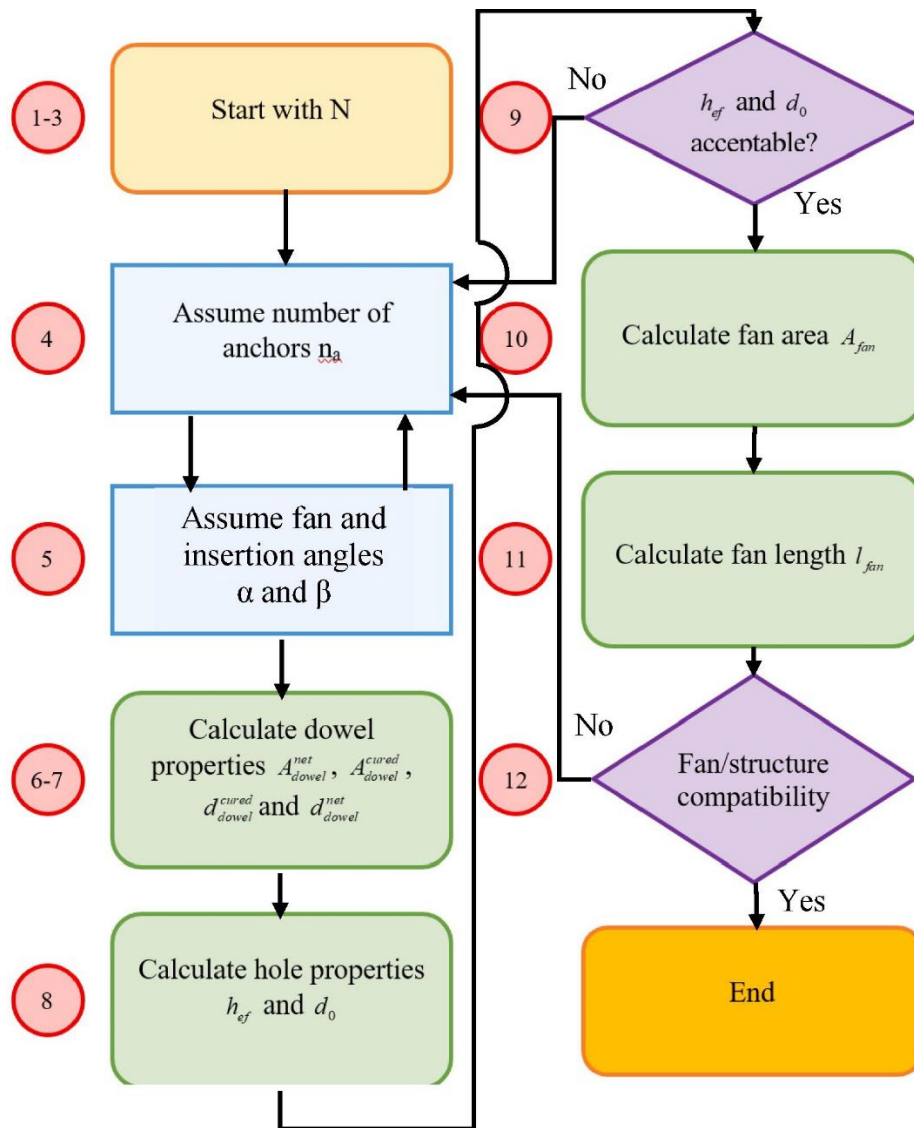


Figure 11: Spike anchor design procedure (Castillo et al., 2019)

In the figure,  $h_{ef}$  and  $d_o$  are the embedment depth and drilled hole diameter, respectively, associated with a single anchor. An anchor's embedment depth and hole diameter increase directly with the tensile force experienced by the anchor. To reduce the fan angle of the anchor(s), which makes the anchor(s) more effective, more anchors should be installed in a more congested configuration.

The use of smaller and more closely spaced anchors was shown to be more effective in flexural and shear strengthening than larger diameter, more widely spaced anchors (Zaki, Rasheed, & Alkhrdaji, 2019).

#### 2.1.1.6 Implementation

The use of FRP spike anchors is increasingly common. The following examples and reports should not be considered an exhaustive list of spike anchor applications.





Two types of near-surface anchors have researched: U-wraps and Staple anchors. The advantages and disadvantages, affiliated research, and current implementation of each anchor type were documented. Design standards for each anchor type were listed, which speaks to their relevance in the existing FRP community.

## 2.2.1 U-Wrap

### 2.2.1.1 Introduction

When FRP laminates are used to strengthen structural members, particularly in flexure and shear, anchorage beyond basic bonding techniques becomes necessary to prevent debonding (peel-off) of the FRP. One method to increase the bond strength of an FRP laminate is by increasing the contact area of the laminate. Increased area permits an increased amount of bonding agent; hence, increased bond strength limits are observed.

The geometry of projects varies and often directs reinforcement procedures. The maximum contact area is utilized by implementing a “complete wrapping” scheme, in which FRP laminate is fixed to all sides of a non-circular member. A completely wrapped member almost eliminates the chance of peel-off failure and yields the highest design strengths. Another less favorable wrapping method is the partial lining of a member with FRP laminate. For rectangular members, partial wrapping includes two-sided bonding (weakest solution) and three-sided bonding. The schematic cited from ACI 440.2R-08 shows each wrapping configuration.

The three-sided wrapping scheme is what is also named a U-wrap. The three-sided wrap is weaker than the completely wrapped solution but stronger than the two-sided configuration. Peel-off failure is also considerably less likely to occur with U-wraps compared to two-sided wraps.

A typical application of U-wraps is the repair of concrete bridge girders damaged by passing vehicles (e.g., a collision between an oversized truck and the bottom of a bridge member). Since the situation requires the strengthening of an already-installed member, in situ procedures must be used. The above bridge deck will always restrict access to at least one face of the bridge girder; therefore, complete wrapping is not possible, and a two-sided or, preferably, a U-wrap must be applied.

U-wraps' application and research are extensive due to their minimal invasiveness and ease of application. In situ demands, like repairing a damaged bridge girder, are often addressed by a U-wrap solution. While simple to implement, U-wraps yield significantly lower design strengths than complete wraps, and peel-off failure is still a concern. Many departments of transportation agencies utilize the U-wrap reinforcement technique. The popularity of the anchorage method prompted the publication of many applicable design standards (ACI 440.2R-08, FIB 14, CSA S806-12, FDOT SDM Vol. 4, etc.). All design standards were produced via empirical data from various research projects and field tests.

### 2.2.1.2 Installation Procedure

Since debonding is a primary concern, proper surface preparation is essential during installation. All surfaces to which CFRP will be bonded must be roughened and cleaned to ensure maximum bond strength. For example, during testing performed by Grelle and Sneed in 2011, all bonded

surfaces were roughened with a diamond cup wheel and cleaned of dust and debris using a vacuum and compressed air.

Two methods are currently available for installing CFRP laminates: wet lay-up and dry lay-up. Wet lay-up involves impregnating the bonding fibers (as suggested by the manufacturer) in a bath saturant before placing the CFRP sheets on the member surface. Dry lay-up consists in impregnating the fibers as the laminates are placed on the surface. Manufacturer specifications and procedures must be followed, especially for adhesives, to ensure bond strength is not less than predicted.

If additional anchorage systems are used (e.g., spike anchors), applicable design provisions and/or modification factors should be considered before construction to prevent debonding.

### 2.2.1.3 Schematics

The three wrapping configurations applied to concrete beams are shown in Figure 13. Strength improvements rapidly decline as the number of wrapped sides decreases. Figure 14 shows a typical construction drawing of an I-shaped girder used to confine a beam's damaged area with CFRP laminate; the Florida Department of Transportation used the girder shown.

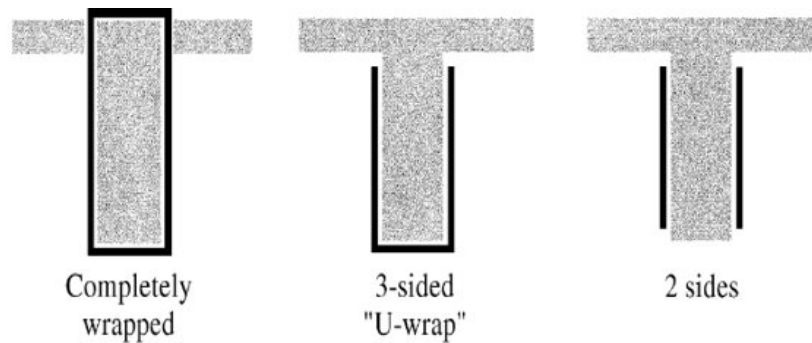


Figure 13: FRP wrapping schemes (ACI 440.2R-08, 2008)

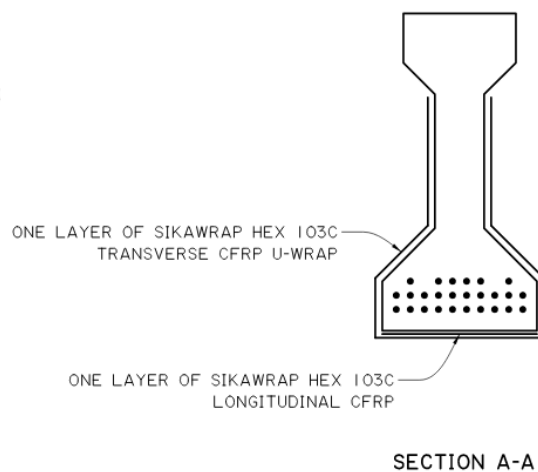


Figure 14: County Road 514 over I-75 bridge repair (SDR Eng. Consultants, Inc. 2017)



### 2.2.1.4 Results

Figure 15 shows the results of 20 reinforced concrete beams and can be interpreted using the following key:

U-wrap types: U is continuum, and G is a grid  
 Adhesive types: E is epoxy bonding, and H is epoxy and SMP hybrid bonding  
 Loading types: M is monotonic loading, and C is cyclic loading  
 U-wrap coverage: 25, 50, 75, and 100% percentage of coverage in the shear span  
 Grid size:  $w \times d$ , where  $w$  and  $d$  are the width and depth of each grid, respectively  
 CONT: Control without U-wraps.

Ultimate capacity increased in all categories tested under monotonic loading, and as the shear span coverage rose, so did the load-carrying capacity. Grid spacing also influences the failure of strengthened beams. It could be seen here that if the U-wrap is not anchored (i.e., only epoxy is used to attach the wrap), the maximum increase in the load-carrying capacity of the beam is 25%.

**Table 1—Details of test beams**

Beam ID	U-wrap configuration	Coverage of shear span, %	Loading*	$P_u$ , kN	Failure sequence†
CONT	No U-wraps	0	M	91.1	FC → SC → DL
UEM25	Continuum with epoxy bonding	25	M	103.3	FC → IC → LR
UEM50	Continuum with epoxy bonding	50	M	107.4	FC → IC → LR
UEM75	Continuum with epoxy bonding	75	M	109.9	FC → IC → LR
UEM100	Continuum with epoxy bonding	100	M	116.1	FC → IC → LR
GEM25	Grid with epoxy bonding	25	M	101.5	FC → SC → GR → DL
GEM50	Grid with epoxy bonding	50	M	104.2	FC → SC → GR → DL
GEM75	Grid with epoxy bonding	75	M	107.2	FC → SC → GR → DL
GEM100	Grid with epoxy bonding	100	M	113.7	FC → SC → GR → DL
GEM100-20 x 20	Grid with epoxy bonding	100	M	114.8	FC → SC → GR → DL
GEM100-40 x 75	Grid with epoxy bonding	100	M	104.4	FC → SC → GR → DL
GEM100-75 x 40	Grid with epoxy bonding	100	M	107.0	FC → SC → GR → DL
GHM25	Grid with hybrid bonding	25	M	100.1	FC → GR → DL → CC
GHM50	Grid with hybrid bonding	50	M	106.2	FC → CS → CC
GHM75	Grid with hybrid bonding	75	M	107.7	FC → CS → CC
GHM100	Grid with hybrid bonding	100	M	111.8	FC → CS → CC
GHC-25	Grid with hybrid bonding	25	C	86.2	FC → CS → CC
GHC-50	Grid with hybrid bonding	50	C	88.2	FC → CS → CC
GHC-75	Grid with hybrid bonding	75	C	91.8	FC → CS → CC
GHC-100	Grid with hybrid bonding	100	C	93.7	FC → CS → CC

\*M is monotonic, and C is cyclic.

†FC is flexural crack; SC is shear crack; IC is intermediate crack-induced CFRP debonding; LR is local CFRP rupture; GR is grid rupture; DL is delamination; CC is concrete crushing; and CS is CFRP shearing.

Note:  $P_u$  is ultimate load; 1 kN = 0.225 kip.

Figure 15: Girder test results (Kim and Bhiri, 2020)

### 2.2.1.5 Design Guidance

ACI 440.2R-17 should be referenced for design procedures. The strength and elastic modulus of FRP materials can be determined by the requirements of ASTM D3039/D3039M, D7205/D7205M, or D7565/D7565M. For bond-critical applications, tension adhesion testing of cored samples should be conducted according to ASTM 7522/D7522.

1. Determine design flexural strength  $\phi M_n$  using the nominal member strength.
2. Ensure the effective strain in FRP reinforcement is limited to the strain at which debonding may occur ( $\varepsilon_{fd}$ ) using the following equation:

$$\varepsilon_{fd} = 0.083 \sqrt{\frac{f'_c}{nE_f t_f}} \leq 0.9\varepsilon_{fu} \quad \text{Eq. 2.7}$$

3. Find the initial strain on the bonded substrate,  $\varepsilon_{bi}$ , from an elastic analysis of the existing member based on cracked section properties.
4. Calculate the effective strain in the FRP reinforcement at the ultimate limit state can be found using the following equation:

$$\varepsilon_{fe} = \varepsilon_{cu} \left( \frac{d_f - c}{c} \right) - \varepsilon_{bi} \leq \varepsilon_{fd} \quad \text{Eq. 2.8}$$

5. Calculate the effective stress in the FRP laminate from the strain in the FRP, assuming perfectly elastic behavior, using the following equation:

$$f_{fe} = E_f \varepsilon_{fe} \quad \text{Eq. 2.9}$$

6. Apply a strength reduction factor given by the following equation, where  $\varepsilon_t$  is the net tensile strain in extreme tension steel at nominal strength, as defined in ACI 318.

$$\phi = \begin{cases} 0.90 & \text{for } \varepsilon_t \geq 0.005 \\ 0.65 + \frac{0.25(\varepsilon_t - \varepsilon_{sy})}{0.005 - \varepsilon_{sy}} & \text{for } \varepsilon_{sy} < \varepsilon_t < 0.005 \\ 0.65 & \text{for } \varepsilon_t < \varepsilon_{sy} \end{cases} \quad \text{Eq. 2.10}$$

7. Ensure the stress in the steel reinforcement under service load is limited to 80 percent of the yield strength and the compressive stress in concrete under service load is limited to 60 percent of the compressive strength.
8. Check creep rupture and fatigue stress limit shown in Figure 16.

**Table 10.2.9—Sustained plus cyclic service load stress limits in FRP reinforcement**

Stress type	Fiber type		
	GFRP	AFRP	CFRP
Sustained plus cyclic stress limit	$0.20f_u$	$0.30f_u$	$0.55f_u$

Figure 16: FRP stress limits (ACI Committee 440, 2008)

Refer to ACI 440.2R-17 for provisions on pre-stressed concrete members and guidelines for strengthening members in categories other than flexure. Section 4.1 American Concrete Institute (ACI 440.2R-17) explains how to verify adequate shear strength is available, which is based on the concept that total shear strength is the sum of the contribution of the FRP shear reinforcement and the steel shear reinforcement; it is limited by the criteria given for steel alone.

#### 2.2.1.6 Implementation

In 2017, SDR Engineering Consultants, Inc. used U-wrap to repair a girder in Sumter County. The County Road 514 bridge over I-75 experienced major and minor spalls, damaged shear reinforcement, and five broken strands. The repairs utilized strand splicing for the broken strands and restored the concrete sections. A composite CFRP lamination system of U-wrapping was used to provide concrete and shear resistance to the restored damaged areas. The u-wrap was chosen to provide higher carrying capacity and improved long-term durability and performance, because of its bonding directly to the surface using adhesive epoxy.

### 2.2.2 U-Anchor

#### 2.2.2.1 Introduction

A difference among the U-shaped reinforcing methods must be noted. A “U-wrap”, as previously defined, is the simple bonding of CFRP laminate(s) to a member. No support beyond the bond strength of the adhesive used is provided. Debonding is a primary concern upon installation of a U-wrap; it is, therefore, often necessary to provide additional anchorage. A “U-anchor” provides additional support to U-wraps via more invasive installation techniques.

To install a U-anchor, grooves must be cut into the substrate to accommodate longitudinal bars. Each end of the CFRP laminate is wrapped around/below a longitudinal bar before the entire system is coated in epoxy. The additional adhesive and connection to a reinforcing bar, which may be steel or composite-based, significantly decreases the likelihood of debonding controlling design.

#### 2.2.2.2 Installation Procedure

Although provisions do not change from typical U-wrap design, installation procedures vary significantly. The following steps should be followed to attain the predicted strengths and strains found using ACI 440.2R-17:

1. Cut grooves into the concrete member along the length required to receive longitudinal bar reinforcement. Grooves should be slightly wider and deeper than the diameter of the reinforcing bars. These details were included in Task 2 of the research project.  
\*Care must be taken not to damage existing reinforcement (e.g., rebar).
2. Remove dust and debris from grooves and clean and roughen surfaces according to the chosen manufacturer’s recommendations.
3. Cut reinforcing rods to appropriate length. If rods are composite-based, care should be taken to avoid splintering while cutting.
4. Fill grooves with appropriate adhesive (i.e., epoxy).
5. Lay CFRP laminate over grooves, align reinforcing bars over laminate along the grooves, and press firmly until the entire laminate-bar system is encased by the adhesive. The additional adhesive should be placed atop the reinforcing bar to ensure the entire groove is filled.

6. Wipe/trowel surface to create a level finish and remove air voids from grooves.

### 2.2.2.3 Schematics

The groove-epoxy-bar system described above is detailed in Figure 17. The groove dimensions depend on the bar geometry, and the laminate encased in the epoxy channel. Figure 18 shows a broader view of two U-anchor schemes, one that contacts three sides of a concrete beam to increase shear strength and one used to flexural strengthen a slab system.

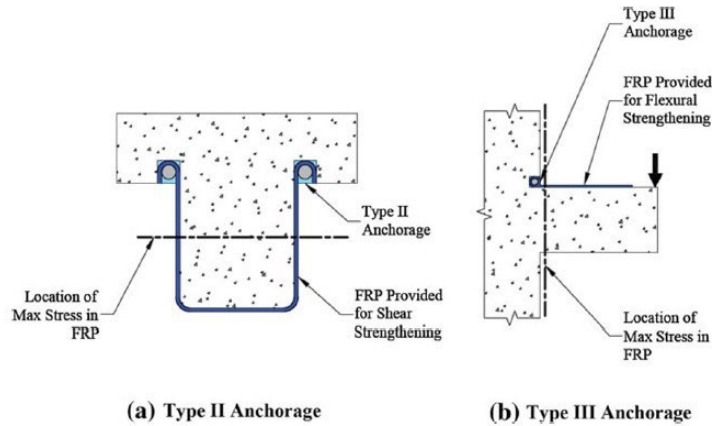


Figure 17: Type II and III anchorage (Grelle and Sneed, 2013)

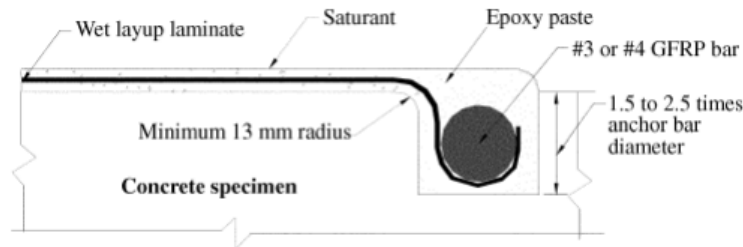


Figure 18: Example of near-surface mounted laminate (McGuirk, G., 2011)

### 2.2.2.4 Results

Figure 19 shows three beams tested by Khalifa in 1999 (Khalifa, Nanni, Alkhrdaji, & Lansburg, 1999), each of which was outfitted with linear variable differential transformers (LVDTs) to measure linear displacement and strain gauges. The first beam, BT1, served as a control test to compare strengthened beams. The second beam, BT2, consisted of a CFRP U-wrap only. The third beam, BT3, was reinforced with a CFRP U-wrap and end anchors (similar to Figure 16). Results showed that the installation of end anchorage significantly increased ultimate flexural strength when tested until failure, as illustrated in Figure 20.

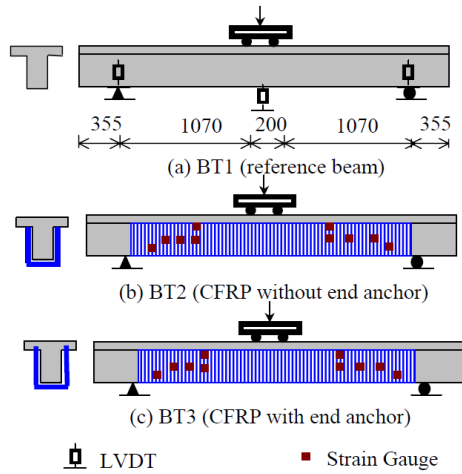


Figure 19: Types of anchors tested (Khalifa et al., 1999)

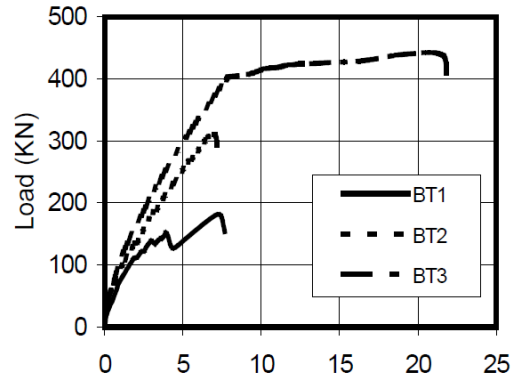


Figure 20: Strength increase from U-anchors (Khalifa et al., 1999)

### 2.2.2.5 Design Guidance

Design procedures align closely with typical U-wraps since the anchorage system is identical with the addition of additional adhesive and longitudinal reinforcement. ACI 440.2R-17 should be referenced for design procedures. The strength and elastic modulus of FRP materials can be determined by the requirements of ASTM D3039/D3039M, D7205/D7205M, or D7565/D7565M.

For CFRP sheets anchored with a grooved system (i.e., U-anchors), the prediction of shear capacity must incorporate a groove factor,  $G_{FS}$  (Mohamed, Abdalla, & Hawileh, 2020). The factor accounts for the shear strength contribution of the grooves in the shear strength of the CFRP, where the shear strength of the CFRP is  $V_f$  in the shear design equation of ACI440.2R-17.

$$V_n = V_c + V_s + G_{FS}\Psi_f V_f \quad \text{Eq. 2.11}$$

$$G_{FS} = f(x) = \begin{cases} 2.086e^{-0.01G_w}, & \text{for } 5\text{mm} \leq G_w \leq 40\text{mm} \\ 1.0, & \text{Otherwise} \end{cases} \quad \text{Eq. 2.12}$$

$V_n$  = Nominal shear strength

$V_s$  = Shear strength contribution of reinforcing steel

$V_f$  = Shear strength contribution of CFRP

$G_{FS}$  = Groove factor

$G_w$  = Groove width (mm)

$\Psi_f$  = FRP strength reduction factor

= 0.85 for flexure (calibrated based on design material properties)

= 0.85 for shear (based on reliability analysis) for three-sided FRP U-wrap or two-sided strengthening schemes

= 0.95 for shear fully wrapped sections

### 2.2.2.6 Implementation

U-anchor usage is extremely limited. While research and performance testing are plentiful, the application of U-anchors in the engineering and construction industry is not prevalent. A

manufacturer of U-anchor products, Sika, was contacted to gain insight into industry preferences and uses of their applicable products. Sika reported that they no longer recommend their U-anchor product to those looking for general concrete strengthening. While specific projects that necessitate the use of U-anchors do exist, other anchorage types are much more popular. For example, Sika recommends their spike anchor for common shear and flexural strengthening projects. No known applications were found for bridges or buildings in the United States. Likewise, no design codes address the installation of non-CFRP materials, making U-anchor design varying and test-based.

## 2.2.3 Staple Anchor

### 2.2.3.1 Introduction

A test report published by the University of Miami in 2016 outlined the performance of what is known as a “staple anchor” (University of Miami, 2016). The unique anchor type increases the bond strength between a CFRP laminate or strip and the substrate. Debonding, or peel-off, is the most commonly observed failure mode among CFRP reinforcement that is directly epoxied to its member’s surface. The goal of staple anchors is to create a condition where the controlling failure mode is concrete substrate breakage (i.e., concrete breaks before debonding).

The anchor solution comprises two components: a flat, prefabricated “staple” made of a pre-cured, carbon FRP piece and a saturated fiber sheet that wraps around or covers the flat staple and externally bonded FRP sheet or laminate.

### 2.2.3.2 Installation Procedure

Given the limited application of staple anchors, the installation procedure is based on existing test reports (University of Miami, 2016).

1. Concrete blocks were cast in a single batch, conforming to ASTM C192/C192M-13a.
2. The surface of each concrete block was sandblasted to a surface roughness of CPS 3 as defined by the International Concrete Repair Institute (ICRI).
3. A typical anchor is 6" long by 2" wide with 1" legs and a uniform thickness of 0.14". To install staple anchors, grooves must be cut into the concrete substrate. The grooves must accommodate the leg geometry and epoxy required to bond the anchor to the surface. It is recommended to install the CFRP laminate and anchor it simultaneously onto the substrate.

Load measurements were recorded via load cells conforming to ASTM E4-16.

### 2.2.3.3 Schematics

Figure 21 shows the testing apparatus used by the University of Miami to tension the FRP laminate. Figure 22 summarizes the capacity of the system under the three different testing conditions, along with the most common failure mode observed for each condition.

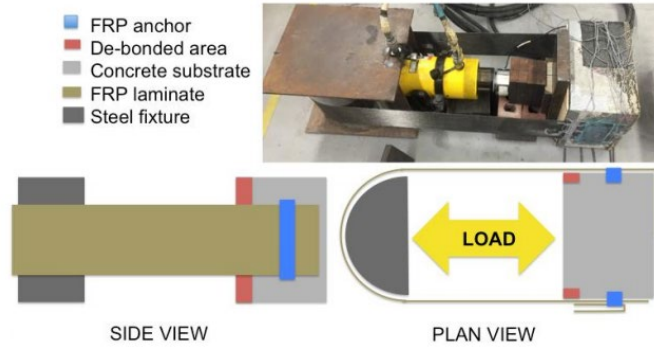


Figure 21: Staple anchor testing apparatus (University of Miami, 2016)

SPECIMEN ID	Total peak load ( $P_{max}$ )		Total load sustained by anchor ( $P_{max}/2$ )		Increase in performance	Failure Mode
	lbf	kips	lbf	kips	%	
B_01	13041	13.04	6521	6.52	-19.7	FRP de-bonding
B_02	17034	17.03	8517	8.52	4.9	FRP de-bonding
B_03	18635	18.63	9317	9.32	14.8	FRP de-bonding
<b>Average</b>	<b>16237</b>	<b>16.24</b>	<b>8118</b>	<b>8.12</b>		
Stand. Dev.	2352	2.35	1176	1.18	<b>0.0</b>	
Coef. of Var. (%)	14.5	14.5	14.5	14.5		
S_01	24628	24.63	12314	12.31	51.7	FRP de-bonding and slippage beneath the anchor
S_02	30118	30.12	15059	15.06	85.5	FRP de-bonding and slippage beneath the anchor/FRP rupture
S_03	29170	29.17	14585	14.58	79.7	FRP de-bonding and slippage beneath the anchor/FRP rupture
<b>Average</b>	<b>27972</b>	<b>27.97</b>	<b>13986</b>	<b>13.99</b>		
Stand. Dev.	2396	2.40	1198	1.20	<b>72.3</b>	
Coef. of Var. (%)	8.6	8.6	8.6	8.6		
Z_01	34480	34.48	17240	17.24	112.4	Failure in concrete substrate
Z_02	43131	43.13	21566	21.57	165.6	Anchor failure and FRP de-bonding
Z_03	45927	45.93	22964	22.96	182.9	Failure in concrete substrate
Z_04	41412	41.41	20706	20.71	155.1	Failure in concrete substrate
Z_05	42833	42.83	21417	21.42		Anchor failure and FRP de-bonding
<b>Average</b>	<b>41556</b>	<b>41.56</b>	<b>20778</b>	<b>20.78</b>		
Stand. Dev.	3829	3.83	1915	1.91	<b>155.9</b>	
Coef. of Var. (%)	9.2	9.2	9.2	9.2		

Figure 22: Staple anchor test results (University of Miami, 2016)

### 2.2.3.4 Results

The effectiveness of the staple anchor was determined by comparing the strength of the FRP-Concrete system with and without the installation of the anchor. An FRP laminate was anchored to a concrete substrate and pulled in tension until the FRP, bonding agent, or concrete failed. The following three conditions were tested until failure:

1. FRP bonded to concrete without a staple anchor (Condition B)
2. FRP bonded to concrete with the staple anchor (Condition S)
3. FRP bonded to concrete with staple anchor and saturated fiber wrap (Condition Z)

Condition B was used as a reference specimen and proved the effectiveness of the staple anchor. When compared to no anchorage (Condition B), a 72% increase in load-carrying capacity was measured for the anchor alone (Condition S). In comparison, a 156% increase in strength was measured for the anchor with a saturate FRP wrap (Condition Z). Debonding, an undesired failure mode, was observed for Condition B and S. Failure in the concrete substrate was the primary failure mode for Condition Z, rendering the anchoring method a viable solution.



### 2.2.3.5 Design Guidance

Limited standards and test criteria have been developed since the creation of staple anchors. To quantify the performance of FRP anchor systems, data-driven and practical design guides have been developed through research studies, some of which have been published in peer-reviewed papers. The method adopted by the University of Miami to evaluate the performance of FRP anchors is based on a double shear bond test, where two bonded areas are engaged in shear.

### 2.2.3.6 Implementation

The application of staple anchors is limited to laboratory testing, but promising results have led to increased market availability and the likelihood of field studies. The manufacturer cited two case studies when a request for implementation information was sent to the company's Director of Development. The first project strengthened double-tee beams in the Omni Hotel parking garage of Dallas, Texas (Fortec Stabilization, 2021). Steel reinforcement, especially at weld locations, failed due to corrosion, tension, and shear stress. Single layers of unidirectional CFRP have been wrapped around (three-sided wrap) the damaged ends of the beam, each of which was anchored by Fortec's staple anchor. The second case study involved reinforcing structural components of a distribution warehouse in Matawan, Michigan (Fortec Stabilization, 2017). The concrete slab, columns, and beams of the warehouse were experiencing corrosion and spalling. After patching critical areas, unidirectional CFRP wraps were installed on members subject to flexural and shear loads; each wrap was anchored with a staple anchor.

Fortress/Fortec Stabilization systems, the producer of staple anchors, must be contacted directly for anchor acquisition. The company sells its products directly to contractors or other parties with a proven need. The anchors are available for educational use, and Fortress/Fortec encourages formal testing of their products before use, given variations in site conditions. The geometric constraints of every project are unique; therefore, Fortress/Fortec offers customization, meaning the company can produce anchors of any size or shape. The manufacturer highly recommends testing unusual shapes and sizes to ensure adequate product performance.

## 2.3 FRP Strip and Sheet

### 2.3.1.1 Introduction

Fiber reinforcing is most commonly bonded to concrete using a bonding agent. The bonding agent is often an epoxy-based solution applied as a liquid and cured before service. When FRP laminates are used to strengthen structural members, particularly in flexure and shear, anchorage beyond basic bonding techniques becomes necessary to prevent debonding (peel-off) of the FRP. When debonding occurs, the full capacity of the FRP reinforcement has not been reached. Hence, all efforts should be made to prevent debonding failure. Additional FRP strips and/or sheets are often applied over the main FRP laminate to increase bonding strength and force failure to occur through FRP rupture or concrete breakage.

FRP strips and sheets are typically fixed to the concrete substrate using a bonding agent like the primary FRP laminate. Although the bonding agent's failure is intended to be prevented by using FRP strips and/or sheets, the increased amount of agent and additional FRP reinforcement provides sufficient bonding strength to prevent debonding failure.



Research on FRP strip and sheet application is extensive and is one of the most common FRP reinforcement techniques. Ease of application and minimal invasiveness make FRP strips and sheets popular among applicable agencies. While the application is non-invasive, overall strengthening is low compared to other anchor types (U-anchor, plate anchor, etc.). State Departments of Transportation favor stronger but equally invasive FRP application methods.

### 2.3.1.2 Installation Procedure

FRP strips and sheets closely resemble U-wraps and U-anchors. The similarity in appearance solidifies the notion that installation procedures between the anchor types are identical, with the exception of FRP geometry and orientation. Both installation methods used for CFRP laminates, wet and dry lay-up, may be used for FRP strips or sheets. Like with U-wraps, manufacturer specifications and procedures must be followed to ensure bond strength is not less than predicted.

### 2.3.1.3 Figures

FRP strips vary significantly in size, shape (although they are typically rectangular), quantity and orientation. Figure 23 details a generic strengthening layout using FRP strips, where rectangular sheets of CFRP are laid perpendicular to the main laminate adhered to the tension face of the member.

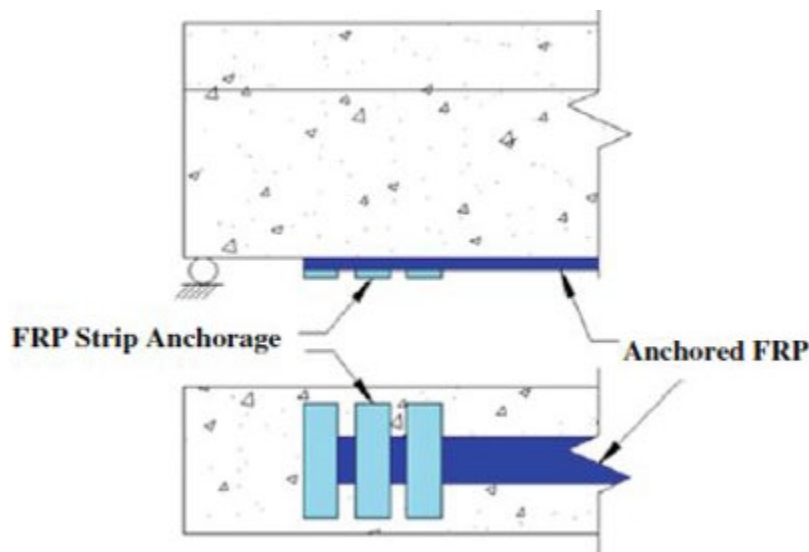


Figure 23: FRP strip anchor (Grelle and Sneed, 2013)

### 2.3.1.4 Results

ElSafty and Graeff tested many strip configurations (ElSafty & Graeff, 2012). As seen Figure 24, all wrapping schemes stiffened beams (decreased maximum deflection before failure) and resulted in increased ultimate strength. Increasing the number of vertical strips seemed to minimally enhance flexural performance, and the presence of a full CFRP wrap did not appear beneficial, suggesting that increased material usage does not correlate to an increase in ultimate strength (Figure 25).

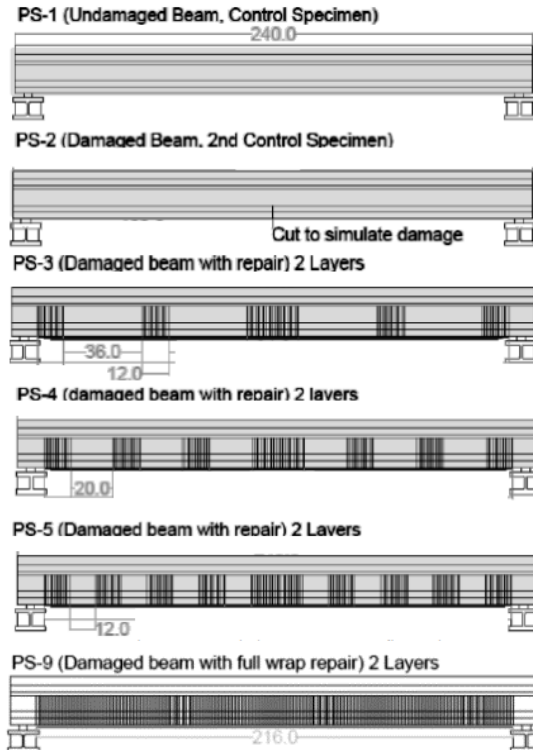


Figure 24: Beam reinforcement configurations (ElSafty & Graeff, 2012)

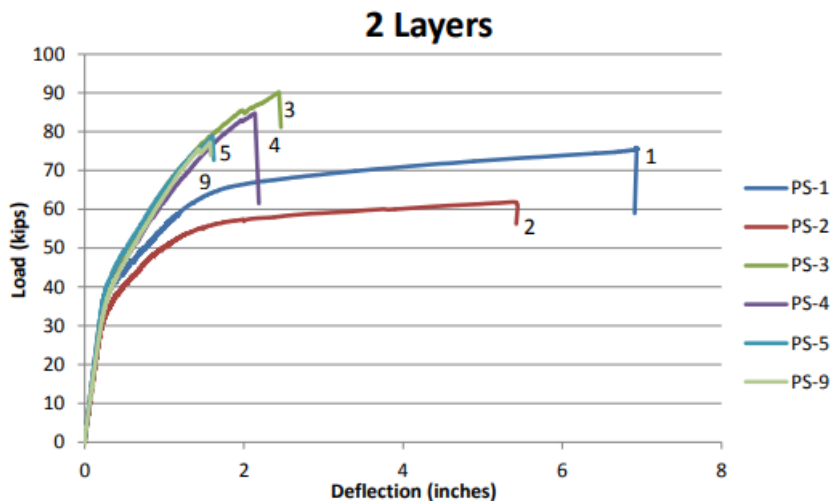


Figure 25: Maximum load and strain of reinforced beams (ElSafty & Graeff, 2012)

The design procedures commonly used for FRP strips and sheets are similar to the methods applied for the design of U-anchors and U-wraps. Likewise, ACI 440.2R-17 should be referenced for design procedures. The strength and elastic modulus of FRP materials can be determined by the requirements of ASTM D3039/D3039M, D7205/D7205M, or D7565/D7565M.

Although much research has been performed regarding the flexural strengthening of concrete members using FRP strips and sheets, the effect of bonded FRP strips and sheets on member shear strength is still under development (Khalifa, Gold, Nanni, & Aziz M.I., 1998). Since 1998,

much data has been collected to aid in developing design approaches. ACI 440.2R-17 outlines a strain-based approach to estimate shear strength contribution and is the referenced standard in the United States. The following design procedure is an alternative approach developed by Khalifa et al. and depends on the bonded surface configuration:

1. Determine the bonded surface configuration.
2. Find the reduction factor  $R$ , which is taken as the least of the following:

$$R = 0.50 \quad \text{Eq. 2.13}$$

$$R = 0.5622(\rho_f E_f)^2 - 1.2188(\rho_f E_f) \quad \text{Eq. 2.14}$$

$$R = \frac{0.0042(f'_c)^{\frac{2}{3}} w_{fe}}{(E_f t_f)^{0.58} \varepsilon_{fu} d_f} \quad \text{Eq. 2.15}$$

\*The second expression for  $R$  applies when  $\rho_f E_f < 1.1 \text{ GPa}$

$f'_c$  = nominal concrete compressive strength (MPa)

$\rho_f$  = FRP shear reinforcement ratio =  $\left(\frac{2t_f}{b_w}\right) \left(\frac{w_f}{s_f}\right)$

$w_f$  = width of FRP strip (mm)

$s_f$  = spacing of FRP strips (mm)

$E_f$  = FRP modulus of elasticity (GPa)

$t_f$  = thickness of FRP sheet on one side of beam (mm)

$w_{fe}$  = effective width of FRP sheet (mm)

$\varepsilon_{fu}$  = ultimate strain of FRP (mm)

$d_f$  = effective depth of CFRP shear reinforcement (mm)

=  $d$  for rectangular members

=  $d - t_s$  for T sections

3. Calculate the shear contribution of the FRP

$$V_f = \frac{A_f f_{fe} (\sin \beta + \cos \beta) d_f}{s_f} \leq \left( \frac{2\sqrt{f'_c} b_w d}{3} - V_s \right) \text{ if } s_f \leq w_f + \frac{d}{4} \quad \text{Eq. 2.16}$$

$f_{fe}$  = Effective tensile stress in FRP sheet in direction of principal fibers

=  $R f_{fu}$

$f_{fu}$  = Ultimate tensile strength of FRP sheet in direction of principal fibers

$R$  = reduction factor = ratio of effective stress or strain in FRP sheet to its ultimate strength or elongation

$\beta$  = Angle between principal fiber orientation and longitudinal axis of beam

$d_f$  = effective depth of CFRP shear reinforcement (mm)

=  $d$  for rectangular members

=  $d - t_s$  for T sections

$s_f$  = Spacing of FRP strips (mm)

$f'_c$  = Nominal concrete compressive strength (MPa)  
 $b_w$  = cross-sectional width of concrete member (mm)  
 $d$  = distance from centroid of steel reinforcement to the top of the concrete section (mm)  
 $V_s$  = shear contribution of steel reinforcement  
 $w_f$  = width of FRP strip (mm)

4. Calculate shear capacity of concrete member

$$\phi V_n = 0.85(V_c + V_s) + 0.70V_f \quad \text{Eq. 2.17}$$

$\phi$  = Strength reduction factor  
 $V_n$  = nominal shear strength  
 $V_c$  = shear contribution of concrete  
 $V_s$  = shear contribution of steel reinforcement  
 $V_f$  = shear contribution of FRP

The Fédération Internationale du Béton (FIB 14) provides the following comments on the design of FRP strips and sheets, most of which is derived from Eurocode 2004:

Shear capacity of a strengthened member (European Committee for Standardization, 2004)

$$V_{Rd} = \min(V_{cd} + V_{wd} + V_{fd}, V_{Rd2}) \quad \text{Eq. 2.18}$$

Contribution of FRP to shear capacity:

$$V_{fd} = 0.9\varepsilon_{fd,e}E_{fu}\rho_f b_w d(\cot(\theta) + \cot(\alpha)) \sin(\alpha) \quad \text{Eq. 2.19}$$

$\varepsilon_{fd,e}$  = design value of effective FRP strain  
 $b_w$  = minimum width of cross-section over the effective depth  
 $d$  = effective depth

$$\rho_f = \text{FRP reinforcement ratio} = \begin{cases} \frac{2t_f \sin(\alpha)}{b_w} & \text{for continuously bonded FRP} \\ \left(\frac{2t_f}{b_w}\right)\left(\frac{b_f}{s_f}\right) & \text{for FRP strips or sheets} \end{cases}$$

$s_f$  = FRP spacing (Figure 26)  
 $E_{fu}$  = FRP modulus of elasticity  
 $\theta = 45^\circ$  = angle of diagonal crack with respect to the member axis  
 $\alpha$  = angle between principal fiber orientation and longitudinal axis of member

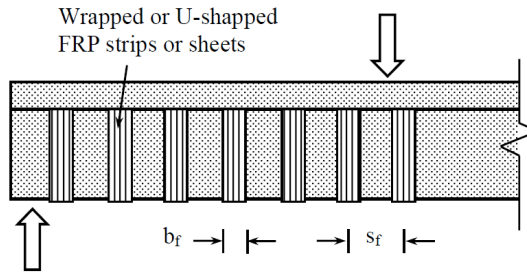


Figure 26: Strip and sheet nomenclature

While FIB and Eurocode are not primary design guides in the United States, their applicability to the design of FRP systems makes their content invaluable. In the United States, ACI 440.2R-17 should be referenced for design procedures. The strength and elastic modulus of FRP materials can be determined in accordance with the requirements of ASTM D3039/D3039M, D7205/D7205M, or D7565/D7565M.

### 2.3.1.5 Implementation

The use of CFRP strips and sheets is most common for concrete repair. Departments of transportation acknowledge FRP strips and sheets as a non-invasive, easy-to-apply solution to restore strength to concrete members damaged by various sources (e.g., an oversized truck colliding with a bridge girder supporting an interstate overpass).

In Winnipeg, Manitoba, Canada, a twenty-seven-year-old bridge (Maryland Bridge) needed to be strengthened to support new truck traffic that imposed service loads higher than those used during the original design of the bridge. Since little design guidance was available at the time (1998), scale models of the bridge's prestressed concrete girders were tested to failure after applying CFRP sheets. Sheet-reinforced members were tested under four wrapping configurations, including vertical CFRP, diagonal CFRP, horizontal and vertical CFRP, and horizontal and diagonal CFRP. The horizontal and diagonal CFRP configuration improved shear capacity by 36%; hence, testing provided the data necessary to use CFRP sheets and strips to strengthen the Maryland bridge girders (Hutchinson, Abdelrahman, & Rizkalla, 1998).

## 2.4 Mechanical & Metallic Anchor (Bolted or Nailed)

### 2.4.1.1 Introduction

The strength of a structural member reinforced with FRP is controlled by its failure mode. Failure of a single element of a system can lead to total system failure. For example, a system with only a simple bonded FRP laminate can fail (when subjected to flexural and/or shear forces) in one of three ways: FRP rupture, debonding (peel-off), or concrete breakout. The number of possible failure modes increases with system complexity, but so should overall strength. Regardless of the anchorage type, the preferred failure mode is the breakage of the concrete substrate. Concrete failure implies that the strength of the anchor applied was fully utilized. To guarantee debonding does not occur, anchorages using mechanical components (i.e., bolts, nails, etc.) were developed. While much more invasive than surface-mounted strips and sheets, mechanical anchors prove rigid, reliable, and effective in preventing peel-off failure.

### 2.4.1.2 Installation Procedure

The installation procedures for mechanical and metallic anchors align similarly with the guidelines applied for spike anchor installation. Given the large variability of mechanical anchors in terms of geometry, material, and manufacturer, a single installation procedure is not identifiable. The provisions used for the installation of spike anchors should be referenced for the installation of mechanical anchors due to the similar, intrusive nature of the anchors' installation. Steel, angled anchor, for example, requires embedment of a bolt, nail, etc., into the concrete substrate. While each type of mechanical anchor yields unique benefits, all mechanical anchors share complex and strenuous application and installation.

### 2.4.1.3 Figures

A plethora of mechanical anchors is available, each of which is associated with a unique geometry, installation procedure, and strengthening capabilities. Plate anchors, a frequently tested anchor type, are depicted in Figure 27, where they were used to strengthen a girder during comprehensive testing of different anchorages (Aljaafreh, Performance of Precast Concrete Bridge Girders with Externally Bonded Anchored CFRP, 2019). When mechanical anchors are used to mounting two or three-sided U-wraps, their method of supporting the CFRP can vary; Figure 28 details two connection possibilities.



Figure 27: Mechanical plate anchors for girder (Aljaafreh, Performance of Precast Concrete Bridge Girders with Externally Bonded Anchored CFRP, 2019)

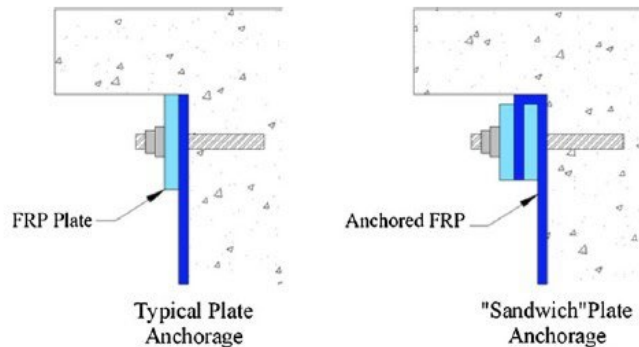


Figure 28: Plate anchorage system (Grelle & Sneed, Review of Anchorage Systems for Externally Bonded FRP Laminates, 2013)

### 2.4.1.4 Results

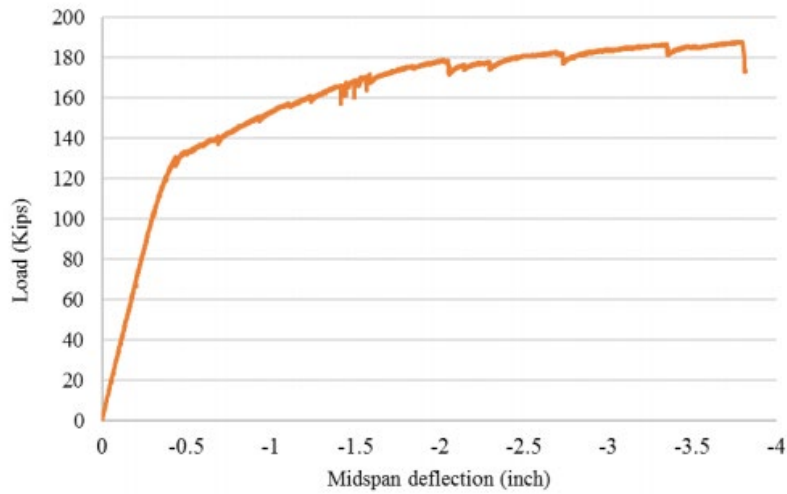


Figure 29: Load & deflection – girder with plate anchors (Aljaafreh, Performance of Precast Concrete Bridge Girders with Externally Bonded Anchored CFRP, 2019)

Item	Girder-1	Girder-2	Girder-3	Girder-4	Girder-5
Type of anchor	Control	No-anchor	Fan-anchor (FAN)	Mechanical-anchor (MA)	U-wrap-anchor
Measured ultimate load (kips)	175.06	186.7	182.6	187.7	168.7
Maximum deflection	2.42	3.4	4	3.8	2.04
Maximum tensile strain for CFRP ( $\mu\epsilon$ )	-	6173	5772	6443	2336

Figure 30: Ultimate strengths – girder with various anchor types (Aljaafreh, Performance of Precast Concrete Bridge Girders with Externally Bonded Anchored CFRP, 2019)

Girder designation	Damage simulating	Strengthening technique
Girder1 – Control	No simulated damage	No strengthening
Girder 2-No anchor	Simulated damage	Pre-saturated CFRP and no anchor.
Girder 3 – Fan anchor	Simulated damage	Pre-saturated CFRP and anchored using CFRP anchor (FAN).
Girder 4 - Mechanical anchor (MA)	Simulated damage	Pre-saturated CFRP anchored with mechanical anchor (MA)
Girder 5 – U-wrap	Simulated damage	Pre-saturated CFRP and anchored with u-wrap.

Figure 31: Tested girder designations (Aljaafreh, T., 2019)

The test results, shown in Figure 29 and Figure 30, are not representative of all anchor capabilities. Due to large cracks between the repair mortar and existing concrete, premature failure of the U-wrapped girder was observed; hence, ultimate load and maximum deflection and strain for the U-wrapped girder should not be considered accurate performance indicators. Regardless, the results shown in Figure 29 provide a concise comparison of the strengthening abilities of the anchor types described in Figure 31.

#### 2.4.1.5 Design Guidance

The use of mechanical anchors complicates the design. The introduction of additional anchoring elements creates new failure modes. Plate anchorage systems, for example, can fail via debonding, concrete rupture, or plate yielding/rupture (as opposed to a U-wrap or strip anchor system where debonding and failure of the concrete or laminate are the only failure modes). ACI 440.2R-17 should be referenced to design the FRP laminate portion of the system. The strength and elastic modulus of FRP materials should be determined in accordance with the requirements of ASTM D3039/D3039M, D7205/D7205M, or D7565/D7565M. The strength of a mechanical anchor should be provided by its manufacturer. Appropriate testing should be conducted prior to application if no strength data is available. For example, if a plate anchor is to be used, the plate and its accompanying hardware (nuts, bolts, etc.) should be rigorously tested to failure in both isolated and fully assembled tests.

#### 2.4.1.6 Implementation

Although a significant strength increase is observed, mechanical and metallic anchors are not common or preferred. The anchors' intrusiveness and protrusion from the member's surface make their application rare. Also, the interaction between dissimilar metals makes galvanic corrosion a prominent risk.

### 2.4.2 Longitudinal Chase

#### 2.4.2.1 Introduction

A longitudinal chase is unlike any other anchorage system. In the case of a rectangular beam, a groove is cut into the tensioned face along the length of the concrete member. The groove is filled with epoxy and, in some cases, a steel or FRP bar. The main FRP laminate is bonded to the concrete directly over the filled groove. The longitudinal chase anchorage system utilizes the mechanical properties of the bonding material (e.g., epoxy) to distribute the interfacial shear stresses to a larger area of concrete. The additional bonded area is equal to the width and twice the depth of the groove times the length of the groove (Grelle & Sneed, Review of Anchorage Systems for Externally Bonded FRP Laminates, 2013).

#### 2.4.2.2 Installation Procedure

Before filling the groove with epoxy, it is recommended that additional protection be applied to the reinforcement. For example, glass fiber fabric (120 mm × 400 mm) was applied centrally over the reinforcement bar to prevent galvanic corrosion of the reinforcement during Kalfat and Al-Mahaidi's testing (Kalfat & Al-Mahaidi, 2010).

1. Determine member geometry (width, depth, and length). In the case of a box girder or other non-solid or non-symmetrical shape, concrete thickness and depth limitations should be noted.



2. Determine the size of the reinforcing bar to be used. No minimum or maximum bar size may be used; bar diameter is controlled by geometric constraints.
3. Cut chase in concrete. Like the bar diameter, no provisions exist for chase sizing; therefore, member geometry dictates design. A channel slightly larger than the diameter of the reinforcing bar is necessary to allow complete penetration of the added epoxy.
4. Before inserting the reinforcing bar, appropriately prime the concrete surface.
5. Bond the reinforcement bar and add additional protection if necessary (e.g., glass fiber fabric).
6. Centrally apply the laminate strip to the concrete surface. The laminate should be pressed onto the member to ensure accurate adhesive thickness and central placement.

### 2.4.2.3 Figures

Grelle and Sneed performed isolated testing on the effectiveness of longitudinal chases to increase bond strength and reduce the likelihood of debonding (Grelle & Sneed, Review of Anchorage Systems for Externally Bonded FRP Laminates, 2013). The typical specimen composition is shown in Figure 32. Although Grelle and Sneed used a steel reinforcing bar, other bar types (e.g., fiberglass) may be used.

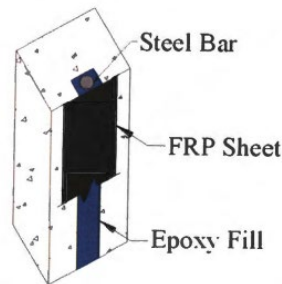


Figure 32: Longitudinal chase cross-section (Grelle, S., Sneed, L., 2011)

### 2.4.2.4 Results

Due to their highly invasive nature, longitudinal chases are seldom tested or used in the construction industry. Exclusion of the bar from the chase system does not affect the strength of the anchorage system (Kalfat & Al-Mahaidi, 2010). The groove has the potential to cause stress concentrations in the substrate and can weaken a section at the groove location.

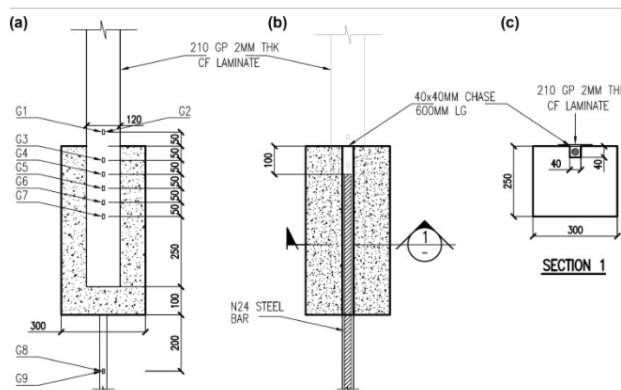


Figure 33: Longitudinal chase test configuration (Kalfat and Al-Mahaidi, 2010)

	Reference	Failure load (kN)	Max elongation ( $\mu\epsilon$ )	
			GA/AR	GA
Control specimen	WG9	99.6	2535	2706
Stage 1 – anchorage	WG1	194.4	4640	4434
	WG2	198.5	4881	4733

Figure 34: Longitudinal chase test results (Kalfat and Al-Mahaidi, 2010)

Seven strain gauges (G1 through G7) were attached to the surfaces of CFRP plates (Figure 33). G1 and G2 were installed to monitor bending in the CFRP plate during testing; bending of the plate would imply eccentric loading was present. G1 and G2 were placed at the back and front, respectively, of the laminate at the same location. A significant increase in failure load (approximately 95 kN) was observed upon the installation of the longitudinal bar/epoxy-filled groove (Figure 34).

#### 2.4.2.5 Design Guidance

The laminate bond strength to be placed over the longitudinal chase must be calculated as it often controls a system's strength limits. The equations used to determine the bond strength of a longitudinal chase were developed by Kalfat and Al-Mahaidi in 2010 (Kalfat & Al-Mahaidi, 2010) using bond strength models developed by Täljsten and Yuan, and Wu (Yuan & Wu, 1999). The thickness of the concrete member can significantly affect the stress distribution within the reinforced member (Kalfat & Al-Mahaidi, 2010).

$$P_u = b_p \sqrt{\frac{2G_f E_p t_p}{1 + \left(\frac{E_p t_p b_p}{E_c t_c b_c}\right)}} \quad \text{Eq. 2.20}$$

$$P_u = 0.427 \beta_p \beta_L \sqrt{f'_c} L_e \quad \text{Eq. 2.21}$$

$$L_e = \sqrt{E_p t_p / \sqrt{f'_c}} \quad \text{Eq. 2.22}$$

$$\beta_p = \left[ \frac{2 - \left(\frac{b_p}{b_c}\right)}{1 + \left(\frac{b_p}{b_c}\right)} \right] \quad \beta_L = \begin{cases} 1, & L \geq L_e \\ \sin\left(\frac{\pi L}{2L_e}\right), & L < L_e \end{cases} \quad \text{Eq. 2.23}$$

$$\text{Eq. 2.24}$$

$b_c$  = Member width (mm)

$b_p$  = Width of bonded FRP laminate (mm)

$t_p$  = Thickness of bonded FRP laminate (mm)

$t_c$  = Member thickness (mm)

$E_p$  = Modulus of elasticity of bonded FRP laminate (MPa)

$E_c$  = Modulus of elasticity of concrete (MPa)

$G_f$  = Fracture energy

$f'_c$  = Concrete compressive strength

$L$  = Bonded length (mm)  
 $L_e$  = Effective bonded length  
 $P_u$  = Bond strength of a joint (N)  
 $\beta_L$  = Geometric bond length coefficient  
 $\beta_P$  = Geometric width coefficient

The effective strain of a CFRP laminate is also a common governing failure mode. Effective strain is the maximum strain of the FRP laminate prior to failure. ACI 440.2R-02 states that for face-bonded applications, the maximum strain in the FRP is given by the following equation:

$$\varepsilon_{fe} = k_v \varepsilon_{fu} \leq 0.004 \quad \text{Eq. 2.25}$$

$k_v$  = Bond reduction coefficient applicable to shear  
 $\varepsilon_{fu}$  = Ultimate strain of the CFRP laminate at rupture

#### 2.4.2.6 Implementation

Longitudinal chases were created with the intent to be used for combined shear and torsional strengthening of box girder bridge webs. After a brief testing period, it was soon realized that more applications existed for the FRP strengthening method. The original anchorage system included a steel reinforcing bar encased in the epoxied groove. The report by Kalfat and Al-Mahaidi (Kalfat & Al-Mahaidi, 2010) claims that exclusion of the reinforcing bar does not affect the strength of the system.

#### 2.5 Summary and Comparison

Table 1 summarizes various anchor systems, their invasiveness to existing concrete structures, predominant failure mode, and implementation. Out of the six anchor systems, only the FRP strip is not invasive to the concrete structures as it relies on the adhesive bond to anchor the main CFRP sheet. Consequently, it also led to the least desirable failure mode of debonding. Spike and mechanical anchors provide the most desirable failure mode of concrete breakout. However, they are invasive to the existing concrete structures. The best of both worlds could be combining the FRP strip and spike anchor, but more research is needed to validate this. Only three systems have been utilized in actual projects. These systems are spike anchors, U-wrap with no anchor, and FRP strip (only flexural strengthening).

Table 1: Summary of anchor details

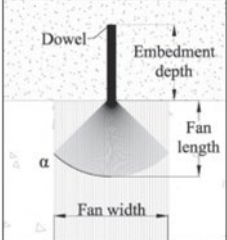
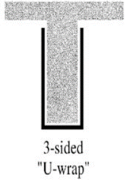
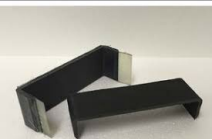
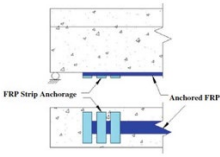
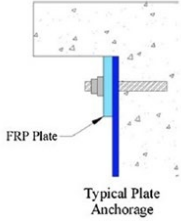
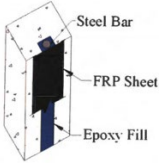
Anchor Name	Schematic	Invasiveness (Dimension of Penetration)	Predominant Failure Mode	Implementation	Manufacturer
Spike Anchor	 <p>(a) Straight anchor – Front view</p>	One hole drilled into concrete per anchor (depth determined by equations developed by Castillo et al., 2019)	Concrete Breakout (preferred) *Dependent upon embedment depth.	<ul style="list-style-type: none"> <li>– Strengthening of AASHTO concrete girders (Palm Beach County, FL)</li> <li>– Repair of AASHTO Type III Girder (Palm Beach Gardens, FL)</li> <li>– Sunshine Skyway Bridge Approach Spans (2013/2019)</li> </ul>	Various (Structural Technologies, CTech-LLC, Fyfe, Simpson Strong Tie, etc.)
U-wrap/anchor	 <p>3-sided "U-wrap"</p>	None *Channels must be cut if a U-wrap is to be anchored with embedded bar reinforcement)	Debonding (Not preferred) *Wraps should be designed not to fail via peel-off from member	– County Road 514 Repaired major spalls and damaged shear reinforcement (Sumter County, FL, 2017)	Various (Structural Technologies, Fyfe, Sika, etc.)
Staple Anchor		Two grooves need to be cut to insert legs of the staple into concrete: 2" x 1" x 0.14" thick	Concrete Rupture *Debonding was observed if a saturated wrap or anchor was not used	– Limited to laboratory testing	Fortec Stabilization Systems
FRP Strip and Sheet		None	Debonding (Not preferred) *Strips/sheets should be designed not to fail via peel-off from member	<ul style="list-style-type: none"> <li>– County Road 514 Br. I-75 Girder Repair (Sumter County, FL)</li> <li>– Strengthening of an old bridge in Manitoba, Canada to accommodate heavier, modern traffic.</li> </ul>	Various (Structural Technologies, Fyfe, Sika, etc.)

Table 1: Summary of anchor details

Anchor Name	Schematic	Invasiveness (Dimension of Penetration)	Predominant Failure Mode	Implementation	Manufacturer
Mechanical and Metallic	 <p>FRP Plate Typical Plate Anchorage</p>	<p>Varies *Drilling, screwing, and/or nailing into concrete always required. *Fasteners protrude from surface</p>	<p>Concrete Breakout (Preferred) *Anchors must be tested to ensure mechanical failure does not occur</p>	<p>– Sunshine Skyway Bridge Approach Spans (2008) – No known applications in the United States *Use in strengthening of walls may be permitted</p>	<p>Various (Structural Technologies, Fyfe, Sika, etc. for CFRP; Simpson Strong Tie, Hilti, etc. for hardware)</p>
Longitudinal Chase	 <p>Steel Bar FRP Sheet Epoxy Fill</p>	<p>Channel slightly larger than reinforcing bar is cut along the length of the member.</p>	<p>Debonding (Not preferred) *Only when laminate is tensioned. If member is flexed, FRP strain limit is typically reached</p>	<p>– No known applications in the United States</p>	<p>Various (Structural Technologies, Fyfe, Sika, etc. for CFRP; Owens Corning, Rhino, etc. for bar)</p>

### 3. Design Standards

The rapid increase in the use of CFRP to strengthen and repair concrete forced industry standards and codes to update their provisions. Providing widely accepted CFRP-based design standards is necessary to ensure safety and uniformity for their various applications. Engineers applying different design procedures for spike anchors, for example, could lead to over or under-designed members, resulting in wasteful or unsafe projects. Five national/international design standards were examined and compared. For all design standards, only sections pertaining to FRP design and application were summarized. Differences between the codes were present but, given that each standard applies to a different jurisdiction, conflicts are not concerning. If a procedure or requirement differs from another code within the same jurisdiction, the more stringent of the codes is assumed to apply. The five design guides investigated are as follows:

1. American Concrete Institute (ACI 440.2R-17)
2. Japan Society of Civil Engineers (JSCE)
3. Fédération Internationale du Béton (FIB 14)
4. Florida Department of Transportation (FDOT SDM Volume 4)
5. Canadian Standards Association (CSA S806-12)

ACI Committee 440, ACI's governing body for fiber-reinforced polymer reinforcement, produces literature specifically for FRP design. ACI 440.2R is the official ACI design guide for concrete reinforced with fibrous polymers. ACI 440.2R-08 was recently replaced with ACI 440.2R-17. Between the 2008 and 2017 versions, no changes were made to the shear strengthening design criteria, but the ACI 440.2R-17 does include a new seismic strengthening section. As a result, Sections 13, 14, and 15 of ACI 440.2R-08 were revised to Sections 14, 15, and 16, respectively. Considering that ACI 440.2R-17 is the current ACI version, the updated code was used in this project. The proposed modification to Volume 4 of FDOT SDM will reflect the changes made by ACI 440.2R-17. Most research and work performed in the United States, including the TxDOT study cited herein, references ACI 440.2R-08 as the primary design approach for CFRP strengthening. The 2012 AASHTO Guide Specifications for Design of Bonded FRP Systems for Repair and Strengthening of Concrete Bridge Elements (1st Edition) is also heavily referenced.

According to ACI 440.2R-17 (ACI Committee 440, 2017), the shear strength provided by FRP reinforcement depends on the tensile stress in the FRP shear reinforcement, which is calculated using the nominal FRP strain. The following equations outline the loss of design strength for non-fully wrapped (i.e., U-wrapped) members:

$$\text{Completely Wrapped with FRP:} \quad \varepsilon_{fe} = 0.004 \leq 0.75\varepsilon_{fu} \quad \text{Eq. 3.1}$$

$$\text{Partially Wrapped with FRP:} \quad \varepsilon_{fe} = \kappa_v \varepsilon_{fu} \leq 0.004 \quad \text{Eq. 3.2}$$

$\kappa_v$  is a “bond-reduction coefficient” that is a function of the concrete strength, the type of wrapping scheme used, and the laminate's stiffness. Properly anchored U-wraps can be designed to fail via FRP rupture. Regardless, the FRP shear reduction factor is equal to 0.85 ( $\psi_f = 0.85$ ).

The Fédération Internationale du Béton (fib) publishes Bulletin 14, a technical report of Task Group 9.3 on “Design and use of externally bonded fiber reinforced polymer reinforcement (FRP EBR) for reinforced concrete structures.” The bulletin is considered a consensus report for Europe as it adopts many European countries' practices. However, as noted earlier in the Michigan report, there are other guide specifications specific for each European country. The fib approach for shear strengthening is detailed in Section 5. It is less restrictive than other guide specifications as there is no limit in terms of maximum effective strain in the CFRP for shear strengthening. A restriction on strain for serviceability is provided:

$$\varepsilon_{fk,e} \leq \frac{0.8f_{yk}}{E_s} \quad \text{Eq. 3.3}$$

$\varepsilon_{fk,e}$  = Eff. FRP strain       $f_{yk}$  = Steel yield strength       $E_s$  = Steel mod. of elasticity

The guide did indicate that some researchers recommend the maximum effective strain in the CFRP to be 0.006, which is still much higher than 0.004 specified in ACI 440.2R-08. The research will further examine this to see the best limits for FDOT shear strengthening with various anchorage systems. Peel-off failure is only considered when calculating strain of two or three-sided wrapping configurations:

Fully Wrapped: 
$$\varepsilon_{f,e} = 0.17 \left( \frac{f_{cm}^{\frac{2}{3}}}{E_{fu}\rho_f} \right)^{0.30} \varepsilon_{fu} \quad \text{Eq. 3.4}$$

U-Wrapped or Two-sided: 
$$\varepsilon_{f,e} = \min \left\{ \begin{array}{l} 0.65 \left( \frac{f_{cm}^{\frac{2}{3}}}{E_{fu}\rho_f} \right)^{0.56} * 10^{-3} \\ 0.17 \left( \frac{f_{cm}^{\frac{2}{3}}}{E_{fu}\rho_f} \right)^{0.30} \varepsilon_{fu} \end{array} \right. \quad \text{Eq. 3.5}$$

$f_{cm}$  = Mean concrete compressive strength

$E_{fu}$  = FRP modulus of elasticity

$\rho_f$  = FRP reinforcement ratio

$\varepsilon_{fu}$  = Ultimate FRP strain

Section 11 of the Canadian Standards Association’s CSA-S806-12 provides flexural and shear strengthening specifications for concrete beams. Like other specifications, the approach is the same with ACI 440.2R-08 but using different limits and factors. It is also the only design specification with an effective strain limit for the CFRP of the three-sided U-wrap with a proven anchoring system. This effective strain limit is the least of 0.005 and 0.75 times the CFRP's ultimate strain, which is greater than ACI 440.2R-08. No singular section is given for non-masonry structures; therefore, Chapter 11 is the only chapter applicable to the strengthening of concrete members using CFRP laminates.

The Japan Society of Civil Engineers (JSCE) design specification differs from other guides because it uses a safety factor approach. The approach defines factors for elements such as material type, member type, structure environment, and loads. For shear strengthening using CFRP laminates, two methods of analysis are recommended. The first method applies only to completely wrapped schemes and uses an equation similar to ACI with added adjustment factors derived from regression analysis of experimental test results. The second method is more rigorous because it uses bond constitutive law to determine the shear contribution of the CFRP laminates. For a U-wrap, JSCE recommends using a mechanical anchor to prevent peel-off failure from occurring. No anchorage analysis or detail is provided, but preliminary testing is recommended to confirm shear capacity. Below are a few of the many design factors defined by JSCE:

$\gamma_{mf}$  = Material Coefficient of CFRP

$f_k$  = Characteristic value

$\gamma_m$  = Material factor

$\sigma_{fp}$  = Increase in reinforcement stress due to permanent load.

A detailed review of each design guidance is presented in the sections below.

### 3.1 American Concrete Institute (ACI 440.2R-17)

FRP systems should be qualified for use on a project based on independent laboratory test data of the FRP-constituent materials and the laminates made with them, structural test data for the type of application being considered, and durability data representative of the anticipated environment.

Chapter 7 of ACI 440.2R-17 gives requirements for inspection, evaluation, and acceptance of materials and adhesion strength. Strength and elastic modulus of FRP materials can be determined in accordance with the requirements of ASTM D3039/D3039M, D7205/D7205M, or D7565/D7565M. For bond-critical applications, tension adhesion testing of cored samples should be conducted in accordance with the requirements of ASTM D7522/D7522. Such tests cannot be performed when using near-surface-mounted (NSM) systems. The sampling frequency should be specified. Tension adhesion strengths should exceed 200 psi (1.4 MPa) and should exhibit failure of the concrete substrate.

General design considerations are given in Chapter 9. Design recommendations are based on limit-states design principles. The approach sets acceptable levels of safety for the occurrence of both serviceability limit states (excessive deflections and cracking) and ultimate limit states (failure, stress rupture, and fatigue).

Chapter 10 begins ACI's detailed design provisions with flexural strengthening. The strength design approach requires that the design flexural strength exceeds its required factored moment  $M_u$  (found via structural analysis), as indicated by Eq. 3.6. The design flexural strength  $\phi M_n$  refers to the nominal strength of the member,  $M_n$  (Eq. 3.17), multiplied by a strength reduction factor,  $\phi$  (Eq. 3.10).



$$\phi M_n \geq M_u \quad \text{Eq. 3.6}$$

To prevent such an intermediate crack-induced debonding failure mode, the effective strain in FRP reinforcement should be limited to the strain at which debonding may occur,  $\varepsilon_{fd}$ , as defined in Eq. 3.7.

$$\varepsilon_{fd} = 0.083 \sqrt{\frac{f'_c}{nE_f t_f}} \leq 0.9\varepsilon_{fu} \quad \text{Eq. 3.7}$$

The following assumptions are made in calculating the flexural resistance of a section strengthened with an externally applied FRP system:

- a) Design calculations are based on the dimensions, internal reinforcing steel arrangement, and material properties of the existing member being strengthened.
- b) The strains in the steel reinforcement and concrete are directly proportional to their distance from the neutral axis. That is, a plane section before loading remains plane after loading.
- c) There is no relative slip between external FRP reinforcement and the concrete.
- d) The shear deformation within the adhesive layer is neglected because the adhesive layer is very thin with only slight variations in its thickness.
- e) The maximum usable compressive strain in the concrete is 0.003.
- f) The tensile strength of concrete is neglected.
- g) The FRP reinforcement has a linear elastic stress-strain relationship to failure.

When FRP reinforcement is being used to increase the flexural strength, the member should be capable of resisting the shear forces associated with the increased flexural strength. The potential for shear failure of the section should be considered by comparing the design shear strength of the section to the required shear strength. If additional shear strength is needed, FRP laminates oriented transverse to the beam longitudinal axis can be used to resist shear forces, as described in Chapter 11.

The initial strain on the bonded substrate,  $\varepsilon_{bi}$ , can be determined from an elastic analysis of the existing member, considering all loads on the member during the installation of the FRP system. The elastic analysis of the existing member should be based on cracked section properties.

Because FRP materials are linear elastic until failure, the strain in the FRP will dictate the stress developed in the FRP. The maximum strain that can be achieved in the FRP reinforcement will be governed by either the strain developed in the FRP at the point at which concrete crushes, the point at which the FRP ruptures, or the point at which the FRP debonds from the substrate. The effective strain in the FRP reinforcement at the ultimate limit state can be found in Eq. 3.8.

$$\varepsilon_{fe} = \varepsilon_{cu} \left( \frac{d_f - c}{c} \right) - \varepsilon_{bi} \leq \varepsilon_{fd} \quad \text{Eq. 3.8}$$

where  $\varepsilon_{bi}$  is the initial substrate strain as described in 10.2.3, and  $d_f$  is the effective depth of FRP reinforcement, as indicated in Figure 35.

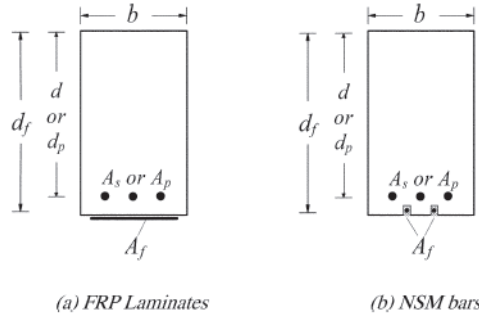


Figure 35: ACI 440.2R-17 Fig. 10.2.5-Beam schematic

The effective stress in the FRP reinforcement is the maximum level of stress that can be developed in the FRP reinforcement before flexural failure of the section. This effective stress can be found from the strain in the FRP, assuming perfectly elastic behavior.

$$f_{fe} = E_f \varepsilon_{fe} \quad \text{Eq. 3.9}$$

The use of externally bonded FRP reinforcement for flexural strengthening will reduce the ductility of the original member. The approach taken by this guide follows the philosophy of ACI 318. A strength reduction factor given by Eq. 3.10 should be used, where  $\varepsilon_t$  is the net tensile strain in extreme tension steel at nominal strength, as defined in ACI 318.

$$\phi = \begin{cases} 0.90 & \text{for } \varepsilon_t \geq 0.005 \\ 0.65 + \frac{0.25(\varepsilon_t - \varepsilon_{sy})}{0.005 - \varepsilon_{sy}} & \text{for } \varepsilon_{sy} < \varepsilon_t < 0.005 \\ 0.65 & \text{for } \varepsilon_t < \varepsilon_{sy} \end{cases} \quad \text{Eq. 3.10}$$

The stress in the steel reinforcement under service load should be limited to 80 percent of the yield strength, as shown in Eq. 3.11. In addition, the compressive stress in concrete under service load should be limited to 60 percent of the compressive strength, as shown in Eq. 3.12.

$$f_{s,s} \leq 0.8f_y \quad \text{Eq. 3.11}$$

$$f_{c,s} \leq 0.6f'_c \quad \text{Eq. 3.12}$$

As stated in 4.4.1 of ACI 440.2R-17, research has indicated that glass, aramid, and carbon fibers can sustain approximately 0.3, 0.5, and 0.9 times their ultimate strengths, respectively, before encountering a creep rupture problem (Yamaguchi, Kato, Nishimura, & Uomoto, 1997).

$$f_{f,s} \leq \text{Sustained plus cyclic stress limit} \quad \text{Eq. 3.13}$$

given in Figure 36

Stress type	Fiber type		
	GFRP	AFRP	CFRP
Sustained plus cyclic stress limit	$0.20f_{fu}$	$0.30f_{fu}$	$0.55f_{fu}$

Figure 36: ACI 440.2R-17-Sustained plus cyclic load limits

For any assumed depth to the neutral axis,  $c$ , the strain in the FRP reinforcement can be computed from Eq. 3.14. This equation considers the governing mode of failure for the assumed neutral axis depth. If the left term of the inequality controls, concrete crushing controls flexural failure of the section. Suppose the right term of the inequality controls, FRP failure (rupture or debonding) controls flexural failure of the section.

Strain in the nonprestressed steel reinforcement can be found in Eq. 3.14

$$\varepsilon_s = (\varepsilon_{fe} + \varepsilon_{bi}) \left( \frac{d - c}{d_f - c} \right) \quad \text{Eq. 3.14}$$

The stress in the steel is determined from Eq. 3.15

$$f_s = E_s \varepsilon_s \leq f_y \quad \text{Eq. 3.15}$$

With the stress in the FRP and steel reinforcement determined for the assumed neutral axis depth, internal force equilibrium may be checked using Eq. 3.16

$$\alpha_1 f'_c \beta_1 b c = A_s f_s + A_f f_{fe} \quad \text{Eq. 3.16}$$

$\varepsilon_t$  = net tensile strain in extreme tension steel at nominal strength, in./in.

$\varepsilon_{sy}$  = strain corresponding to yield strength of steel reinforcement, in./in.

$\varepsilon_s$  = strain in nonprestressed steel reinforcement, in./in.

$\varepsilon_{fe}$  = effective strain in FRP reinforcement attained at failure, in./in.

$\varepsilon_{bi}$  = strain in substrate at time of FRP installation (tension is positive), in./in.

$d$  = distance from extreme compression fiber to centroid of tension reinforcement, in.

$c$  = distance from extreme compression fiber to the neutral axis, in.

$d_f$  = effective depth of FRP flexural reinforcement, in.

$E_s$  = modulus of elasticity of steel, psi

$f_y$  = yield strength of nonprestressed steel reinforcement, psi

$\alpha_1$  = multiplier on  $f'_c$  to determine intensity of an equivalent rectangular stress distribution for concrete

$f'_c$  = compressive strength of concrete, psi

$\beta_1$  = ratio of depth of equivalent rectangular stress block to depth of neutral axis.

$b$  = width of compression face of member, in.

$c$  = distance from extreme compression fiber to the neutral axis, in.

$A_s$  = area of nonprestressed steel reinforcement, in.<sup>2</sup>

$f_s$  = stress in nonprestressed

$A_f$  = area of FRP external reinforcement, in.<sup>2</sup>

$f_{fe}$  = effective stress in the FRP, psi

An initial value for  $c$  is first assumed and the strains and stresses are calculated using Eq. 3.8, 3.9, 3.14, and 3.15. A revised value for the depth of neutral axis,  $c$ , is then calculated from Eq. 3.16. The calculated and assumed values for  $c$  are then compared. If they agree, then the proper value of  $c$  is reached. If the calculated and assumed values do not agree, another value for  $c$  is selected, and the process is repeated until convergence is attained. The nominal flexural strength of the section with FRP external reinforcement is computed from Eq. 3.17. The recommended value of  $\Psi_f$  is 0.85.

$$M_n = A_s f_s \left( d - \frac{\beta_1 c}{2} \right) + \Psi_f A_f f_{fe} \left( d_f - \frac{\beta_1 c}{2} \right) \quad \text{Eq. 3.17}$$

$A_s$  = area of nonprestressed steel reinforcement, in.<sup>2</sup>

$f_s$  = stress in nonprestressed steel reinforcement, psi

$d$  = distance from extreme compression fiber to centroid of tension reinforcement, in.

$\beta_1$  = ratio of depth of equivalent rectangular stress block to depth of neutral axis.

$c$  = distance from extreme compression fiber to the neutral axis, in.

$\Psi_f$  = FRP strength reduction factor (0.95 for U-wraps and 0.85 for three-sided or two-sided wraps)

$A_f$  = area of FRP external reinforcement, in.<sup>2</sup>

$f_{fe}$  = effective stress in the FRP, psi

$d_f$  = effective depth of FRP flexural reinforcement, in.

The stress in the steel reinforcement can be calculated based on a cracked-section analysis of the FRP-strengthened reinforced concrete section, as indicated by Eq. 3.18.

$$f_{s,s} = \frac{\left[ M_s + \varepsilon_{bi} A_f E_f \left( d_f - \frac{kd}{3} \right) \right] (d - kd) E_s}{\left[ A_s E_s \left( d - \frac{kd}{3} \right) + A_f E_f \left( d_f - \frac{kd}{3} \right) (d_f - kd) \right]} \quad \text{Eq. 3.18}$$

$f_{s,s}$  = stress in nonprestressed steel reinforcement at service loads, psi

$M_s$  = service moment at section, in.-lb.

$\varepsilon_{bi}$  = strain in substrate at time of FRP installation (tension is positive), in./in.

$A_f$  = area of FRP external reinforcement, in.<sup>2</sup>

$E_f$  = tensile modulus of elasticity of FRP, psi

$d_f$  = effective depth of FRP flexural reinforcement, in.

$kd$  = depth from top fo member to neutral axis, in.

$d$  = distance from extreme compression fiber to centroid of tension reinforcement, in.

$E_s$  = modulus of elasticity of steel, psi

$A_s$  = area of nonprestressed steel reinforcement, in.<sup>2</sup>

$d_f$  = effective depth of FRP flexural reinforcement, in.

The depth to the neutral axis at service,  $kd$ , can be computed by taking the first moment of the areas of the transformed section as shown in Figure 37. The transformed area of the FRP may be obtained by multiplying the area of FRP by the modular ratio of FRP to concrete.

The stress in the steel under service loads computed from Eq. 3.18 should be compared against the limits described in 10.2.8 of ACI 440.2R-17. The value of  $M_s$  from Eq. 3.18 is equal to the moment due to all sustained loads (dead loads and the sustained portion of the live load) plus the maximum moment induced in a fatigue loading cycle.

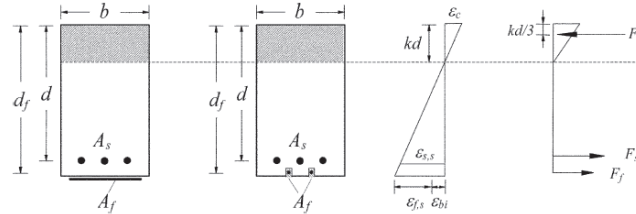


Figure 37: ACI 440.2R-17-Elastic stress and strain distribution

The stress in the FRP reinforcement can be computed using Eq. 3.19 with  $f_{s,s}$  from Eq. 3.18.

$$f_{f,s} = f_{s,s} \left( \frac{E_f}{E_s} \right) \left( \frac{d_f - kd}{d - kd} \right) - \varepsilon_{bi} E_f \quad \text{Eq. 3.19}$$

The stress in the FRP under service loads computed from Eq. 3.19 should be compared against the limits described in 3.18.

The following assumptions are made in calculating the flexural resistance of a prestressed section strengthened with an externally applied FRP system:

- a) Strain compatibility can be used to determine strain in the externally bonded FRP, strain in the nonprestressed steel reinforcement, and the strain or strain change in the prestressing steel.
- b) Additional flexural failure mode controlled by prestressing steel rupture should be investigated.
- c) For cases where the prestressing steel is draped or harped, several sections along the span of the member should be evaluated to verify strength requirements.
- d) The initial strain of the concrete substrate,  $\varepsilon_{bi}$ , should be calculated and excluded from the effective strain in the FRP.

Chapter 11 expands on shear strengthening with FRP, beginning with wrapping schemes. Orienting FRP fibers transverse to the axis of the member or perpendicular to potential shear cracks is effective in providing additional shear strength (Sato, Ueda, Kakuta, & Tanaka, 1996).

In beam applications where an integral slab makes it impractical to wrap the member completely, the shear strength can be improved by wrapping the FRP system around three sides (U-wrap) or bonding to two opposite sides of the member as illustrated in Figure 38. Although all three

techniques have been shown to improve the shear strength of a rectangular member, completely wrapping the section is the most efficient, followed by the three-sided U-wrap. Bonding to two sides of a beam is the least efficient scheme.

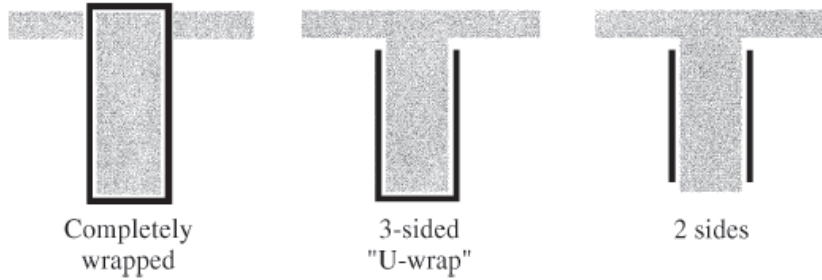


Figure 38: ACI 440.2R-17 wrapping schemes

Design shear strength should exceed the required shear strength:

$$\phi V_n \geq V_u \quad \text{Eq. 3.20}$$

$$\phi V_n = \phi(V_c + V_s + \Psi_f V_f) \quad \text{Eq. 3.21}$$

$V_n$  = nominal shear strength, lb

$V_u$  = required shear strength, lb

$V_c$  = nominal shear strength provided by concrete with steel flexural reinforcement, lb

$V_s$  = nominal shear strength provided by steel stirrups, lb

$\Psi_f$  = FRP strength reduction factor

$V_f$  = nominal shear strength provided by FRP stirrups, lb

where  $V_c$  and  $V_s$  are the concrete and internal reinforcing steel contributions to shear capacity (respectively) according to ACI 318.

$\Psi_f = 0.95$  for completely wrapped members

$\Psi_f = 0.85$  for completely wrapped members

The contribution of the FRP system to shear strength of a member is based on the fiber orientation and an assumed crack pattern (Khalifa, Gold, Nanni, & Aziz M.I., 1998). The shear contribution of the FRP shear reinforcement is then given by Eq. 3.22.

$$V_f = \frac{A_{fv} f_{fe} (\sin \alpha + \cos \alpha) d_{fv}}{s_f} \quad \text{Eq. 3.22}$$

For Rectangular

$$A_{fv} = 2nt_f w_f$$

Eq. 3.23

Sections:

For Circular

$$A_{fv} = \left(\frac{\pi}{2}\right) nt_f w_f$$

Eq. 3.24

Sections:

Note:  $d_{fv}$  is taken as 0.8 times the diameter of the section for circular sections.

The tensile stress in the FRP shear reinforcement at nominal strength is given by Eq. 3.25.

$$f_{fe} = E_f \varepsilon_{fe} \quad \text{Eq. 3.25}$$

- $V_f$  = nominal shear strength provided by FRP stirrups, lb  
 $A_{fv}$  = area of FRP shear reinforcement with spacing  $s$ , in.<sup>2</sup>  
 $f_{fe}$  = effective stress in the FRP; stress attained at section failure, psi  
 $\alpha$  = angle of application of primary FRP reinforcement direction relative to longitudinal axis of member  
 $d_{fv}$  = effective depth of FRP shear reinforcement, in.  
 $s_f$  = center-to-center spacing of FRP strips, in.  
 $n$  = number of FRP strips  
 $t_f$  = nominal thickness of one ply of FRP reinforcement, in.  
 $w_f$  = width of FRP reinforcing plies, in.  
 $E_f$  = tensile modulus of elasticity of FRP, psi  
 $\varepsilon_{fe}$  = effective strain in FRP reinforcement attained at failure, in./in.

The maximum strain used for design should be limited to the effective strain given in Table 2.

Table 2: ACI effective strain (ACI Committee 440, 2017)

ACI Reference	Equation	Failure Mode	Eq. Number
11.4.1.1 Completely wrapped members	$\varepsilon_{fe} = 0.004$ $\leq 0.75\varepsilon_{fu}$	Maximum design shear limited to 0.4%	Eq. 3.26
11.4.1.2 Bonded U-wraps or bonded face plies (two- and three-sided wraps)	$\varepsilon_{fe} = \kappa_v \varepsilon_{fu} \leq 0.004$	Delamination occurs before the loss of aggregate interlock.	Eq. 3.27

where  $\kappa_v$  is the bond-reduction coefficient; it is a function of concrete strength, wrapping scheme, and laminate stiffness.

- $\varepsilon_{fe}$  = effective strain in FRP reinforcement attained at failure, in./in.  
 $\varepsilon_{fu}$  = design rupture strain of FRP reinforcement, in./in.

For bonded U-wraps or bonded face plies:

$$\kappa_v = \frac{k_1 k_2 L_e}{468 \varepsilon_{fu}} \text{ (in.-lb) (Khalifa et al. 1998)} \quad \text{Eq. 3.28}$$

$L_e$  is the active bond length (length over which the majority of the bond stress is maintained).  $k_1$  and  $k_2$  are modification factors that account for concrete strength and wrapping scheme, respectively.

$$L_e = \frac{2500}{(nt_f E_f)^{0.58}} \quad \text{Eq. 3.29}$$

$$k_1 = \left( \frac{f'_c}{4000} \right)^{2/3} \quad \text{Eq. 3.30}$$

$$k_2 = \begin{cases} \frac{d_{fv} - L_e}{d_{fv}} & \text{for three - sided wraps} \\ \frac{d_{fv} - 2L_e}{d_{fv}} & \text{for two - sided wraps} \end{cases} \quad \text{Eq. 3.31}$$

The effective strain in an anchored FRP U-wrap should never exceed the lesser of 0.004 or  $0.75\varepsilon_{fu}$ , and  $\Psi_f = 0.85$ .

Spacing of FRP strips used for shear should adhere to ACI 318 limits for internal steel shear reinforcement. Total shear strength is the sum of the contribution of the FRP shear reinforcement and the steel shear reinforcement; it is limited by the criteria given for steel alone (Eq. 3.32).

$$V_f + V_s \leq 8\sqrt{f'_c}b_wd \quad (\text{in.-lb}) \quad \text{Eq. 3.32}$$

$V_f$  = nominal shear strength provided by FRP reinforcement, lb

$V_s$  = nominal shear strength provided by steel stirrups, lb

$f'_c$  = specified compressive strength of concrete, psi

$b_w$  = web width, in.

$d$  = distance from extreme compression fiber to centroid of tension reinforcement, in.

### 3.2 Japan Society of Civil Engineers (JSCE)

JSCE provides guidelines for the handling and preparation of CFRP materials and surfaces prior to and during construction. Handling instructions, while important for quality control and assurance, do not directly affect the shear or flexure capacity of any type of fiber reinforcing polymer. Figure 39 and Figure 40, respectively, illustrate the flowchart for computing the design strength without and with samples.

The “maximum size” of CFRP used is found using the following procedure:

1. Obtain at least five, 1m samples of the FRP used.
2. Measure the maximum diameter in the two orthogonal directions to the nearest 0.1 mm. Measurements should be taken at both ends and in the center of each test piece.
3. The average maximum diameter of the sample shall be taken as the “maximum size”.

Prior to construction, it is necessary to estimate the “guaranteed capacity” of the CFRP used. The capacity estimation shall be the minimum of the values obtained from at least twenty applicable tests by subtracting three times the standard deviation from the average of the test results of at least 20 test pieces conducted in accordance with JSCE-E 531.”Test Method for Tensile Properties of Continuous Fiber Reinforcing Materials” (rounded to the nearest 100 N). However, JSCE also provides guidelines in the case where samples cannot be taken from existing



structures. Figure 38 and Figure 39 illustrate this process for structures without and with samples, respectively.  $\gamma_m$  is the material factor that depends on the design criteria listed in Table 3 and Table 4 for CFRP sheet and strands, respectively.

The JSCE design criteria for CFRP sheet depends on the following factors:

- Breakage of CFRP after yielding of steel reinforcement
- Crushing of concrete after yielding of steel reinforcement
- Crushing of concrete
- Anchorage failure of CFRP
- Interfacial fracture of the CFRP to concrete due to the flexural and shear cracking.

However, the above factors can only be achieved so long as there is no peel-off failure in the CFRP sheet.

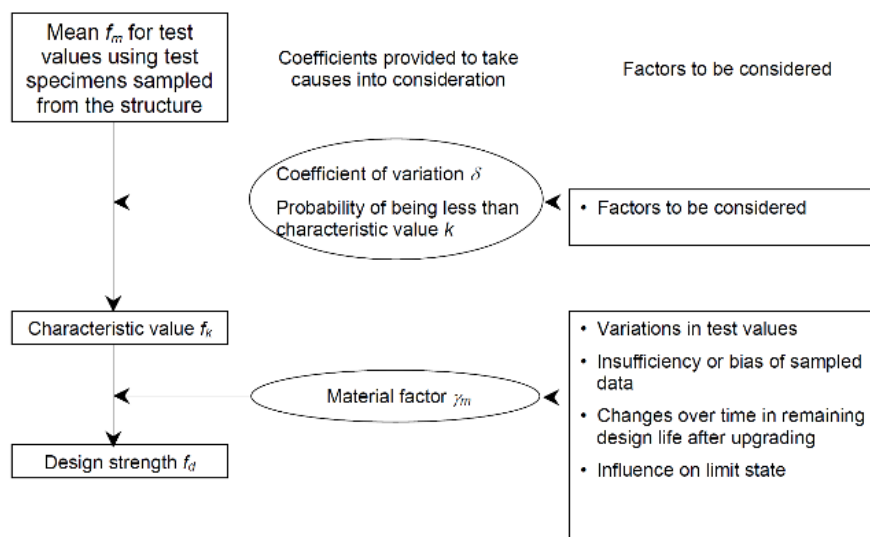
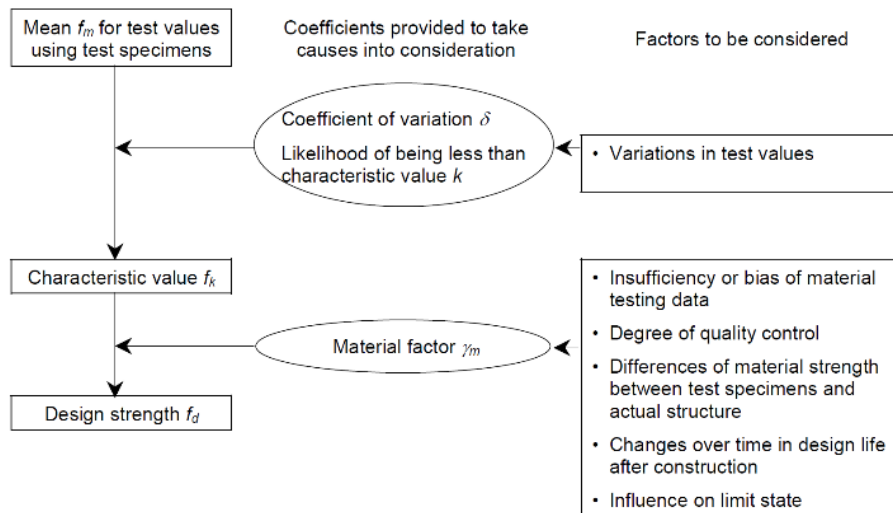


Table 3: JSCE material factor for CFRP sheets

Consideration	Material Factor ( $\gamma_m$ )
Safety and Restorability	1.2-1.3
Serviceability	1.0

Table 4: JSCE material factor for CFRP strands

Consideration	Material Factor ( $\gamma_m$ )
Safety and Restorability	1.2-1.3
Serviceability	1.0

Peel-off failure will not occur if the following equation is satisfied:

$$\sigma_f \leq \sqrt{\frac{2G_f E_f}{t_f n_f}} \quad \text{Eq. 3.33}$$

$\sigma_f$  = Stress of CFRP at location of flexural cracking caused by the maximum bending moment.

$n_f$  = Number of plies of continuous fiber sheets

$E_f$  = Modulus of elasticity for continuous fiber sheet (N/mm<sup>2</sup>)

$t_f$  = Thickness of one layer of continuous fiber sheet (mm)

$G_f$  = Interfacial fracture energy between continuous fiber sheet and concrete (N/mm)

If peel-off failure does not occur, the design flexural capacity and axial load-carrying capacity of the member may be determined using the same method used for standard reinforced concrete members.

If the equation used to determine if peel-off failure will occur is not satisfied but the member does not fail from CFRP peel-off, then the flexural capacity and axial load-carrying capacity of the member may be calculated by multiplying the peel-off failure equation for  $\sigma_f$  by a reduction factor of 0.9.

If the member fails from CFRP peel-off, the flexural capacity and axial load-carrying capacity of the member may be calculated using the following equation:

$$\Delta\sigma_f \leq \sqrt{\frac{2G_f E_f}{t_f n_f}} \quad \text{Eq. 3.34}$$

$\Delta\sigma_f$  = Maximum value of the difference in tensile stresses in the continuous fiber sheet between the flexural cracking locations due to the maximum bending moment (N/mm<sup>2</sup>).

$n_f$  = Number of plies of continuous fiber sheets

$E_f$  = Modulus of elasticity for continuous fiber sheet (N/mm<sup>2</sup>)

$t_f$  = Thickness of one layer of continuous fiber sheet (mm)

$G_f$  = Interfacial fracture energy between continuous fiber sheet and concrete (N/mm)

The design shear capacity of members reinforced with CFRP sheets ( $V_{fyd}$ ) may be expressed as the sum of the contribution from concrete ( $V_{cd}$ ), the contribution from steel ( $V_{sd}$ ) and the contribution from the CFRP sheets ( $V_{fd}$ ).

$$V_{fyd} = V_{cd} + V_{sd} + V_{fd} \quad \text{Eq. 3.35}$$

$V_{cd}$  = Design shear contribution from concrete

$$V_{cd} = \beta_d \beta_p \beta_n f_{vcd} b_w \left( \frac{d}{\gamma_b} \right)$$

$$f_{vcd} = 0.20^3 \sqrt{f'_{cd}} \text{ (N/mm}^2\text{)}, \text{ however, } f_{vcd} \leq 0.72 \text{ (N/mm}^2\text{)}$$

$$\beta_d = \sqrt[4]{\frac{1}{d}} \text{ (d:m)}, 1.5 \text{ when } \beta_d > 1.5$$

$$\beta_p = \sqrt[3]{100p_w} \text{ (d:m)}, 1.5 \text{ when } \beta_p > 1.5$$

$$\beta_n = \begin{cases} 1 + \frac{M_o}{M_d} (N'_d \geq 0), 1.5 \text{ when } \beta_n > 2.0 \\ 1 + \frac{2M_o}{M_d} (N'_d \geq 0), 1.5 \text{ when } \beta_n > 0 \end{cases}$$

$N'_d$  = Design axial compressive force

$M_d$  = Design bending moment

$M_o$  = Decompression moment

$b_w$  = Web width

$d$  = Effective depth

$$p_w = \frac{A_s}{b_w d}$$

$A_s$  = Cross-sectional area of reinforcing bars in tension

$f'_{cd}$  = Design compressive strength of concrete (N/mm<sup>2</sup>)

$\gamma_b$  = Member factor (Typically,  $\gamma_b = 1.3$ )

$V_{sd}$  = Design shear contribution from shear reinforcing bars

$A_w$  = Total cross-sectional area of shear reinforcement in space  $s_s$

$f_{wyd}$  = Design tension yield strength of shear reinforcement (400 N/mm<sup>2</sup> max.)

$\alpha_s$  = Angle formed by shear reinforcement about the member axis

$s_s$  = Spacing of shear reinforcement

$z$  = Lever arm length =  $d/1.15$  (typ.)

$\gamma_b$  = Member factor = 1.15 (typ.)

$V_{fd}$  = Design shear contribution from continuous fiber sheets obtained by *Method (1)* or *(2)* (as follows):

(1) Coefficient expressing the shear reinforcing efficiency of the continuous fiber sheet is used to evaluate the ultimate mean stress of the sheet and to determine the shear contribution of the sheet

$$V_{fd} = K \left[ \frac{A_f f_{fud} (\sin \alpha_f + \cos \alpha_f)}{s_f} \right] \left( \frac{z}{\gamma_b} \right)$$

$K$  = Shear reinforcing efficiency of CFRP

$A_f$  = Total cross-sectional area of CFRP in space  $s_f$

$s_f$  = Spacing of CFRP sheet

$f_{fud}$  = Design tensile strength of CFRP sheet (N/mm<sup>2</sup>)

$E_f$  = CFRP modulus of elasticity (kN/mm<sup>2</sup>)

$\rho_f$  = Angle formed by CFRP sheet about the member axis

$\gamma_b$  = Member factor = 1.25 (typ.)

(2) Stress distribution of the CFRP sheets is evaluated based on the bond constitutive law to determine the shear contribution of the sheet. This method uses numerical calculation based on five hypothesis (Japan Society of Civil Engineers, 2001) to evaluate the stress distribution of the CFRP that are illustrated in Figure 41.

The following assumptions must be made to perform a stress analysis during the determination of CFRP shear capacity:

- Cracked concrete is a rigid body.
- CFRP sheets are elastic bodies.

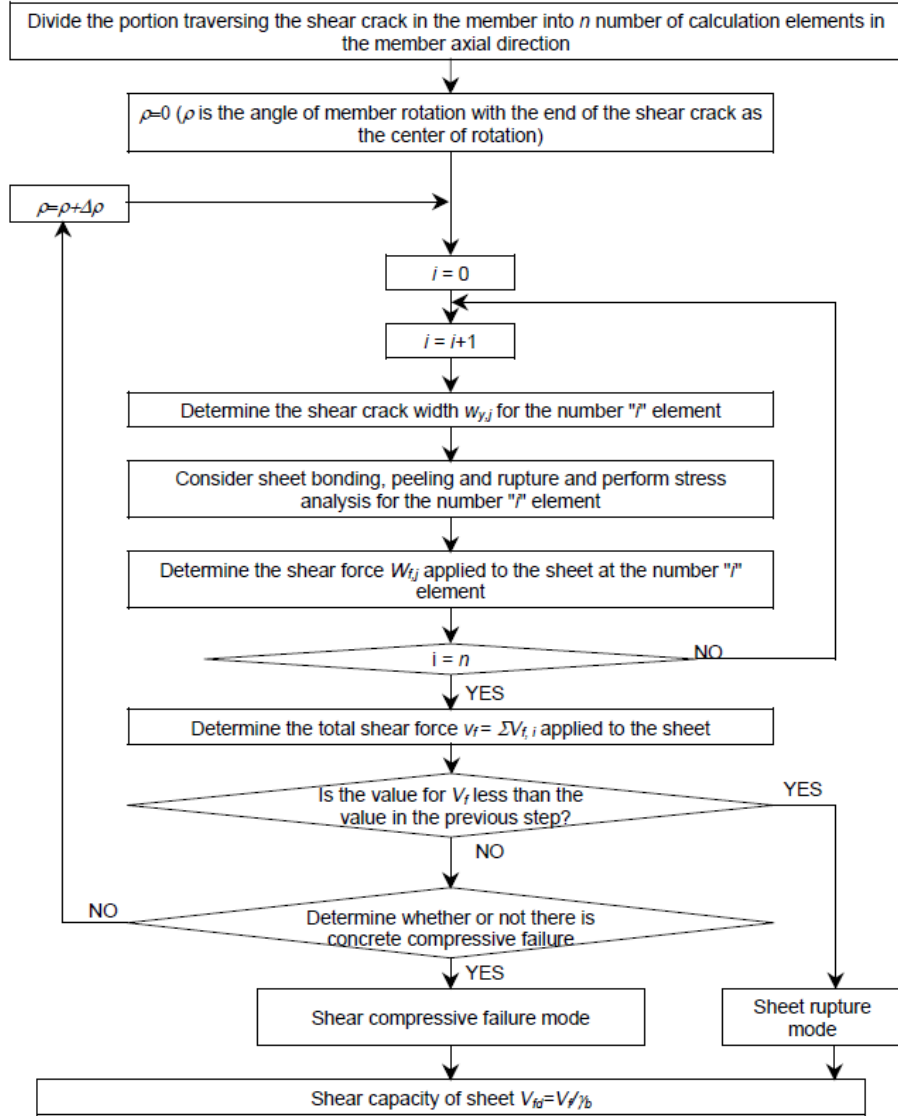


Figure 41: CFRP wrap shear capacity (JSCE, 2001)

A three-stage progression of CFRP peel-off failure is provided in *JSCE: Recommendations for Upgrading of Concrete Structures with Use of Continuous Fiber Sheets* based on crack width and tensile strength during loading. If member deformation progresses and the applied CFRP sheet(s) break(s), the total shear force supported by the sheet(s),  $V_f$ , begin(s) to decline. In such cases, the member failure mode is sheet rupture.

If member deformation has progressed without CFRP rupture, the failure mode is concrete compression failure (see Figure 42). The compressive edge strain,  $\varepsilon'_b$ , of the concrete should be calculated with the following equation:

$$\varepsilon'_b = \rho \sqrt{y_e/d} \quad \text{Eq. 3.36}$$

The compressive strain of the concrete during compression failure should be set to equal 0.0025. The value of  $V_f$  is the ultimate shear force experienced by the CFRP sheet(s) when compression failure occurs.

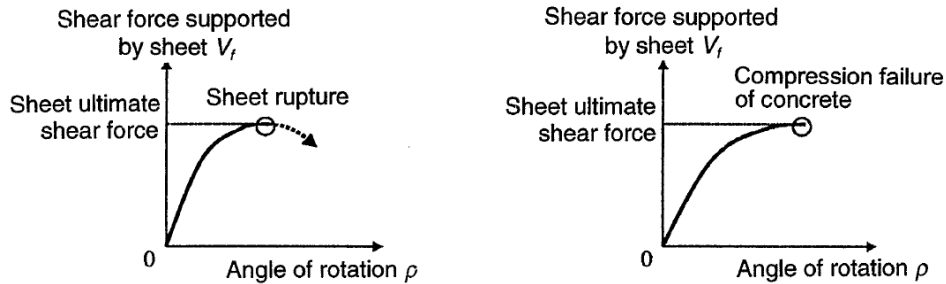


Figure 42: JSCE Fig. C6.4.6-Failure mode and shear capacity

When CFRP sheets are bonded to the sides of girders for shear reinforcement, mechanical anchoring (i.e., anchor bolts and anchor plates) should be used. It is necessary to confirm that peel-off failure does not occur between the CFRP sheets and the anchors under the design loads, and that anchor bolt or concrete failure does not occur.

### 3.3 Fédération Internationale du Béton (FIB 14)

Flexural strengthening using FRP is given in Chapter 4 of FIB 14, beginning with the assumption that the slip at the concrete-FRP interface may be ignored (justified for most structural adhesives applied at thicknesses of 1.0-1.5 mm) as illustrated in Figure 43.

- Renders viscoelastic phenomena (i.e., axial and interlaminar shear creep and relaxation) negligible
- Forms basis for ultimate strength limit state analysis of concrete strengthened in flexure

If the service moment ( $M_o$ ) is smaller than the cracking moment ( $M_{cr}$ ),  $M_o$  may be neglected.

The initial situation is described by the following figures and equations:

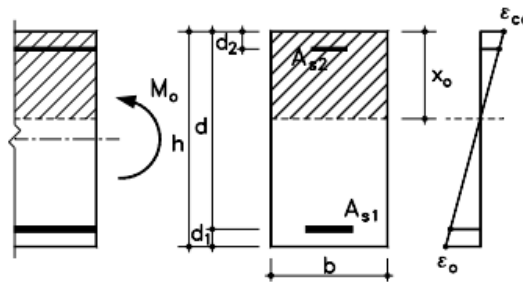


Figure 43: FIB-14 Beam nomenclature

Equation 3.38 can be solved to find the neutral axis depth ( $x_o$ )

$$\frac{1}{2}bx_o^2 + (\alpha_s - 1)A_{s2}(x_o - d_2) = \alpha_s A_{s1}(d - x_o) \quad \text{Eq. 3.37}$$

$\alpha_s = E_s/E_c$   
 $E_c$  = concrete modulus of elasticity  
 $E_s$  = steel modulus of elasticity  
 $b$  = width of member  
 $A_{s1}$  = area of steel reinforcement in tension  
 $A_{s2}$  = area of steel reinforcement in compression  
 $d$  = effective depth of member  
 $d_2$  = distance from centroid of compressive steel to extreme compressive fiber  
 $x_o$  = depth of the compression zone before strengthening

Concrete strain in top fiber

$$\varepsilon_{co} = \frac{M_o x_o}{E_c I_{co}} \quad \text{Eq. 3.38}$$

$M_o$  = Acting moment during strengthening  
 $x_o$  = depth of the compression zone before strengthening  
 $E_c$  = concrete modulus of elasticity  
 $I_{co}$  = moment of inertia of concrete section

Moment of Inertia of Cracked Section

$$I_{co} = \frac{bx_o^3}{3} + (\alpha_s - 1)A_{s2}(x_o - d_s)^2 + \alpha_s A_{s1}(d - x_o)^2 \quad \text{Eq. 3.39}$$

$\alpha_s = E_s/E_c$   
 $E_c$  = Concrete modulus of elasticity  
 $E_s$  = steel modulus of elasticity  
 $b$  = width of member  
 $A_{s1}$  = area of steel reinforcement in tension  
 $A_{s2}$  = area of steel reinforcement in compression  
 $d$  = effective depth of member  
 $d_s$  = diameter of steel reinforcement  
 $x_o$  = depth of the compression zone before strengthening

Concrete strain in extreme tension fiber

$$\varepsilon_o = \varepsilon_{co} \frac{h - x_o}{x_o} \quad \text{Eq. 3.40}$$

$h$  = Member depth  
 $x_o$  = depth of the compression zone before strengthening

Two “classes” of failure modes are outlined in section 4.3 based on ultimate limit states.

1. Full composite action maintained until concrete crushes in compression or the FRP fails in tension.
  - a. Steel yielding followed by concrete crushing
  - b. Steel yielding followed by FRP fracture
  - c. Concrete crushing
2. Composite action lost prior to crushing or FRP tension failure (i.e., peel-off of the FRP).
  - a. Debonding and bond failure modes as illustrated in Figure 44.

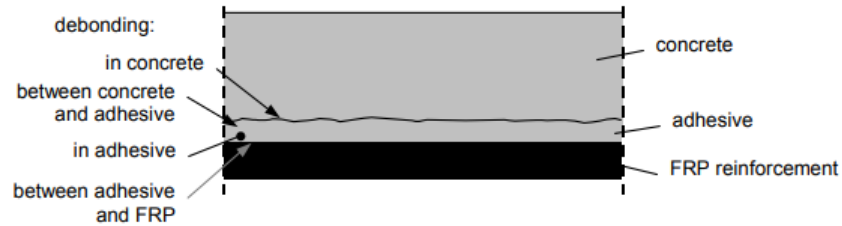


Figure 44: Debonding interfaces (FIB-14, 2001)

The analysis of ultimate limit states is given in section 4.4, starting with steel yielding followed by concrete crushing.

- Most desirable failure types
- Reinforced element may not be fully unloaded during strengthening (initial strain in the extreme tensile fiber must be considered)
- Tensile steel reinforcement must yield and the FRP strain is limited to the ultimate strain.

Equation 3.42 can be solved to find the neutral axis depth ( $x_o$ )

$$0.85\Psi f_{cd}bx + A_{s2}E_s\varepsilon_{s2} = A_{s1}f_{yd} + A_fE_{fu}\varepsilon_f \quad \text{Eq. 3.41}$$

$$\Psi = 0.8$$

$\varepsilon_{s2}$  = strain in compression steel

$\varepsilon_f$  = strain in FRP

$$\varepsilon_{s2} = \varepsilon_{cu} \frac{(x - d_2)}{x}$$

$$\varepsilon_f = \varepsilon_{cu} \frac{(h - x)}{x} - \varepsilon_o$$

$\varepsilon_{cu}$  = ultimate strain in concrete

$\varepsilon_o$  = initial strain at the extreme tension fiber before strengthening

$f_{cd}$  = design value of the concrete compressive strength

$b$  = width of member

$x$  = depth of the compression zone



$A_{s1}$  = area of steel reinforcement in tension  
 $A_{s2}$  = area of steel reinforcement in compression  
 $A_f$  = area of FRP reinforcement  
 $E_s$  = steel modulus of elasticity  
 $E_{fu}$  = FRP modulus of elasticity at ultimate strength  
 $f_{yd}$  = design value of the steel yield strength

The design bending moment capacity can be determine using cross-sectional analysis as illustrated in Figure 45 and the equation below.

$$M_{Rd} = A_{s1}f_{yd}(d - \delta_G x) + A_f E_f \varepsilon_f (h - \delta_G x) + A_{s2} E_s \varepsilon_{s2} (\delta_G x - d_2) \quad \text{Eq. 3.42}$$

$\delta_G = 0.4$  = stress block centroid coefficient  
 $A_{s1}$  = area of steel reinforcement in tension  
 $A_{s2}$  = area of steel reinforcement in compression  
 $A_f$  = area of FRP reinforcement  
 $f_{yd}$  = design value of the steel yield strength  
 $d$  = effective depth of the member  
 $d_2$  = distance from centroid of compressive steel to extreme compression fiber  
 $h$  = member depth  
 $x$  = depth of the compression zone  
 $E_{fu}$  = FRP modulus of elasticity  
 $E_s$  = steel modulus of elasticity  
 $\varepsilon_f$  = strain in FRP  
 $\varepsilon_{s2}$  = strain in compression steel

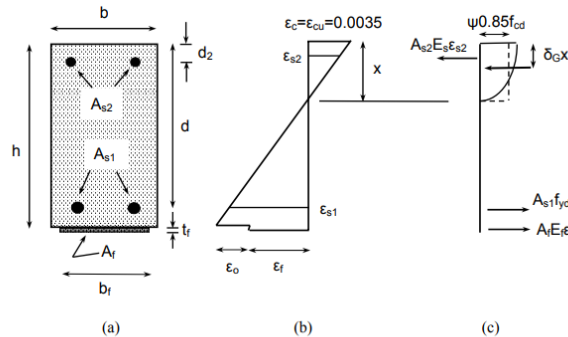


Fig. 4-11: Analysis of cross section for the ultimate limit state in bending: (a) geometry, (b) strain distribution and (c) stress distribution.

Figure 45: FIB-14 Fig. 4-11 Cross-sectional analysis of beam under bending

For steel yielding followed by FRP fracture

- Unlikely since premature FRP debonding often precedes FRP fracture
- Analysis identical to procedure used for *steel yielding followed by concrete crushing* with the following modifications:

$\varepsilon_{cu}$  is replaced by  $\varepsilon_c$   
 $\varepsilon_f$  is replaced by  $\varepsilon_{fud}$

$\Psi$  and  $\delta_G$  given by Eq. 4-11 and 4-12 in, FIB Bulletin 14

For concrete crushing

- Analysis governed by reinforced concrete procedures presiding over applicable jurisdiction

For debonding and bond failure modes

- Occurrence of peel-off is dictated by the vertical crack opening displacement, the flexural and shear rigidity of the FRP, and the tensile strength of the concrete.
- Although analysis equations are provided, it is noted that peel-off caused by shear cracks has not yet been researched to sufficient detail.
- Many design models and approaches exist to analyze peel-off at the end anchorage and at flexural cracks, end shear failure, and peel-off caused by the unevenness of the concrete surface. Most approaches utilize empirical formulas and may be referenced in FIB Bulletin 14 Appendix A.

FIB 14 also outlines serviceability limit states through linear elastic analysis depicted in Figure 46. The neutral axis depth is not independent from the acting moment.

Two analysis states:

1. Cracked

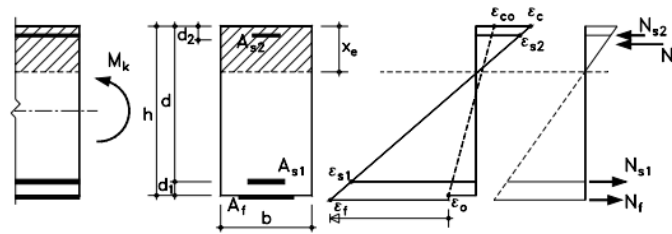


Figure 46: FIB-14 Fig. 4-15 Linear elastic analysis of cracked section

Equation 3.43 can be solved to find the neutral axis depth ( $x_e$ )

$$\frac{1}{2}bx_e^2 + (\alpha_s - 1)A_{s2}(x_e - d_2) = \alpha_a A_{s1}(d - x_e) + \alpha_f A_f \left[ h - \left( 1 + \frac{\epsilon_o}{\epsilon_c} \right) x_e \right] \quad \text{Eq. 3.43}$$

$$\alpha_f = E_f/E_c$$

$$\alpha_s = E_s/E_c$$

$E_c$  = concrete modulus of elasticity

$E_s$  = steel modulus of elasticity

$E_f$  = FRP modulus of elasticity

$b$  = width of member

$A_{s1}$  = area of steel reinforcement in tension

$A_{s2}$  = area of steel reinforcement in compression

$d$  = effective depth of member

$x_e$  = depth of the compression zone from linear elastic analysis

$\varepsilon_o$  = initial strain at the extreme tension fiber before strengthening

For low values of  $\varepsilon_o$ :

$\left(1 + \frac{H_o}{H_c}\right) \approx 1$ , so Eq. 4-19 can be solved for  $x_e$ .

For high values of  $\varepsilon_o$ :

$x_e$  should be solved from Eq. 4-19 and 4-20 found in FIB Bulletin 19.

Moment of inertia of cracked section:

$$I_2 = \frac{bx_e^3}{3} + (\alpha_s - 1)A_{s2}(x_e - d_2)^2 + \alpha_s A_{s1}(d - x_e)^2 + \alpha_f A_f(h - x_e)^2 \quad \text{Eq. 3.44}$$

Cracking Moment:

$$M_{cr} \approx f_{ctm} \left( \frac{bh^2}{6} \right) \quad \text{Eq. 3.45}$$

$f_{ctm}$  = mean value of the concrete tensile strength

$b$  = width of member

$h$  = depth of member

## 2. Uncracked

Analysis performed identical to analysis used for cracked section with the following modifications to the moment of inertia (neglecting the contribution of steel reinforcement):

$$I_1 \approx \frac{bh^3}{12} \quad \text{Eq. 3.46}$$

## Stress Limitation

Under service load conditions, concrete, FRP, and steel stresses must be limited.

Eurocode 2 provides such limitations, which can be referenced in FIB bulletin 14 section 4.6.2.

## Deflection Verification

An accurate but complex method of predicting deflection uses numerical integration of curvature, which is determined by accounting for tension stiffening and by performing a non-linear analysis of the cracked section.

The CEB bilinear method is a simpler, reasonably accurate deflection estimating procedure. According to the CEB method, Eq. 3.49 can be used to predict the mean deflection.

$$a = a_1(1 - \zeta_b) + a_2\zeta_b \quad \text{Eq. 3.47}$$

$$a_1 = k_M l^2 \left( \frac{M_k}{E_c I_1} \right)$$

$$a_2 = k_M l^2 \left( \left( \frac{M_0}{E_c I_{o2}} \right) + \left( \frac{M_k - M_0}{E_c I_2} \right) \right) M_k > M_0$$

$$M_k > M_{cr}: \quad \zeta_b = 0$$

$$M_k > M_{cr}: \quad \zeta_b = 1 - \beta_1 \beta_2 \left( \frac{M_{cr}}{M_k} \right)^{\frac{n}{2}}$$

$k_M$  = coefficient depending on type of loading

$l$  = span length

$M_{cr}$  = cracking moment

$a_1$  and  $a_2$  are the deflections in the uncracked and the fully cracked state, respectively.

$\zeta_b$  is a distribution coefficient

$M_k$  is the characteristic value of moment

$I_1$  = moment of inertia of transformed uncracked section

$I_2$  = moment of inertia of transformed cracked section

According to Eurocode 2:

$\beta_1 = 0.5$  and  $1$  for smooth and deformed steel (respectively)

$\beta_2 = 0.5$  and  $1$  for long-term and short-term loading (respectively).

### Crack Width Verification

For RC beams with FRP, new cracks will appear in between existing cracks, leading to denser cracking and smaller crack widths. The small crack widths make the verification of crack widths not necessary.

### Bond Interface Cracking Verification

Stress concentrations are obtained at the FRP end and crack locations.

Maximum shear stress  $\tau_{f1}$  at the FRP end, calculated according to linear elastic analysis, must be smaller than the characteristic value of the concrete tensile strength  $f_{ctk}$ . Refer to FIB Bulletin 14 section 4.6.5 for one approach to calculating  $\tau_{f1}$ .

If extra anchorage is provided at the FRP end, bond interface cracking verification is no longer necessary.

Chapter 5 of FIB 14 addresses shear and torsion strengthening using FRP. When a concrete member with FRP is loaded to its shear capacity, the FRP is stretched strained in the “principal fiber direction” (also known as effective strain and is denoted by  $\varepsilon_{f,e}$ ) less than the tensile fracture strain  $\varepsilon_{fu}$ . Multiplying  $\varepsilon_{f,e}$  by the elastic modulus of the FRP,  $E_{fu}$ , and the FRP’s cross-sectional area yields the force carried by the FRP at shear failure.

FRP will fail under shear in one of three methods: shear fracture and peel-off, simultaneous shear and FRP fracture, or delayed shear and FRP fracture (see Figure 47 for a visualization of the load as strain increases during each failure method).

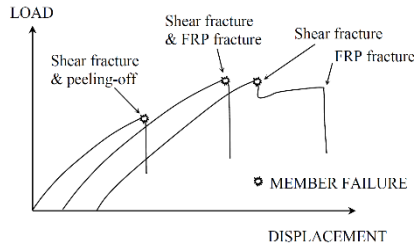


Figure 47: FIB-14 - Failure mode based on load and displacement

Shear capacity of a strengthened member (European Committee for Standardization, 2004)

$$V_{Rd} = \min(V_{cd} + V_{wd} + V_{fd}, V_{Rd2}) \quad \text{Eq. 3.48}$$

Contribution of FRP to shear capacity:

$$V_{fd} = 0.9\varepsilon_{fd,e}E_{fu}\rho_f b_w d (\cot(\theta) + \cot(\alpha)) \sin(\alpha) \quad \text{Eq. 3.49}$$

$\varepsilon_{fd,e}$  = design value of effective FRP strain

$b_w$  = minimum width of cross-section over the effect depth

$d$  = effective depth

$$\rho_f = \text{FRP reinforcement ratio} = \begin{cases} \frac{2t_f \sin(\alpha)}{b_w} & \text{for continuously bonded FRP} \\ \left(\frac{2t_f}{b_w}\right) \left(\frac{b_f}{s_f}\right) & \text{for FRP strips or sheets} \end{cases}$$

$s_f$  = FRP spacing as illustrated in Figure 48

$E_{fu}$  = FRP modulus of elasticity

$\theta = 45^\circ$  = angle of diagonal crack with respect to the member axis

$\alpha$  = angle between principal fiber orientation and longitudinal axis of member

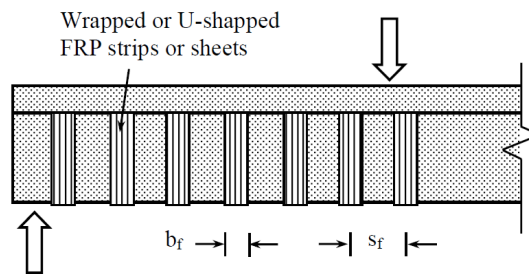


Figure 48: FIB-14 FRP shear reinforcement nomenclature

The design value of the effective FRP strain:

$$\frac{\varepsilon_{fk,e}}{\gamma_f} \quad \text{Eq. 3.50}$$

$$\begin{aligned} \varepsilon_{fk,e} &= k\varepsilon_{f,e} \\ \varepsilon_{f,e} &= \text{effective FRP strain} \\ k &= 0.8 = \text{reduction factor} \\ \gamma_f &= \begin{cases} \text{see Figure 49 if FRP fracture controls} \\ 1.3 \text{ if debonding failure (peel – off) controls} \end{cases} \end{aligned}$$

FRP type	Application type A <sup>(1)</sup>	Application type B <sup>(2)</sup>
CFRP	1.20	1.35
AFRP	1.25	1.45
GFRP	1.30	1.50

<sup>(1)</sup> Application of prefab FRP EBR systems under normal quality control conditions. Application of wet lay-up systems if all necessary provisions are taken to obtain a high degree of quality control on both the application conditions and the application process.

<sup>(2)</sup> Application of wet lay-up systems under normal quality control conditions. Application of any system under difficult on-site working conditions.

Figure 49: FIB-14 FRP Material Safety Factors

Assuming effective FRP strain is larger than the yield strain of internal steel reinforcement, the following equations may be used to find the effective FRP strain:

$$\text{Fully Wrapped:} \quad \varepsilon_{f,e} = 0.17 \left( \frac{f_{cm}^2}{E_{fu}\rho_f} \right)^{0.30} \varepsilon_{fu} \quad \text{Eq. 3.51}$$

$$\text{U-Wrapped or Two-sided:} \quad \varepsilon_{f,e} = \min \begin{cases} 0.65 \left( \frac{f_{cm}^2}{E_{fu}\rho_f} \right)^{0.56} * 10^{-3} \\ 0.17 \left( \frac{f_{cm}^2}{E_{fu}\rho_f} \right)^{0.30} \varepsilon_{fu} \end{cases} \quad \text{Eq. 3.52}$$

$f_{cm}$  = Mean concrete compressive strength

$E_{fu}$  = FRP modulus of elasticity

$\rho_f$  = FRP reinforcement ratio

$\varepsilon_{fu}$  = Ultimate FRP strain

Note: The above equations were derived based on metric units (MPa for  $f_{cm}$  and GPa for  $E_{fu}$ )

If vertical FRP strips are used, their spacing should adhere to the following limits:

Rectangular Cross-sections:	$s_f \leq 0.9d - \frac{b_f}{2}$	Eq. 3.53
T-beams (i.e., bridge girder):	$s_f \leq d - h_f - \frac{b_f}{2}$	Eq. 3.54

FRP reinforcement is also limited by serviceability criteria:

$$\varepsilon_{fk,e} \leq \frac{0.8f_{yk}}{E_s} \quad \text{Eq. 3.55}$$

$\varepsilon_{fk,e}$  = Design FRP strain

$f_{yk}$  = Steel yield strength

$E_s$  = Steel modulus of elasticity

Note: if provided, manufacturer criteria should be used.

### 3.4 Florida Department of Transportation (FDOT SDM Volume 4)

Chapter 4 of FDOT's *Structural Design Manual* explains the department's requirements and modifications to ACI 440.2R-17 regarding structural strengthening using carbon fiber reinforced Polymer (CFRP), which are summarized in Table 5.

- Primary Reinforcement: carbon (CFRP).
- Resin and adhesive must be a thermoset epoxy formulation specifically designed to be compatible with the fibers or pre-cured shapes (if a pre-cured laminate or wet layup system is used).
- Maximum number of reinforcement layers: 3 (except as required for anchorages).
- ACI 440.2R-17 should be referenced for all design except as noted herein.
- All loads should be obtained using AASHTO LRFD.

Table 5: FDOT SDM vol. 4 modifications to ACI 4040.2R-17

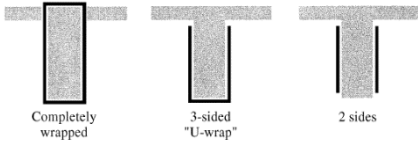
Modified Section	ACI 440.2R-17 Equation	FDOT SDM Volume 4 Equation/Modification	Definitions
Section 9.2	<p>When <math>S_{DL}</math> is not likely to be present for a sustained period of time:</p> $(\phi R_n)_{Existing} \geq (1.1S_{DL} + 0.75S_{LL})$ <p>When <math>S_{DL}</math> is likely to be present for a sustained period of time:</p> $(\phi R_n)_{Existing} \geq (1.1S_{DL} + 1.0S_{LL})$	<p>When strengthening a single girder in a span containing <math>\geq 4</math> similar girders:</p> $(\phi R_n)_{Existing} \geq (1.1S_{DL} + 0.75S_{LL})$ <p>When multiple girders in a single span are strengthened:</p> $(\phi R_n)_{Existing} \geq (1.1S_{DL} + 1.0S_{LL})$	<ul style="list-style-type: none"> <li>• <math>(\phi R_n)_{Existing}</math> = capacity of the member considering ONLY the existing reinforcement.</li> <li>• <math>S_{DL}</math> and <math>S_{LL}</math> = unfactored dead load and live load effects, respectively, that occur after the member has been strengthened</li> </ul>

Table 5: FDOT SDM vol. 4 modifications to ACI 4040.2R-17

Modified Section	ACI 440.2R-17 Equation	FDOT SDM Volume 4 Equation/Modification	Definitions																								
Section 9.4	<table border="1" data-bbox="391 327 760 562"> <caption>Table 9.1—Environmental reduction factor for various FRP systems and exposure conditions</caption> <thead> <tr> <th>Exposure conditions</th> <th>Fiber type</th> <th>Environmental reduction factor <math>C_E</math></th> </tr> </thead> <tbody> <tr> <td rowspan="3">Interior exposure</td> <td>Carbon</td> <td>0.95</td> </tr> <tr> <td>Glass</td> <td>0.75</td> </tr> <tr> <td>Aramid</td> <td>0.85</td> </tr> <tr> <td rowspan="3">Exterior exposure (bridges, piers, and unenclosed parking garages)</td> <td>Carbon</td> <td>0.85</td> </tr> <tr> <td>Glass</td> <td>0.65</td> </tr> <tr> <td>Aramid</td> <td>0.75</td> </tr> <tr> <td rowspan="3">Aggressive environment (chemical plants and wastewater treatment plants)</td> <td>Carbon</td> <td>0.85</td> </tr> <tr> <td>Glass</td> <td>0.50</td> </tr> <tr> <td>Aramid</td> <td>0.70</td> </tr> </tbody> </table>	Exposure conditions	Fiber type	Environmental reduction factor $C_E$	Interior exposure	Carbon	0.95	Glass	0.75	Aramid	0.85	Exterior exposure (bridges, piers, and unenclosed parking garages)	Carbon	0.85	Glass	0.65	Aramid	0.75	Aggressive environment (chemical plants and wastewater treatment plants)	Carbon	0.85	Glass	0.50	Aramid	0.70	Use an environment reduction factor $C_E = 0.85$ for bridge applications.	<ul style="list-style-type: none"> <li>• <math>C_E</math> = environment reduction factor</li> </ul>
Exposure conditions	Fiber type	Environmental reduction factor $C_E$																									
Interior exposure	Carbon	0.95																									
	Glass	0.75																									
	Aramid	0.85																									
Exterior exposure (bridges, piers, and unenclosed parking garages)	Carbon	0.85																									
	Glass	0.65																									
	Aramid	0.75																									
Aggressive environment (chemical plants and wastewater treatment plants)	Carbon	0.85																									
	Glass	0.50																									
	Aramid	0.70																									
Sec. 10.2.8/10.3.1.4	<p>Stress in steel under service load limited to:</p> $f_{s,s} \leq 0.80f_y \text{ (Eq. 10-6)}$ $f_{ps,s} \leq 0.82f_{py} \text{ (Eq. 10-20a)}$ $f_{ps,s} \leq 0.74f_{pu} \text{ (Eq. 10-20b)}$	Check stresses in existing reinforcement (using Eqs. 10-6 or 10-20a/b) using Service I Load Combination from LRFD.	<ul style="list-style-type: none"> <li>• <math>f_{s,s}</math> = stress in steel</li> <li>• <math>f_y</math> = yield strength of steel</li> <li>• <math>f_{ps,s}</math> = stress in prestressed steel</li> <li>• <math>f_{py}</math> = yield strength of prestressed steel</li> <li>• <math>f_{pu}</math> = ultimate strength of prestressed steel</li> </ul>																								
Sec. 10.2.9/10.3.1.5	<p>Stress in the FRP reinforcement computed using elastic analysis and an applied moment due to all sustained loads plus the max. moment induced in a fatigue loading cycle. The sustained stress is limited to:</p> $f_{f,s} \leq 0.55f_{fu}$	Use the standard fatigue truck from LRFD to check fatigue stresses in CFRP composites. Check allowable fatigue stresses in prestressing or mild steel using Ch. 5 of the LRFD.	<ul style="list-style-type: none"> <li>• <math>f_{f,s}</math> = sustained stress plus cyclic fatigue stress in FRP</li> <li>• <math>f_{fu}</math> = ultimate strength of FRP</li> </ul>																								
Sec. 10.2.10	<p>Stress in FRP:</p> $f_{fe} = E_f \varepsilon_{fe}$ <p>Stress in Steel:</p> $f_s = E_s \varepsilon_s \leq f_y$ <p>Strain in FRP (Eq. 10-3):</p> $\varepsilon_{fe} = \varepsilon_{cu} \left( \frac{d_f - c}{c} \right) - \varepsilon_{bi} \leq \varepsilon_{fd}$	Calculate strength of non-prestressed concrete repaired with CFRP using Section 10.2.10. Strain in the CFRP at ultimate capacity shall not exceed the bond critical limit (Eq. 10-3).	<ul style="list-style-type: none"> <li>• <math>E_f</math> = FRP Elas. Mod.</li> <li>• <math>\varepsilon_{fe}</math> = FRP Strain</li> <li>• <math>E_s</math> = Steel Elas. Mod.</li> <li>• <math>\varepsilon_s</math> = Steel Strain</li> <li>• <math>\varepsilon_{cu}</math> = ultimate strain of unconfined concrete</li> <li>• <math>d_f</math> = FRP Eff. Depth</li> <li>• <math>c</math> = dist. from extreme comp. fiber to neutral axis</li> <li>• <math>\varepsilon_{bi}</math> = concrete strain at time of FRP install.</li> <li>• <math>\varepsilon_{fd}</math> = FRP debond. strain</li> </ul>																								



Table 5: FDOT SDM vol. 4 modifications to ACI 4040.2R-17

Modified Section	ACI 440.2R-17 Equation	FDOT SDM Volume 4 Equation/Modification	Definitions
Sec. 10.3.1	Strain in FRP (Eq. 10-16): $\epsilon_{fe} = \epsilon_{cu} \left( \frac{d_f - c}{c} \right) - \epsilon_{bi} \leq \epsilon_{fd}$	Calculate strength of prestressed concrete repaired with CFRP using equil. and strain compatibility. Strain in the CFRP at ultimate capacity shall not exceed the bond critical limit (Eq. 10-16).	<ul style="list-style-type: none"> <li>• <math>\epsilon_{cu}</math> = ultimate strain of unconfined concrete</li> <li>• <math>d_f</math> = FRP Eff. Depth</li> <li>• <math>c</math> = dist. from extreme comp. fiber to neutral axis</li> <li>• <math>\epsilon_{bi}</math> = concrete strain at time of FRP install.</li> <li>• <math>\epsilon_{fd}</math> = FRP debond. strain</li> </ul>
Chapter 11		Shear strengthening using FRP restricted to complete wrapping or three-sided  U-wrapping. If U-wrapping is used, the termination of the wrap must be anchored to prevent debonding.	N/A
Chapter 13	Area of the transverse clamping FRP U-wrap reinforcement: $A_{fanchor} = \frac{(A_f f_{fu})_{longitudinal}}{(E_f \kappa_v \epsilon_{fu})_{anchor}}$	Place transverse CFRP reinforcement at the termination points of each ply of CFRP and from end to end of the CFRP at a max. spacing of $d$ .  Width of the transverse reinforcement $\geq \frac{3}{4}d$ along the member axis. Intermediate transverse reinforcement $\geq \frac{d}{4}$	<ul style="list-style-type: none"> <li>• <math>A_f</math> = area of FRP external reinforcement</li> <li>• <math>f_{fu}</math> = ultimate strength of FRP</li> <li>• <math>E_f</math> = FRP Elas. Mod.</li> <li>• <math>\kappa_v</math> = bond-dependent coefficient for shear</li> <li>• <math>\epsilon_{fu}</math> = Design FRP rupture strain</li> </ul>

### 3.5 Canadian Standards Association (CSA S806-12)

The CSA Design Guide (Canadian Standards Association, 2012) is a comprehensive resource that describes usage and properties of FRP and outlines design of members with FRP reinforcement. The guide is comparable to ACI 440.2R-17 in that it speaks direct to FRP reinforcement design through equations based on proven research.

Chapter 8 of CSA S806-12 provides design guidance for composite/fiber-based reinforcing bars. While material property equations are applicable to projects using FRP wraps, equations for flexural and shear strength are not relevant. Instead, Chapter 11, *Strengthening of Concrete Masonry and Steel Components with FRP*, must be referenced.

Design requirements for concrete beam strengthening are outlined in section 11.3. Concrete beams strengthened with FRP laminates, including near-surface anchors, can be analyzed using the following equations. The code states that if the clear cover is less than 20 mm, FRP reinforcing bars shall not be used. A perfect bond is assumed to exist between concrete, steel, and FRP laminates.

The maximum strain in the extreme compression fiber is assumed to be 0.0035, while the maximum tensile strain in the FRP laminate shall not exceed 0.007:

$$\varepsilon_{f,max} = 0.41 \sqrt{\frac{f'_c}{n_F E_F t_F}} \leq 0.007 \quad \text{Eq. 3.56}$$

$\varepsilon_{f,max}$  = Maximum tensile strain in the FRP laminate

$f'_c$  = Concrete compressive strength

$n_F$  = Number of plies of FRP

$t_F$  = Nominal thickness of one ply of FRP

$E_F$  = FRP modulus of elasticity

Stresses are calculated based on a linear elastic analysis. The specification considers the following failure modes during design:

- Concrete crushing prior to rupture of the FRP or yielding of the reinforcing steel.
- Yielding of the steel and/or rupture of the FRP followed by concrete crushing.
- Shear/tension failure of concrete substrate around the FRP termination point
- Debonding of adhesive

$$f_F = E_f(\varepsilon_F - \varepsilon_{ci}) \quad \text{Eq. 3.57}$$

$f_F$  = FRP stress

$E_f$  = FRP modulus of elasticity

$\varepsilon_F$  = Tensile strain at level of FRP under factored loads

$\varepsilon_{ci}$  = Initial concrete strain at FRP level

$l_a$  is the anchorage length at where no further strengthening is required:

$$l_a = \sqrt{\frac{n_F E_F t_F}{\sqrt{f'_c}}}$$

$n_F$  = Number of plies of FRP

$E_f$  = FRP modulus of elasticity

$t_F$  = Nominal thickness of one ply of FRP

$f'_c$  = Concrete compressive strength

If  $l_a < 300$  mm, the FRP must be anchored using a system with test-verified strength under simulated field conditions.

Beams with a total depth less than 300 mm shall not be strengthened for shear unless the beam is fully wrapped, or a proven anchorage system is used to develop necessary design strength of the externally bonded FRP shear reinforcement.

Factored shear resistance of the reinforced beam:

$$V_f = V_c + V_s + V_F \leq 0.25\phi_c f'_c b_w d_v \quad \text{Eq. 3.58}$$

$V_f$  = Shear resistance capacity

$V_c$  and  $V_s$  are calculated using *CAN/CSA-A23.3*

$V_F$  = Contribution of the FRP to the shear resistance of the retrofitted beam

$\phi_c$  = Resistance factor of concrete

$f'_c$  = Concrete compressive strength

$b_w$  = Beam web width

$d_v$  = Effective shear depth for internal steel

$$= \max \begin{cases} 0.9d \\ 0.72h \end{cases}$$

Contribution of the FRP to the shear resistance of the retrofitted beam:

$$V_F = \frac{\phi_F A_F E_F \varepsilon_F d_v (\cot \theta + \cot \alpha_F) \sin \alpha_F}{s_F} \quad \text{Eq. 3.59}$$

$\alpha_F$  = Orientation angle of the fibers with respect to the longitudinal axis of the member.

$A_F$  = Cross-sectional area of FRP (unit width of if continuous wrap is used)

$E_F$  = FRP modulus of elasticity

$\varepsilon_F$  = Tensile strain at FRP composite level under factored loads

$d_v$  = Effective shear depth for internal steel

$$= \max \begin{cases} 0.9d \\ 0.72h \end{cases}$$

$\theta$  = acute fiber direction angle

$s_F$  = spacing of FRP (unit width of if continuous wrap is used)

If the factored shear force is greater than  $0.125\lambda\phi_c f'_c b_w d_v$ , the following spacing, applies:

$$s_F = \min \left\{ \begin{array}{l} w_F + 0.25d_v \\ w_F + 300 \text{ mm} \end{array} \right. \quad \text{Eq. 3.60}$$

$w_F$  = Width of FRP strips  
 $\lambda$  = low density concrete factor  
 $\phi_c$  = Resistance factor of concrete  
 $b_w$  = Beam web width  
 $d_v$  = Effective shear depth for internal steel  
 $= \max \left\{ \begin{array}{l} 0.9d \\ 0.72h \end{array} \right.$

Fully wrapped:  $\varepsilon_F = 0.006 < 0.75\varepsilon_{fu}$   
 U-wrapped with anchors:  $\varepsilon_F = 0.005 < 0.75\varepsilon_{fu}$   
 U-wrapped without anchors or strips:  $\varepsilon_F = \kappa_v \varepsilon_{fu} < 0.004$

$$\kappa_v = \frac{k_1 k_2 L_e}{11900 \varepsilon_{FU}} \leq 0.75 \quad \text{Eq. 3.61}$$

$\kappa_v$  = Bond-reduction coefficient calculation

$$k_1 = \left( \frac{f'_c}{27} \right)^{\frac{2}{3}} \quad k_2 = \frac{d_F - L_e}{d_F}$$

$$L_e = \frac{23300}{(n_F t_F E_F)^{0.58}}$$

= FRP effective anchorage length

$\varepsilon_{FU}$  = Ultimate FRP strain

$k_1$  = Concrete strength factor

$k_2$  = FRP bond configuration factor

$f'_c$  = Concrete compressive strength

$d_F$  = Distance from extreme compression fiber to centroid of tension FRP reinforcement

### 3.6 Comparison of Design Guidance

A Michigan DOT report number OR10-039 (Eamon, 2014) provides a detailed summary of these differences between the AASHTO and ACI as well as four other specifications, i.e., ISIS (Design Manual by Intelligent Sensing for Innovative Structures, which is similar to CSA), JSCE (Japanese Society of Civil Engineer), UK (United Kingdom Concrete Society technical report TR55), and CNR (Italian National Research Council technical document). In general, the AASHTO equations are less restrictive in the computation of the CFRP shear strength than ACI, but the overall shear strength of the beam is slightly lower than the ACI approach (Figure 50 and Figure 51).

FRP-related guidelines for bridges in Michigan were analyzed and compared for the applicability and effectiveness to the needs of the Michigan Department of Transportation (MDOT). The current design approach was found to have six different failure modes, some of which include

brittle failure, ductile failure, and delamination. The six failure modes were split into two types. The first type includes the modes that exhibit composite action up to a failure due to concrete crushing, FRP rupture, or lack of shear resistance. The second type consists of failures that lose composite action due to the debonding of the FRP sheet or when the concrete cover near the support region peels off.

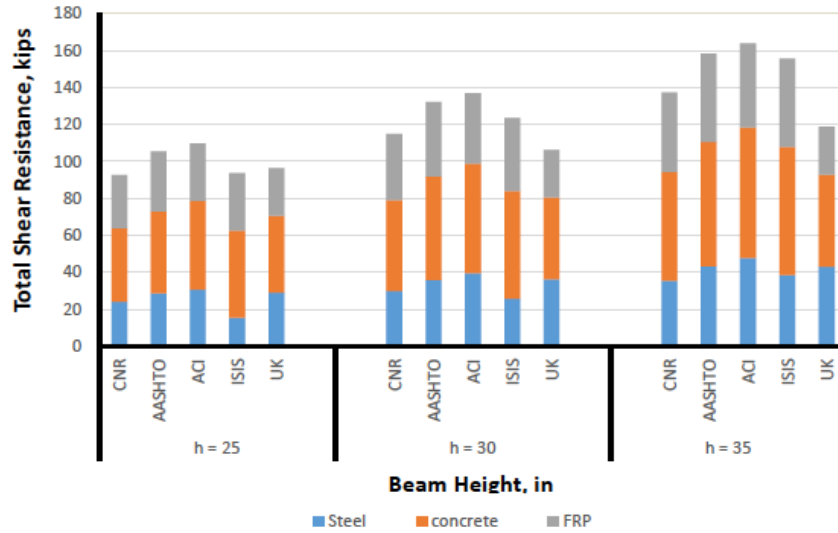


Figure 50: Total shear resistance of a reinforced concrete beam (stirrup spacing = 9 in.) (Eamon 2014)

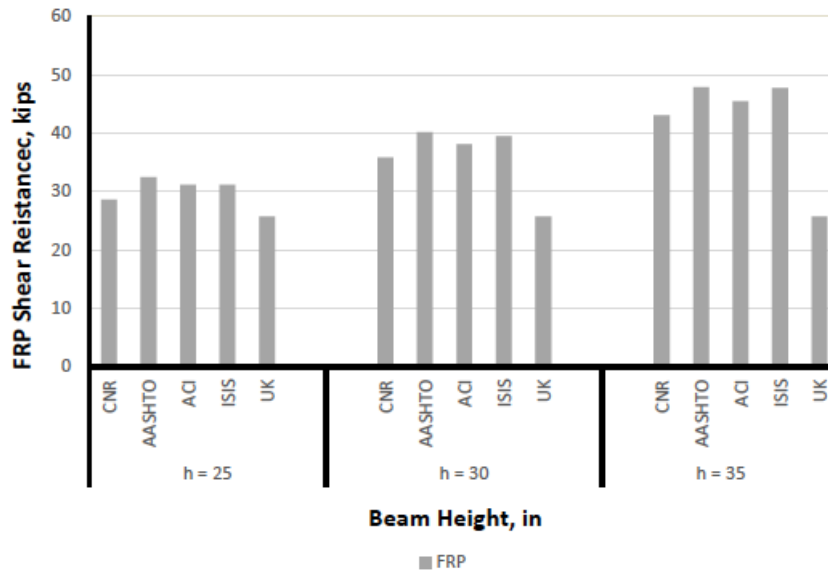


Figure 51: FRP shear resistance of a reinforced concrete beam (stirrup spacing = 9 in.) (Eamon 2014)

The ACI 440.2R-08 framework was used to identify the items that are considered for review and comparison since it offers the most complete coverage of the subject. FRP strengthening systems can enhance flexural strength by 10%-160%; but, by accounting for code-specified strengthening and ductility limits, a 40% enhancement of flexural strength is accepted.

Strengthening qualification limits for a structural member were set by AASHTO, ACI, and ISIS. The limits ensure the adequacy of a member to support a given number of service dead and live loads in the case of severe environmental damage, fire, vandalism, or construction error(s) causing loss of strengthening. Other guides leave the decision to strengthen a structure to an authority having jurisdiction on a case-by-case basis. The differences in the strengthening limits for AASHTO and ACI are similar, but ISIS allows a lower threshold of the existing structure strength. The most comprehensive coverage of environmental factors is given by ACI. For FRP strain limits, AASHTO, ISIS, and TR55 have fixed strain limit volumes, whereas ACI and CNR show an increase in the strain limit with an increase in concrete compressive strength. For the majority of codes, strength reduction factor values are near 0.85, which is a fixed value under AASHTO. The service stress limits for different codes are shown in Figure 52.

	ACI	AASHTO	ISIS	UK	CNR
<b>Steel</b>	$0.80f_y$	$0.80f_y$	$0.80f_y$	$0.80f_y$	
<b>Concrete</b>	$0.45f'_c$	$0.36f'_c$		$0.60f_{cu}$	
<b>CFRP</b>	$0.55f_{fu}$	$0.80f_{fu}$		0.65	$0.80f_{fu}$

Figure 52: ISIS maximum stress level against creep rupture (Eamon, 2014)

Creep rupture and fatigue limits are fixed values under CNR and TR55, while ACI and ISIS set the limits as a function of FRP strength. The most elaborate check for creep and fatigue limits is given by AASHTO as stress limits for concrete, steel, and FRP are provided. Most expressions were developed as a function of tension in the FRP and concrete compressive strength. There is little difference in the wrapping schemes that are recommended by the different codes. AASHTO notes that the 2-sided wrap is the least effective wrapping scheme and that the three-sided (U-wrap) variation is more popular. Adding anchors to any wrap, according to AASHTO, increases effectiveness, particularly in the compression zone. AASHTO and ACI consistently provide the largest design capacity values for the effective FRP strain. Similar to CNR, the strain limit that AASHTO specifies for the confinement of axial compression members is 0.004. Testing of adhesive bond was conducted to assess the pull-off strength of a longer-term FRP application on carbon-wrapped columns. Considerable variation in the test results was observed with a mean overall bond strength of 668 psi and a mean coefficient of variation of 0.29. The failure modes that were observed included concrete rupture, FRP interface, and combined concrete/FRP interface failures. The majority of the failures were concrete breakout due to the bond strength being greater than the concrete strength. The cases where the failure was non-concrete related were attributed to the failure of adhesive and/or FRP (the FRP was not fully saturated with the epoxy, or the adhesive contained air bubbles).

In terms of recommendations to the current provisions, AASHTO’s environmental reduction factors, flexural design when considering compression failures, initial strain for prestressed sections, and strength reduction factors and ductility provisions considering prestressed sections should be altered.

Given that AASHTO does not provide specific environmental reduction factors, Michigan-specific reduction factors for CFRP interface bond strength were recommended (Figure 53).

Time (design years)	Reduction Factor
10	0.73
25	0.66
50	0.54
75	0.42

Figure 53: Reduction factors for CFRP interface bond strength (Michigan-specific) (Eamon, 2014)

A 15-year reduction factor was determined experimentally by measured reduction in the bond strength of a CFRP wrap when exposed to Michigan weather. Additional research can confirm the applicability of a reduction factor corresponding to the expected remaining service life. If the common and appropriate epoxy strengths, surface preparations, and installation techniques are used in union with the other recommendations, it will be unlikely that environmental reductions will be needed.

It is recommended that the AASHTO-specified FRP strain limit should correspond to a maximum concrete compressive strain in the girder of 0.003. The FRP reinforcement strength per unit width should be calculated using the lesser of the FRP tensile strain or 0.005 to avoid bond interface failure.

The initial strain for a prestressed concrete section was not addressed in AASHTO; however, it can be derived theoretically. Regardless, the initial strain given by ACI is shown below:

$$\varepsilon_{bo} = -\frac{p_e}{E_c A_{cg}} \left( 1 + \left( \frac{e y_b}{r^2} \right) \right) + \left( \frac{M_{DL} y_b}{E_c I_g} \right) \quad \text{Eq. 3.62}$$

$\varepsilon_{pi}$  = initial strain in prestressed steel reinforcement, in./in. (mm/mm)

$P_e$  = effective force in prestressing reinforcement, lb. (N)

$A_p$  = area of prestressed reinforcement in tension zone, in.<sup>2</sup> (mm<sup>2</sup>)

$E_p$  = modulus of elasticity of prestressing steel, psi (MPa)

$e$  = eccentricity of prestressing steel, in. (mm)

$r$  = radius of gyration of a section, in. (mm)

The AASHTO limits specify that, in the FRP reinforcement at section's ultimate capacity, the strain developed must be equal to or greater than 2.5 times the strain at the point where the centroid of steel tension reinforcement yields. Structural reliability analysis of FRP-strengthened prestressed concrete girders subjected to Michigan bridge loads is needed to determine the most appropriate resistance factors and associated strain limits.

Table 6 summarizes the available design guide on using externally bonded CFRP. Based on this preliminary review, it is recommended that FDOT continue to adopt the ACI 440 provisions. AASHTO approach is slightly less conservative and uses a higher ultimate strength in the FRP but does not specify an environmental factor. To determine the best design provision, a synthesis of test data on prestressed concrete beams is needed to evaluate the design provision, which is beyond the scope of this research project.

## 4. Anchor System Evaluation

As mentioned early, the anchor system effectiveness is not used in evaluating the anchor system, but this information is provided in Table 7. The staple anchor seems to be the most effective from the table as it increased the ultimate capacity by 156%. However, the result was based on a direct tension test of a small-scale component level testing. There is no indication that this would still be the case if the system was evaluated in full-scale prestressed concrete specimens. Therefore, the anchor system effectiveness is not used in the evaluation. The anchor systems are evaluated based on the following criteria, which are summarized in Table 8:

### *Proprietary*

If the anchor, or all elements of the anchor, is available for public purchase, it is not considered proprietary. For example, staple anchors are not readily available and must be made by an approved manufacturer upon request.

### *Level of Invasiveness*

- 1: no alteration of the concrete substrate; application does not require knowledge of interior reinforcement.
- 2: minor alteration to member surface (i.e., roughing surface via grinding)
- 3: alteration of substrate required; grinding or shallow cutting of surface; knowledge of interior reinforcement is necessary
- 4: penetration beyond cover is often necessary (i.e., drilling of holes to accommodate anchor)
- 5: significant and destructive procedure; cutting of a large channel (in relation to member size) and/or embedment of foreign materials (non-CFRP elements or substances used for bonding).

### *Installation Tolerance*

**GREEN:** high tolerance; anchor can accommodate to any member geometry; no concern for internal reinforcement

**YELLOW:** medium tolerance; anchor can accommodate to most member geometries, but internal reinforcement may be impacted

**RED:** low tolerance; anchor only applicable to members of a specific size and/or shape; conflict with internal reinforcement is likely

### *Installation Complexity*

**GREEN:** low complexity; little design experience required, fast and easy to apply

**YELLOW:** medium complexity; may require advanced treatment of concrete surface or alteration of substrate

**RED:** high complexity; many details and specifications, a detailed layout must be followed, heavy machinery may be required, expensive, slow, and/or dangerous to implement; multiple materials require.



Table 6: Design guide comparison

Design Standard	Description	Flexural Provisions	Shear Provisions	Creep/Fatigue	Reduction Factor(s)	Unique Elements
ACI 440.2R-17	American Concrete Institute: Guide for the Design and Construction of Externally Bonded FRP Systems for Strengthening Concrete Structures (2017)	<ul style="list-style-type: none"> <li>– Design strength must exceed factored moment</li> <li>– Strain in FRP must be less than debonding strain</li> </ul>	<ul style="list-style-type: none"> <li>– Considers existing substrate strain, strain in the FRP, and stress in the FRP</li> </ul>	Limit: 55% of Stress in CFRP	0.65-0.9 (based on net tensile strain) $\phi$ = strength reduction factor	Prestressed concrete: Initial strain of substrate should be calculated and excluded from the effective FRP strain
JSCE	Japan Society of Civil Engineers: Recommendation for Design And Construction of Concrete Structures Using Continuous Fiber Reinforcing Materials	<ul style="list-style-type: none"> <li>– Flexural capacity dependent upon peel-off failure occurring</li> </ul>	<ul style="list-style-type: none"> <li>– Shear capacity equals the sum of the contribution from concrete, steel, and CFRP sheets</li> </ul>	None *JSCE Standard Specification for Concrete Structures still applies	Based on Testing $f_k$ = characteristic value $\gamma_m$ = material factor *Tables used if testing is not possible	Mechanical anchoring recommended when CFRP sheets are bonded to the sides of girders
FIB-14	Fédération Internationale du Béton: Externally bonded FRP reinforcement for RC structures (2001)	<ul style="list-style-type: none"> <li>– Considers concrete strain in top and tension fiber, moment of Inertia of cracked section, and strain in FRP and steel</li> </ul>	<ul style="list-style-type: none"> <li>– References Eurocode 2004 for shear design</li> <li>– Considers FRP strain and orientation</li> <li>*Notes that peel-off caused by shear cracks has not yet been researched to sufficient detail</li> </ul>	Uses CEB method to predict mean deflection	Based on presence of debonding and FRP type (table provided) $\gamma_f$ = material safety factor	Most approaches to analyze end failures utilize empirical formulas References Eurocode 2

Table 6: Design guide comparison

Design Standard	Description	Flexural Provisions	Shear Provisions	Creep/Fatigue	Reduction Factor(s)	Unique Elements
FDOT SDM Volume 4	Florida Department of Transportation: Fiber Reinforced Polymer Guidelines (FRPG) Structures Manual Volume 4	<ul style="list-style-type: none"> <li>– References ACI 440.2R-17</li> <li>– Design loads change based on number of strengthened girders</li> </ul>	<ul style="list-style-type: none"> <li>– References ACI 440.2R-17</li> <li>– Must place transverse CFRP at the termination points of each ply and between ends of the CFRP</li> </ul>	References ACI 440.2R-17	$C_E = 0.85$ , environment reduction factor	<p>Shear strengthening using FRP restricted to complete or three-sided</p> <p>If U-wrapping is used, the termination of the wrap must be anchored</p>
CSA S806-12	Canadian Standards Association: Design and Construction of Building Components with Fiber-Reinforced Polymers	<ul style="list-style-type: none"> <li>– Specifies FRP shape, orientation, spacing, and additional anchorage</li> </ul>	<ul style="list-style-type: none"> <li>– Shear capacity equals the sum of the contribution from concrete, steel, and CFRP sheets</li> <li>– Punching shear considered</li> </ul>	References CSA Design Guide-2012 (CSA S806-12)	Based on material properties $\phi_F$ = FRP resistance factor $\phi_S$ = steel resistance factor $\phi_C$ = concrete resistance factor	Failure controlled by concrete crushing unless factored resistance > 1.6 times the effect of the factored loads, in which case, FRP failure would control

\**Unique Elements* include provisions that are found only in the corresponding design guide.

Table 7: Effectiveness of anchors

Anchor Type	Control Member			Reinforced Member			Test Method	% Difference from Control	Source
	Details	Ultimate Load	Failure Mode	Details	Ultimate Load	Failure Mode			
Spike Anchor	<ul style="list-style-type: none"> <li>- 13.5 ft. AASHTO type IV girder</li> <li>- Steel rebar</li> <li>- No CFRP</li> </ul>	405 kips	Shear Crack	<ul style="list-style-type: none"> <li>- 13.5 ft. AASHTO type IV girder</li> <li>- Steel rebar</li> <li>- 48 anchors with vertical and horizontal strips</li> </ul>	550 kips	Shear Crack	1-point bending	+35.8%	(Fyfe, 2019)
U-Wrap	<ul style="list-style-type: none"> <li>- Dimensions: 1200 mm x 100 mm x 165 mm</li> <li>- Steel Rebar</li> <li>- CFRP laminate on tension face</li> </ul>	91 kN	Flexural Crack	<ul style="list-style-type: none"> <li>- Dimensions: 1200 mm x 100 mm x 165 mm</li> <li>- Steel Rebar</li> <li>- CFRP laminate on tension face</li> <li>- 100% coverage of shear span with CFRP (three-sided wrap)</li> </ul>	116 kN	Flexural crack/ Debonding	4-point bending	+27.4%	(Kim & Bhiri, 2020)
Staple (Round) Anchor	<ul style="list-style-type: none"> <li>- 10" x 10" concrete block</li> <li>- CFRP strip bonded to block without anchor</li> </ul>	16 kips	Debonding	<ul style="list-style-type: none"> <li>- 10" x 10" concrete block</li> <li>- CFRP strip bonded to block with staple anchor and saturated fiber wrap</li> </ul>	41 kips	Concrete break-out	Direct tensile	+155.9%	(University of Miami, 2016)

Table 7: Effectiveness of anchors

Anchor Type	Control Member			Reinforced Member			Test Method	% Difference from Control	Source
	Details	Ultimate Load	Failure Mode	Details	Ultimate Load	Failure Mode			
FRP Strip/Sheet	<ul style="list-style-type: none"> <li>– Dimensions: 1840 mm x 200 mm x 300 mm</li> <li>– Steel rebar</li> <li>– No CFRP</li> </ul>	116 kN	Shear Crack	<ul style="list-style-type: none"> <li>– Dimensions: 1840 mm x 200 mm x 300 mm</li> <li>– Steel rebar</li> <li>– 125 mm CFRP vertical sheet spacing</li> </ul>	190 kN	Debonding	4-point bending	+62.5%	(Mohamed, Abdalla, & Hawileh, 2020)
Mechanical and Metallic Anchor	<ul style="list-style-type: none"> <li>– 1800 mm x 1500 mm concrete wall</li> <li>– Steel Rebar</li> <li>– No CFRP</li> </ul>	341 kN	Tension Cracks	<ul style="list-style-type: none"> <li>– 1800mm x 1500mm concrete wall</li> <li>– Steel Rebar</li> <li>– CFRP: 1 vertical layer, 3 horizontal layers</li> <li>– Steel dowel bolted along base</li> </ul>	633 kN	Concrete crushing at base	Cyclic Flexural Testing	+85.6%	(Woods, 2014)
Longitudinal Chase	<ul style="list-style-type: none"> <li>– Concrete Block Dimensions: 250 mm x 300 mm x 600 mm</li> <li>– Steel Rebar</li> <li>– 120 mm x 2 mm x 1000 mm CFRP strip (bond length = 500 mm)</li> </ul>	99.6 kN	Concrete failure at surface	<ul style="list-style-type: none"> <li>– Concrete Block Dimensions: 250 mm x 300 mm x 600 mm</li> <li>– Steel Rebar</li> <li>– 40 mm x 40 mm x 500 mm chase with</li> <li>– N24 bar and GFRP strip 120 mm x 400 mm</li> <li>– 120 mm x 2 mm x 1000 mm CFRP strip (bond length = 500 mm)</li> </ul>	195 kN	Debonding	Direct tension	+95.8%	(Kalfat & Al-Mahaidi, 2010)

Note: See Section 3. Anchorage Types and/or Table 7 for availability of design and construction guidance for each anchor type.

Table 8: Anchor properties summary

Anchor Type	Proprietary	Level of Invasiveness	Installation Tolerance	Installation Complexity	Design Guidance
Spike Anchor	✘	4	Yellow	Red	TxDOT Reports FHWA/TX-13/5-6306-01-1 FHWA/TX-12/0-6306-1 FHWA/TX-16/0-6783-1
U-Wrap	✘	2	Green	Green	ACI 440.2R-17 JSCE FIB 14 FDOT SDM Vol. 4 CSA S806-12
Staple (Round) Anchor	✓	3	Red	Yellow	None *Design strength given by manufacturer
FRP Strip/ Sheet	✘	1	Green	Green	ACI 440.2R-17 JSCE FIB 14 FDOT SDM Vol. 4 CSA S806-12
Mechanical and Metallic Anchor	✘	5	Yellow	Red	None *Manufacturer/component dependent
Longitudinal Chase	✘	5	Red	Red	ACI440.2R-17 and bond strength/slip models (Chen & Teng, 2001) and (Yuan & Wu, 1999).

## 4.1 Explanation of Properties by Anchor Type

### 4.1.1 Spike Anchor

Spike anchors are readily available for purchase through many manufacturers, making none of their data proprietary. Installation requires drilling into the concrete substrate repeatedly, which may interfere with bar reinforcement and/or may be impossible if thin members are being strengthened; thus, invasiveness and complexity are high with a moderate tolerance for error. Texas DOT reports provide specific guidance on spike anchor design and installation: FHWA/TX-13/5-6306-01-1 (Garcia, Sun, Kim, Ghannoum, & Jirsa, 2014), FHWA/TX-12/0-6306-1 (Kim, et al., 2012), and FHWA/TX-16/0-6783-1 (Jirsa, et al., 2017).

### 4.1.2 U-Wrap

U-wraps consist of only CFRP laminates and are publicly available for purchase. Installation does not involve drilling or cutting into the concrete substrate, rendering invasiveness and complexity low with a high alignment and positioning tolerance. Given their popularity, design guidance for U-wraps is provided by all major design organizations (ACI, FIB, etc.).

U-anchors were not considered during the creation of Table 7 as their use is similar to U-wraps but with much more invasive installation techniques. The superiority of U-wraps over more complex U-anchors has been explained and justifies the exclusion of U-anchors from Table 7. Furthermore, other invasive anchor types, mechanical anchors for example, may be used and could be considered representative of U-anchor performance when compared to all anchor types.

### 4.1.3 Staple Anchor

Staple anchors are new, and their production is limited. Fortec Stabilization is the sole manufacturer of staple anchors, making their information accessible but generally proprietary. Although custom anchors may be ordered, post-production modification is not possible (i.e., lengthening or shortening anchors) and installation requires cutting grooves (or holes in recent modified bar versions) into the substrate to accommodate the anchors' "legs." The flexural, shear, and tensile strength of a staple anchor is provided by the manufacturer, who obtains the design limits from post-production testing.

### 4.1.4 FRP Strip/Sheet

Almost identical to U-wraps, FRP strips and sheets consist of only CFRP laminate and are publicly available for purchase. Installation does not involve drilling or cutting into the concrete substrate, rendering invasiveness and complexity low with a high alignment and positioning tolerance. Lower material usage and waste compared to U-wraps validates FRP strips and sheets' usage as the least invasive anchor type. Like U-wraps, FRP strip and sheet design guidance is provided by all major design organizations (ACI, FIB, etc.). Strips may be used in conjunction with U-wraps to significantly enhance shear strengthening. Although test have shown that flexural and shear strengthening begins to taper after a particular material usage is reached, the addition of U-wraps to existing or new FRP strips or sheets is beneficial to overall strengthening and repair.

### 4.1.5 Mechanical/Metallic Anchors

Mechanical anchors are not popular in the construction industry. Most mechanical anchors are comprised of multiple, heavy components that must be properly assembled to specified standards

to achieve expected design properties, slowing build time, increasing labor, and reducing aesthetic appeal. Their stringent and destructive installation, which often requires deep drilling and/or cutting of the substrate, makes their invasiveness and complexity exceptionally high. Material properties are typically readily available as components are often constructed from widely used materials (e.g., steel); however, design strength of an entire mechanical anchor varies significantly across anchor types and is typically provided by the manufacturer. Galvanic corrosion was not considered in the ranking provided herein but is a concern mentioned by a select group of topic experts. Anchors made of non-ferrous metals (e.g., aluminum) pose the largest threat to degradation of reinforcement; such concerns must be addressed during design and remedied during installation.

#### 4.1.6 Longitudinal Anchors

Longitudinal anchors, which require a channel to be cut along the entire tension face of a member, are the most invasive anchor type and require special tools and labor to install. Research-based design guidelines, like the models developed by Chen and Teng in 2001 and Yuan and Wu in 1999, are the main sources of design support currently available. The bond and steel yield strength of a longitudinal system may be estimated using applicable section of popular design guides (e.g., ACI440.2R-17), but total anchor strength must be found experimentally.

#### 4.2 Anchor System Recommendation

Table 9 summarizes the ranking of the anchor systems based on the established criteria. The top three anchor systems are FRP strip, U-wrap anchor, and spike anchor. However, no manufacturer recommends U-wrap anchor in the United States, and therefore, the next ranked system, mechanical anchor, was selected.

Table 9: Ranking of anchors by detail

<b>Rank</b>	<b>Proprietary (1 = most available)</b>	<b>Level of Invasiveness (1 = least invasive)</b>	<b>Installation Tolerance (1 = highest tolerance)</b>	<b>Installation Complexity (1 = least complex)</b>	<b>Design Guidance (1 = most guidance)</b>
1	FRP Strip/ Sheet	FRP Strip/ Sheet	FRP Strip/ Sheet	FRP Strip/ Sheet	FRP Strip/ Sheet
2	U-Wrap/Anchor	U-Wrap/Anchor	U-Wrap/Anchor	U-Wrap/Anchor	U-Wrap/Anchor
3	Spike Anchor	Staple Anchor	Spike Anchor	Staple Anchor	Spike Anchor
4	Mech./Metallic Anchor	Spike Anchor	Mech./Metallic Anchor	Spike Anchor	Staple Anchor
5	Longitudinal Chase	Mech./Metallic Anchor	Staple Anchor	Mech./Metallic Anchor	Longitudinal Chase
6	Staple Anchor	Longitudinal Chase	Longitudinal Chase	Longitudinal Chase	Mech./Metallic Anchor



### 4.3 Anchor System Details

Detailed drawings and specifications of these anchor systems are provided in Appendix A, which were developed based on existing test results from various publications. The drawing details were developed for prestressed and reinforced concrete sections typically used in Florida. These sections include AASHTO girders, Florida I-beam, bulb-T girder, inverted T-beam, reinforced concrete T-beam, and slab beam (including cast-in-place slab). The anchors' quantity, size, and location were conservatively developed, and the spacing of CFRP strips and laminates was configured to accommodate member geometry. The spike anchor details and specifications are based on TxDOT recommendations. For the FRP strips and mechanical anchors, the authors' engineering judgment combined with test results available from the literature were used to develop the details and specifications. The recommendations are also based on actual projects implemented in Florida. More explanations of the development are described below. It is recommended that the proposed design drawings and details be further evaluated experimentally. The size and spacing of FRP laminates are designed according to the beam types, sizes and, FRP strip orientations. Only vertical and horizontal FRP laminates are considered as minimal testing results are available for beams on which the FRP laminates are installed at an angle, i.e., a strip oriented 45 degrees to the flexural reinforcement of a beam.

The width of vertical FRP laminates is based on ACI 440.2R-17, limiting vertical laminates' spacing based on shear capacity. The on-center spacing between vertical laminates is based on published research (Kim, et al., 2012) and (Garcia, Sun, Kim, Ghannoum, & Jirsa, 2014), which recommends a spacing that should not exceed the sum of the depth of the member divided by four plus the width of one vertical laminate.

Literature detailing spacing and sizing requirements of transverse laminates also referred to as longitudinal or horizontal strips, is much more limited than vertical laminates. Four sources (Table 10) are used to create the recommendations provided.

Table 10: List of reports detailing the size and spacings of FRP transverse laminate

Report Number	Title	Author (Citation)
FHWA/TX-13/5-6306-01-1	Procedures for the Installation and Quality Control of Anchored CFRP Sheets for Shear Strengthening of Concrete Bridge Girders	(Garcia, Sun, Kim, Ghannoum, & Jirsa, 2014)
FHWA/TX-12/0-6306-1	Shear Strengthening of Reinforced and Prestressed Concrete Beams Using Carbon Fiber Reinforced Polymer (CFRP) Sheets and Anchors	(Kim, et al., 2012)
FHWA/TX-16/0-6783-1	Use of Carbon Fiber Reinforced Polymer (CFRP) with CFRP Anchors for Shear-Strengthening	(Jirsa, et al., 2017)
BDK82 977-03	The Repair of Damages Bridge Girders with Carbon-Fiber-Reinforced Polymer "CFRP" Laminates	(ElSafty & Graeff, 2012)

Based on the test results by Kim (Kim, et al., 2012), the on-center spacing of the horizontal strip should not exceed the sum of the depth of the member divided by four plus the width of one horizontal strip. This will result in an excessive number of horizontal strips even though these horizontal strips are anchored with spike anchors. On the other hand, El Safty, who evaluated the flexural performance retrofitted beams with CFRP laminates anchored with U-wrap strip, recommends an ideal spacing for the horizontal strip equal to two-thirds to twice the height of the beam (ElSafty & Graeff, 2012). Considering that existing shear retrofits of FDOT bridges using spike anchors or no anchors do not provide any horizontal strip details, the recommendation by El Safty is used in developing the anchorage details.

#### 4.3.1 Spike Anchor Details

Spike anchor details were developed in alignment with published FDOT projects and research performed by the University of Texas at Austin (Kim, et al., 2012). Table 11 lists the four FDOT projects referenced during spike anchor layout design.

Table 11: Existing spike anchor details

<b>Name of Project</b>	<b>Engineer of Record (Company)</b>	<b>Primary Use</b>
P.G.A. Boulevard over Florida's Turnpike	SDR Engineering Consultants, Inc.	-CFRP Laminate installation procedure.
State Road 30 (U.S. 98) Over Pensacola Bay	Parsons Brickerhoff	- CFRP fan and hole preparation procedure. - CFRP anchor installation procedure.
Glades Road over I-95	WSP USA Inc.	- Typical CFRP fan detail. - CFRP and anchor spacing. - Typical beam span schematic.
Sunshine Skyway Bridge AASHTO Beams Rehabilitation	PB Americas, Inc.	- CFRP installation at beam webs and flanges. - Typical anchor size and patch schematic.

The primary reference for the spike detail includes the TxDOT report number FHWA/TX-12/0-6306-1 (Kim, et al., 2012), which was published in partnership with The University of Texas at Austin's Center for Transportation Research in 2012. Chapter 5 of the report provides spike anchor design recommendations. A balance between redundancy and practicality is stressed and one spike anchor per CFRP strip is recommended. Kim's research (pg. 238-240) provides the following recommendations:

1. Six in. anchor hole depth (4 in. under extenuating circumstances)
2. The anchor hole is 1.4 times the cross-sectional area of the spike anchor used with a chamfer radius of 0.5 in.
3. The material used for anchors is at least twice as large as the material used for strips.
4. Minimum of 0.5 in. fan overhang on all sides with a 60° angle.

5. Two patches should be placed over each anchor (one longitudinal and one transverse to the CFRP strip).

These recommendations were incorporated in developing the spike anchor details illustrated in Appendix A.

#### 4.3.2 FRP Strip Details

ACI 440.2R-17 was predominantly followed for the design of the FRP strip anchoring system. The horizontal strip details were based on the recommendation from the FDOT research project BDK 82 977-03 (ElSafty & Graeff, 2012) with minor modifications to adopt the FRP strip for anchoring shear laminates. They recommended that the optimum spacing for the FRP strip should be two-thirds to twice the height of the beam. However, they also suggested that the end of the FRP strip should extend to the top of the beam as far as possible and anchor with a transverse strip to avoid premature failure debonding. They also recommend additional longitudinal strips should be installed around the tension strut.

In addition to the provisions outlined above, an 18 in. on-center limit was implemented based on the maximum spacing for temperature and shrinkage reinforcement provisions outlined in ACI 318-19. All beams analyzed are geometrically classified as “deep beams” for shear; hence, the entire shear area of each beam is considered a high-compression (strut) area. Given the beam’s “deep beam” classification, spacing requirements for longitudinal reinforcement, according to ACI 318-19, are based on anticipated crack width. Since crack severity associated with laminates is unknown, the 18 in. maximum allowable spacing specified in ACI 318-19 is assumed to control design and serves as the upper limit for horizontal strip spacing. The 18 in. maximum permits the use of fewer horizontal laminates compared to the amount aligning with the theoretical quantities calculated using the results of El Safty’s research. The reduced quantity of horizontal strips improves constructability and aligns with projects published by the FDOT, which utilizes no horizontal laminates.

Additionally, the locations most susceptible to delamination, i.e., the ends and corners of the vertical strips, are anchored with the horizontal strip. Figure 54 shows the locations along the beam’s cross-sectional perimeter most likely to experience delamination (outlined by dotted red lines).

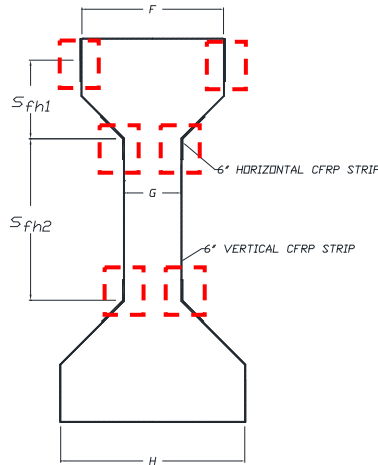


Figure 54: AASHTO Type IV beam schematic

Once horizontal strips were specified at locations outlined in Figure 54, spacing requirements were referenced to determine the need for additional horizontal reinforcement. If the clear distance between any of the horizontal strips already specified (i.e., those along the top region and edges) exceeds 18 in., additional strips were added until a uniform spacing of less than 18 in. was achieved.

### 4.3.3 Mechanical Anchors

Mechanical anchor design is based on University of California San Diego Report No. SSRP-95/01 (Laursen, Seible, Hegemier, & Innamorato, 1995). The University of California San Diego’s department of applied mechanics and engineering sciences published test results from research on seismic retrofit and repair of reinforced concrete with carbon overlays that utilized mechanical anchors to fix CFRP laminates to flexural walls. The study evaluated two types of mechanical anchors: a steel angle and a Simpson Strong-Tie product. Using an entire steel angle was deemed overly conservative; hence, steel plates were used in conjunction with the spacing requirements outlined on page 95 of the report. Like with beam retrofit design, “The strength provided by the horizontal steel and carbon overlays is based on a 45° crack inclination.” (Laursen, Seible, Hegemier, & Innamorato, 1995). Failure of mechanical anchors should be ductile and expected to withstand a predetermined moment. The stress and strain limits outlined in ACI, 2019 should control design. Since the existing literature results were based on testing of walls, the recommendations provided in Laursen’s report are indirectly related; however, application procedures and spacing requirements are assumed to be adequate until additional testing proves otherwise.

## 5. Proposed Testing Program

As stated earlier, these anchorage details need to be further evaluated experimentally to validate their shear resistance capabilities. At the very least, the detail of horizontal strips of all anchor systems needs to be evaluated. The horizontal strip is excluded in existing FDOT shear retrofit details, despite many studies overwhelmingly indicating its importance in enhancing the shear capacity of CFRP laminates. Below is the proposed testing plan.

### 5.1 Testing Procedure

The proposed test procedures are divided into two loading regimes: (1) monotonic load test and an optional (2) cyclic load tests. These tests will be performed at the FDOT Marcus Ansley Structural Research Center (SRC) using the existing strong floor and reaction frames. All tests will be performed using a servo-controlled hydraulic actuator or a hydraulic jack to apply a concentrated load on a 50-ft. long AASHTO Type IV beam, as illustrated in Figure 55 and Figure 56. Two loading locations are proposed to capture web-shear failure (Location 1) and flexural-shear failure (Location 2). It is possible to apply the two loading locations on a single beam by applying the load on opposite ends of the beam. However, the span would have to be moved closer together for the second test (Location 2), i.e., after the completion of the first test (Location 1), the span length would need to be shortened by at least 10 ft. from 49 ft. to 39 ft. to eliminate the damaged portion. The proposed CFRP anchor details will only be installed either on one side (Location 1) or two sides (Location 2) of the beam. The unrepaired side should have higher shear reinforcement or clamped with steel brace to avoid premature shear failure.

The monotonic load test will evaluate the ultimate performance of various anchor systems. The monotonic load test protocol loads the test specimens at a constant rate (approximately 250 lb./sec) until failure. A video recording of the crack initiation and pattern of the concrete beam will also be conducted during the test. Additionally, to reveal any hidden cracks beneath the CFRP laminate, it is also recommended that an infrared camera be used to capture any hidden cracks.

The optional cyclic load test (or crack movement test) will be used to determine the reliability and redundancy of the anchor system after the beam cracks. A servo-controlled hydraulic actuator with load control is needed for the cyclic load test to apply reverse-cyclic load on the test specimens. The cyclic load test protocol first loads the beam until shear cracks are formed on the concrete with an opening of approximately 0.01 in. (0.3 mm). The cracked beam will be subjected to 50% initial load with a maximum of 1,500,000 cycles or until the failure of the anchorage system. It should be noted that the number of cycles will depend on the initial load that causes the beam to crack and should be adjusted accordingly. The crack width will be recorded along with the number of cycles for this test. Upon completing the cyclic load test, the beam will be loaded to failure following the monotonic load test protocol.

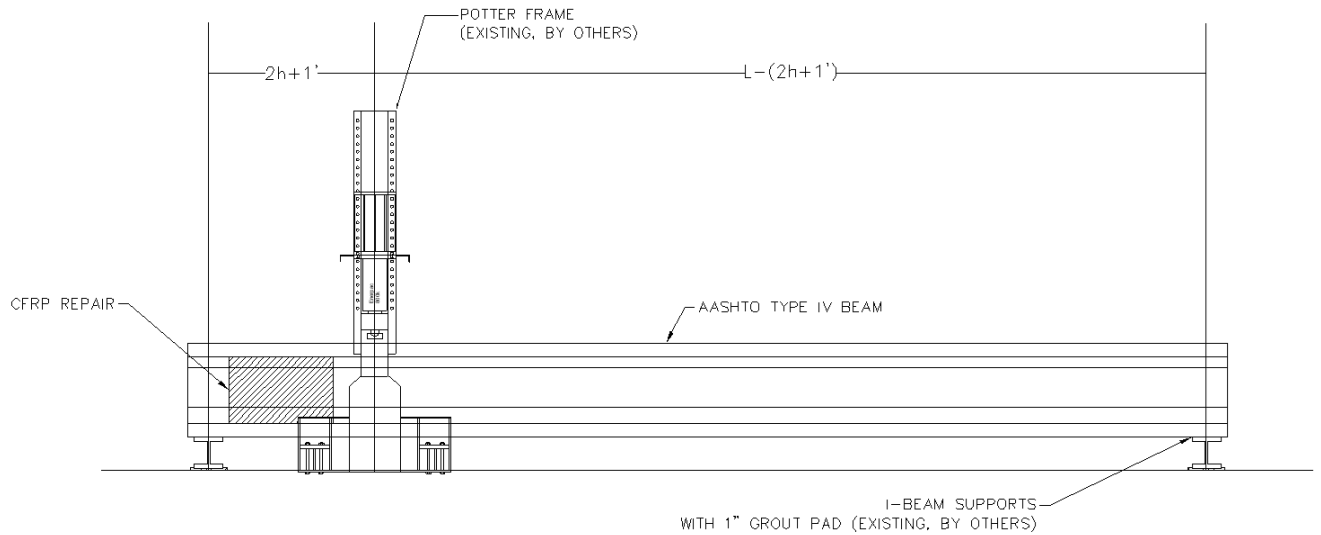


Figure 55: Full-scale shear load test of the AASHTO IV beam repaired with externally bonded CFRP - Test Location 1

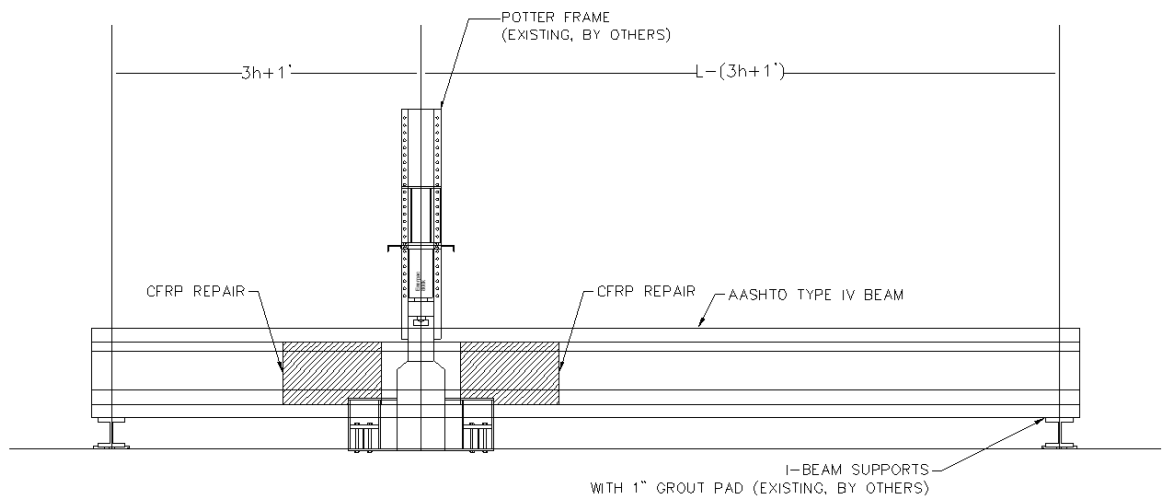


Figure 56: Full-scale shear load test of the AASHTO IV beam repaired with externally bonded CFRP - Test Location 2

## 5.2 Instrumentation

The beam should be minimally instrumented with foil strain gages and displacement sensors. The locations of the foil strain gauges should be closest to the expected shear cracks as much as possible. A finite element analysis will need to be performed to determine the crack's locations from the stress contour or force vector plots. The foil strain gage should be installed in the steel stirrups and on the CFRP laminates (for both vertical and horizontal strips), as illustrated in Figure 57. Additionally, three displacement transducers (e.g., string potentiometers) arranged to

form a right triangle should also be used to capture the shear crack movements that are depicted in Figure 57.

The anchor system will not be directly instrumented with foil gauges to avoid the impact of the gauges on the anchorage performance. However, the anchor system delamination or pull-out (for mechanical anchors) will be monitored using displacement transducers (preferably noncontact sensors) to detect the transverse displacement of the anchorage. The beam deflection will also be monitored at the load point.

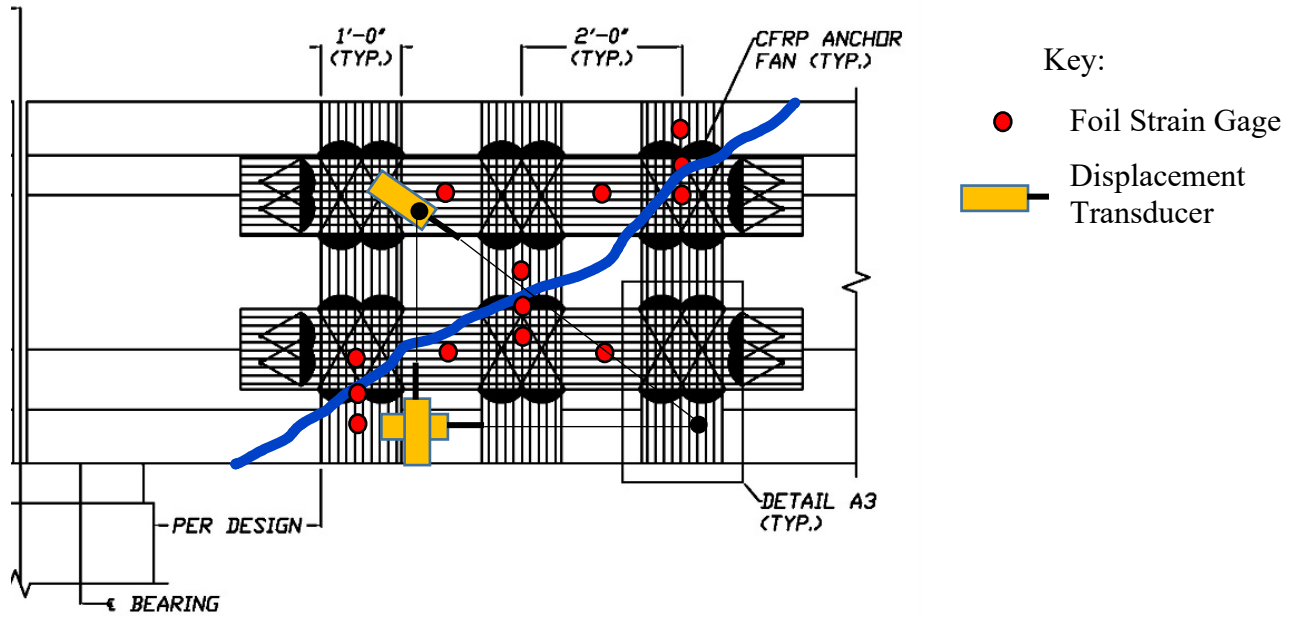


Figure 57: Preliminary foil strain gauge locations

### 5.3 Test Matrices

The test matrices will be used to evaluate anchor systems' performance in enhancing the shear capacity of the CFRP laminates. To this end there will be two control beams, one is a beam with no CFRP and the second is a beam with CFRP but without anchorage. All beams will utilize 2 layers of 12 in. CFRP vertical strip spaced at 24 in. on-center. Table 12 provides a summary of the test matrix. In the table, "uni-direction" denotes the beam is strengthened with only vertical CFRP strip, while "bi-direction" denotes the beam is strengthened with both horizontal and vertical strips, as illustrated in the details provided in the appendix. The proposed test matrix evaluates the proposed anchorage details, it is possible that additional beams are needed to develop optimized details for the three anchorage systems.

Table 12: Test matrix for AASHTO type VI beam

Test	CFRP layout	Variables	Monotonic Load Test	Cyclic Load Test
1	No CFRP	Control	X	
2	Uni-direction, no anchorage	Control CFRP without anchorage		
3	Uni-direction, spike anchor	Existing FDOT details		
4	Bi-direction, spike anchor	Proposed spike anchor detail		
5	Bi-direction, CFRP strip	Proposed CFRP strip anchor detail		
6	Bi-direction, mechanical anchor	Proposed mechanical anchor detail		
7	Bi-direction, spike anchor	Proposed spike anchor detail		X
8	Bi-direction, CFRP strip	Proposed CFRP strip anchor detail		
9	Bi-direction, mechanical anchor	Proposed mechanical anchor detail		

#### 5.4 Fabrication of Test Beams

An approved local prestressed concrete girder plant will produce and deliver all test specimens to the SRC. The Research Team will need to work with the prestressed concrete plant to arrange a time for the Research team to install foil strain gages onto the steel stirrups before casting the test beams. The Research Team will also need to work with the SRC staff to locate an area to store the test specimens and assist the SRC staff with installing the CFRP laminates and all instrumentation. The beams need to be prepared following the specification provided in the details described in the appendix. The Research Team will need to carefully document the test samples' fabrication.



## 6. Conclusion

Carbon fiber reinforced polymer (CFRP) is a flexible and customizable fabric effective in resisting tension loads. Material properties, size, modulus of elasticity, etc., vary significantly between CFRP manufacturers, each of which is associated with unique benefits and specific uses. Wide sheets, for example, are commonly used in U-wrap applications, while bonded strands are used to form spike anchors. The use of CFRP to repair and strengthen concrete has proven successful for all loading conditions. Beams, for example, are strengthened in flexure by bonding a CFRP strip along the bottom (tension) face of the member and support in shear by fixing CFRP strips or wraps to the side faces of the member.

A common failure mode among CFRP laminates is debonding. Debonding is not a preferred failure mode as it indicates the full strength of the concrete member or CFRP has not been reached. To preventing debonding, which is also known as peel-off failure, additional anchorage is often applied to the primary laminate. Anchor systems investigated include spike anchors, U-wraps/anchors, staple anchors, FRP strips and sheets, mechanical and metallic anchors, and longitudinal chases. Most anchor types have been rigorously tested according to applicable standards and have seen use in projects outside of academic settings. Spike anchors, for example, have been used by the Florida and Texas departments of transportation in the repair of highway overpass girders damaged by trucks exceeding posted clearances. It is the goal of the report to outline the effectiveness of each anchor type and showcase additional anchorage options that are less invasive and stronger than current methods. Preliminarily, staple anchors proved to be most effective in providing additional support when laminates are subjected to direct tension, however, no data are available for their use in prestressed girder. A combination of FRP strips and spike anchors showed the largest strength enhancement under flexural conditions, and mechanical anchors displayed the most effective shear resistance. Additional testing in which each anchor type is tested under identical loading conditions should be performed to confirm the claims mentioned. Proposed changes to current design standards from various literature were also compiled in Section 3.6 Comparison of Design Guidance.

Testing procedures varied significantly between existing literature. For example, experimental results were amiable for spike anchors installed in large, AASHTO Type IV girders, while strength data for mechanical anchors was obtained from testing of shear walls. Due to the differences among test specimens, a single control specimen has not been identified. A control for each anchor type has been specified and the increase in member strength resulting from anchorage installation was calculated separately for each test. The percentage differences may, therefore, be compared for general guidance. For example, the literature cited for spike anchor testing showed a 35.8% increase in member capacity after installing spike anchors. The literature cited for U-wrap/anchor testing showed a 27.4% increase in member capacity after installing U-wraps. Although each experiment tested different members, the effectiveness of each anchor type may be mostly compared based on the strengthened system improvement over the control specimen, but not specifically the bond strength improvement that could be used in the design calculation. An experiment testing each anchor type in identical members under uniform loading conditions would be required for an accurate conclusion to be made regarding which anchor type is most effective in increasing member flexural and shear strength.

Additionally, it is not clear from the literature if shear strength increase is contributed by the spike anchor or from a combination of spike anchors and horizontal CFRP strips. Based on Project 0-6306 (Kim, et al., 2012) study, there is no gain in the ultimate shear capacity in the prestressed girder when the girder is rehabilitated with vertical CFRP strips that are anchored with spike anchor only. Whereas the ultimate shear capacity increased by 33% when horizontal CFRP strips are added to provide additional anchorage of the vertical CFRP strips. Therefore, it is recommended that FDOT specify the use of horizontal CFRP strips, similar to the proposed spike anchor details.

For this reason, the Research Team recommends that more testing be conducted to optimize the CFRP anchorage systems. Two types that need to be investigated are a hybrid system with CFRP strip and spike anchors.

## 7. References

- ACI Committee 440. (2008). *ACI 440.2R-08: Guide for the Design and Construction of Externally Bonded FRP Systems for Strengthening Concrete Structures*. American Concrete Institute. Farmington Hills: American Concrete Institute. Retrieved 2022
- ACI Committee 440. (2017). *ACI 440.2R-17: Guide for the Design and Construction of Externally Bonded FRP Systems for Strengthening Concrete Structures*. Farmington Hills: American Concrete Institute. Retrieved 2022
- Aljaafreh, T. (2019). *Performance of Precast Concrete Bridge Girders with Externally Bonded CFRP*. The University of Texas at Arlington. Arlington: The University of Texas at Arlington. Retrieved January 2022
- Aljaafreh, T. (2019). *Performance of Precast Concrete Bridge Girders with Externally Bonded Anchored CFRP*. The University of Texas at Arlington. Arlington: Aljaafreh, Tariq. Retrieved February 14, 2022
- American Concrete Institute. (2019). *ACI 318-19: Building Code Requirements for Structural Concrete*. Farmington Hills: American Concrete Institute. Retrieved 2022
- Canadian Standards Association. (2012). *CSA S806-12: Design and Construction of Building Structures with Fiber-Reinforced Polymers*. Mississauga, Ontario: Canadian Standards Association. Retrieved 2022
- Chen, J., & Teng, J. (2001, July 1). Anchorage Strength Models for FRP and Steel Plates Bonded to Concrete. *Journal of Structural Engineering*, 127(7), 1-8.  
doi:[https://doi.org/10.1061/\(ASCE\)0733-9445\(2001\)127:7\(784\)](https://doi.org/10.1061/(ASCE)0733-9445(2001)127:7(784))
- del Rey Castillo, E., & Kaniitkar, R. (2021). Effect of FRP Spike Anchor Installation Quality and Concrete Repair on the Seismic Behavior of FRP-Strengthened RC Columns. *Journal of Composites for Construction*, 25(1), 1-14. Retrieved February 14, 2022, from [https://doi.org/10.1061/\(ASCE\)CC.1943-5614.0001095](https://doi.org/10.1061/(ASCE)CC.1943-5614.0001095)
- del Rey Castillo, E., Dizhur, D., & Griffith, M. (2019, February 1). Strengthening RC structures using FRP spike anchors in combination with EBR systems. *Composite Structures*, 209, 668-685. doi:<https://doi.org/10.1016/j.compstruct.2018.10.093>
- del rey Castillo, E., Kaniitkar, R., Smith, S., Griffith, M., & Ingham, J. (2019, April 15). Design approach for FRP spike anchors in FRP-strengthened RC structures. *Composite Structures*, 214, 23-33. doi:<https://doi.org/10.1016/j.compstruct.2019.01.100>
- Eamon. (2014). *Checklist To Designate Areas of Evaluation For CFRP*. MDOT.
- ElSafty, A., & Graeff, M. K. (2012). *The Repair of Damaged Bridge Girders with Carbon-Fiber-Reinforced Polymer "CFRP" Laminates*. University of North Florida, College of Computing, Engineering, and Construction. Jacksonville: Florida Department of Transportation. Retrieved February 15, 2022, from <https://www.fdot.gov/docs/default-source/structures/structuresresearchcenter/Final-Reports/BDK82-977-03.pdf>
- European Committee for Standardization. (2004). *Eurocode 2: Design of concrete structures*. Brussels: European Committee for Standardization. Retrieved 2022
- Fédération Internationale du Béton. (2001). *fib Bulletin 14: Externally Bonded FRP Reinforcement for RC Structures*. Lausanne: Fédération Internationale du Béton. Retrieved February 16, 2022
- Florida Department of Transportation. (2021). *FDOT SDM Volume 4: Fiber Reinforced Polymer Guidelines (FRPG)* (Vol. 4). Florida, USA: FDOT. Retrieved February 16, 2022
- Fortec Stabilization. (2017). *BASF Loading Dock*. Matawan: Fortec Stabilization. Retrieved 2022, from <https://fortecstabilization.com/project/fortec-stabilization-case-study-basf/>

- Fortec Stabilization. (2021). *Omin Parking Garage*. Dallas: Fortec Stabilization. Retrieved 2022, from <https://fortecstabilization.com/project/omin-parking-garage-dallas-tx/>
- Fyfe. (2019). *Greenway Bridge End Rehabilitation*. Wisconsin Department of Transportation. Monroe: Fyfe. Retrieved March 21, 2022
- Garcia, J., Sun, W., Kim, C., Ghannoum, W. M., & Jirsa, J. O. (2014). *Procedures for the Installation and Quality Control of Anchored CFRP Sheets for Shear Strengthening of Concrete Bridge Girders*. The University of Texas at Austin, Center for Transportation Research. Austin: TxDOT. Retrieved February 16, 2022
- Grelle, S. V. (2011). *Categorization and experimental evaluation of anchorage systems for fiber-reinforced polymer laminates bonded to reinforced concrete structures*. Missouri University Of Science And Technology, Civil Engineering. Rolla: Scholars' Mine. Retrieved February 22, 2022
- Grelle, S. V., & Sneed, L. H. (2013). Review of Anchorage Systems for Externally Bonded FRP Laminates. *International Journal of Concrete Structures*, 7, 17-33. Retrieved February 22, 2022, from <https://ijcsm.springeropen.com/articles/10.1007/s40069-013-0029-0>
- Hutchinson, R. L., Abdelrahman, A. A., & Rizkalla, S. H. (1998). *Shear Strengthening Using CFRP Sheets for Prestressed Concrete Bridge Girders in Manitoba, Canada*. Manitoba. Retrieved February 22, 2022
- Japan Society of Civil Engineers. (2001). *Recommendations for Upgrading of Concrete Structures with Use of Continuous Fiber Sheets*. Japan: JSCE. Retrieved 2022
- Japan Society of Civil Engineers. (2007). *Standard Specifications for Concrete Structures - Design*. Tokyo: JSCE. Retrieved 2022
- Jinno, Y., Tsukagoshi, H., & Yabe, Y. (2001). RC beams with slabs strengthened by CF sheets and bundles of CF strands. *5th International Conference on Fibre Reinforced Plastics for Reinforced Concrete Structures*. 2, pp. 981-988. London: Thomas Telford. Retrieved February 14, 2022
- Jirsa, J. O., Ghannoum, W. M., Kim, C. H., Sun, W., Shekarchi, W. A., Alotaibi, N. K., . . . Wang, H. (2017). *Use of Carbon Fiber Reinforced Polymer (CFRP) with CFRP Anchors for Shear-Strengthening and Design Recommendations/Quality Control Procedures for CFRP Anchors*. Technical Report, University of Texas, Austin, Austin. Retrieved February 22, 2022
- Kahl, S. (2012). *Design and Construction Guidelines for Strengthening Bridges using Fiber Reinforced Polymers (FRP) OR10-039*. Michigan University. Lansing: Michigan Department of Transportation. Retrieved 2022
- Kalfat, R., & Al-Mahaidi, R. (2010, October 10). Investigation into bond behaviour of a new CFRP anchorage system for concrete utilising a mechanically strengthened substrate. *Composite Structures*, 92(11), 2738-2746. doi:<https://doi.org/10.1016/j.compstruct.2010.04.004>
- Khalifa, A., Gold, W. J., Nanni, A., & Aziz M.I., A. (1998, November). Contribution of Externally Bonded FRP to Shear Capacity of RC Flexural Members. *Journal of Composites for Construction*, 2(4). Retrieved February 22, 2022, from <https://ascelibrary.org/doi/10.1061/%28ASCE%291090-0268%281998%292%3A4%28195%29>
- Khalifa, A., Nanni, A., Alkhrdaji, T., & Lansburg, S. (1999, October). Anchorage of Surface Mounted FRP Reinforcement. *Concrete International: Design and Construction*, 21(10), 49-54. Retrieved February 22, 2022

- Kim, Y. J., & Bhiri, M. (2020, January 1). Grid U-Wrap Anchorage for Reinforced Concrete Beams Strengthened with Carbon Fiber-Reinforced Polymer Sheets. *Structural Journal*, 117(1), 3-15. Retrieved February 22, 2022
- Kim, Y., Quinn, K., Satrom, N., Garcia, J., Sun, W., Channoum, W. M., & Jirsa, J. O. (2012). *Shear Strengthening of Reinforced and Prestressed Concrete Beams Using Carbon Fiber Reinforced Polymer (CFRP) Sheets and Anchors*. University of Texas at Austin, Center for Transportation Research. Austin: Texas Department of Transportation. Retrieved March 1, 2022, from [https://ctr.utexas.edu/wp-content/uploads/pubs/0\\_6306\\_1.pdf](https://ctr.utexas.edu/wp-content/uploads/pubs/0_6306_1.pdf)
- Kobayashi, K., Fujil, S., Yabe, Y., Tsukagoshi, H., & Sugiyama, T. (2001). Advanced wrapping system with CF-anchor – Stress transfer mechanism of CF-anchor. In C. J. Burgoyne (Ed.), *5th International Conference on Fibre Reinforced Plastics for Reinforced Concrete Structures. 1*, pp. 379-388. London: Thomas Telford. Retrieved March 1, 2022, from <http://www-civ.eng.cam.ac.uk/frprcs5/proceedings.htm>
- KSDOT. (2012). *Theoretical Specific Gravity of a Combination of Aggregates*. KSDOT. Retrieved February 14, 2022
- Laursen, P. T., Seible, F., Hegemier, G. A., & Innamorato, D. (1995). *Seismic Repair and Retrofit of Masonry Walls with Carbon Overlays*. (L. Taerwe, Ed.) San Diego, California, USA: University of California. Retrieved February 28, 2022
- McGuirk, G. N., & Brena, S. F. (2012). *Development of Anchorage System for FRP Strengthening Applications Using Integrated FRP Composite Anchors*. University of Massachusetts Amherst, Department of Civil and Environmental Engineering. Amherst: ACI Foundation. Retrieved March 1, 2022, from [https://www.acifoundation.org/Portals/12/Files/PDFs/CRC\\_report-FRP\\_anchors-Brena.pdf](https://www.acifoundation.org/Portals/12/Files/PDFs/CRC_report-FRP_anchors-Brena.pdf)
- Mohamed, K., Abdalla, J. A., & Hawileh, R. A. (2020, September 30). Experimental and Analytical Investigations of the Use of Groove-Epoxy Anchorage System for Shear Strengthening of RC Beams Using CFRP Laminates. *Materials*, 13(19). Retrieved March 1, 2022, from <https://doi.org/10.3390/ma13194350>
- Pudliner, D., Ghannoum, W. M., & Jirsa, J. O. (2019, October). Influence of Anchor Size on Anchored CFRP Systems. *Journal of Composites for Construction*, 23(5). Retrieved March 3, 2022, from [https://doi.org/10.1061/\(ASCE\)CC.1943-5614.0000954](https://doi.org/10.1061/(ASCE)CC.1943-5614.0000954)
- Sato, Y., Ueda, T., Kakuta, Y., & Tanaka, T. (1996). Shear Reinforcing Effect of Carbon Fiber Sheet Attached to Side of Reinforced Concrete Beams. In M. El-Badry (Ed.), *Proceedings of the Second International Conference on Advanced Composite Materials in Bridges and Structures* (pp. 621-627). Quebec: Canadian Society for Civil Engineering. Retrieved 2022
- SDR Engineering Consultants, Inc. (2017, December). County Road 514 Br. I-75 Girder Repair. Florida, United States of America: State Road Department. Retrieved March 3, 2022
- SDR Engineering Consultants, Inc. (2018, October). PGA Boulevard over Florida's Turnpike. Florida, United States of America: Florida Department of Transportation. Retrieved March 3, 2022
- University of Miami. (2016). *Evaluation of Anchoring Solution for Externally Bonded Fiber Reinforced Polymer (FRP) Systems*. Structures and Materials Laboratory, College of Engineering. Coral Gables: Fortress Stabilization Systems. Retrieved 2022
- Woods, J. (2014). *Carleton Shear Wall Tests*. Ontario: Carleton University. Retrieved 2022

- WSP Global Inc. (2020). Load Rating Calculations I-95 Express Lanes Phase 3B-2. Florida, United States of America: Florida Department of Transportation.
- WSP USA Inc. (2020, July). Glades Road Over I-95. Boca Raton, Florida, Palm Beach: Florida Department of Transportation. Retrieved 2022
- Yamaguchi, T., Kato, Y., Nishimura, T., & Uomoto, T. (1997). Creep Rupture of FRP Rods Made of Aramid, Carbon, and Glass Fibers. *3rd International Symposium on Non-Metallic (FRP) Reinforcement for Concrete Structures, 2*, pp. 179-186. Sapporo. Retrieved 2022
- Yuan, H., & Wu, Z. (1999). Interfacial fracture theory in structures strengthened with composite of continuous fiber. *Proceedings of the symposium of China and Japan: Science and technology of 21st century*, (pp. 142-155). Tokyo. Retrieved 2022
- Zaki, M. A., Rasheed, H. A., & Alkhrdaji, T. (2019, November 1). Performance of CFRP-strengthened concrete beams fastened with distributed CFRP dowel and fiber anchors. *Composites Part B: Engineering, 176*.  
doi:<https://doi.org/10.1016/j.compositesb.2019.107117>


# Appendix A: Design Details of Top Three Ranked Anchoring Systems

CARBON FIBER REINFORCED POLYMER REPAIR NOTES—SPIKE ANCHORS

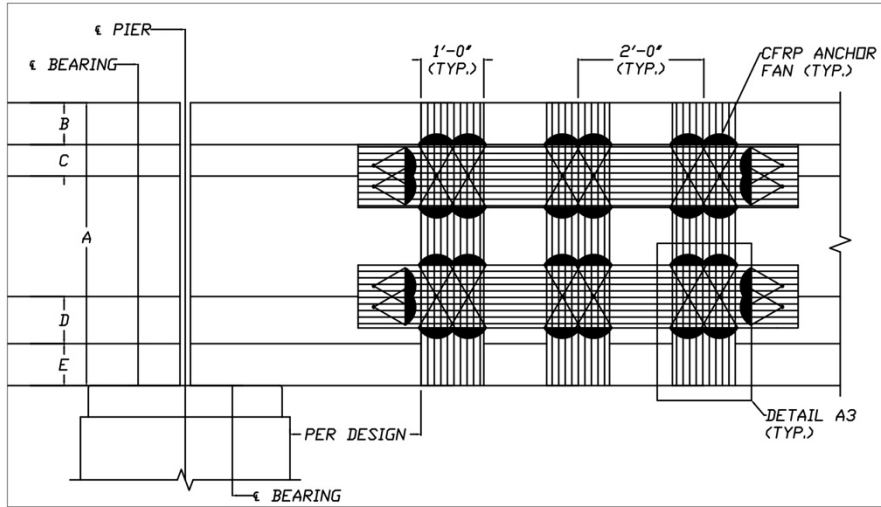
1. NUMBER OF CFRP SPIKE ANCHORS AND AMOUNT OF CFRP LAMINATE DETERMINED BASED ON MOST CURRENT RESEARCH.
2. THE EXTENT OF REPAIR WILL DICTATE THE NUMBER OF VERTICAL STRIPS USED.
3. VERTICAL STRIP WIDTH VARIES BASED ON MEMBER GEOMETRY AND ANCHOR TYPE.
4. HORIZONTAL STRIP WIDTH VARIES BASED ON MEMBER GEOMETRY.
5. FAN ANGLE (60 DEG.) REMAINS CONSTANT AMONG ALL MEMBERS.
6. ANCHORS SHOULD ALWAYS BE PLACED WITHIN THE VOLUME OF CONCRETE ENCLOSED BY THE TRANSVERSE REINFORCEMENT.
7. IF A STEEL BAR/REINFORCEMENT IS ENCOUNTERED DURING INSTALLATIONS, THE HOLE MAY BE USED BUT INCLINED 10 DEG. TO EITHER SIDE OF THE OBSTRUCTION.
8. IT IS RECOMMENDED THAT EACH ANCHOR HOLE AREA EQUAL 1.4 TIMES THE AREA OF THE CFRP ANCHOR.
9. AN ANCHOR HOLE CHAMFER RADIUS OF 0.5" IS RECOMMENDED (WHERE APPLICABLE).
10. ANCHOR FAN LENGTH OF AT LEAST 6" IS RECOMMENDED FOR ALL APPLICATIONS.
11. ALL HORIZONTAL AND VERTICAL CFRP STRIPS SERVE AS "PATCHING" (A PRACTICE COMMONLY UTILIZED FOR CFRP ANCHORAGE); HENCE, NO INDIVIDUAL PATCHES ARE NECESSARY.
12. SURFACE MUST BE CLEAN, SOUND AND DRY. REMOVE DUST, LAITANCE, GREASE, CURING COMPOUNDS, IMPREGNATIONS, WAXES, FOREIGN ARTICLES, DISINTEGRATED MATERIALS, AND OTHER BOND INHIBITING MATERIALS.
13. EXISTING UNEVEN SURFACES MUST BE FILLED WITH AN APPROPRIATE REPAIR MORTAR.
14. CRACKS WITH A WIDTH GREATER THAN OR EQUAL TO 0.008" MUST BE STABILIZED USING EPOXY INJECTION METHODS, PRIOR TO APPLICATION OF CFRP.
15. A UV PROTECTIVE COATING IS RECOMMENDED TO BE APPLIED TO ALL ANCHOR AREAS WITHIN 24 HOURS OF ANCHOR INSTALLATION.
16. THE RECOMMENDATIONS PROVIDED HEREIN SHOULD BE EVALUATED EXPERIMENTALLY PRIOR TO ADOPTION.

CFRP SPIKE ANCHOR INSTALLATION SEQUENCE

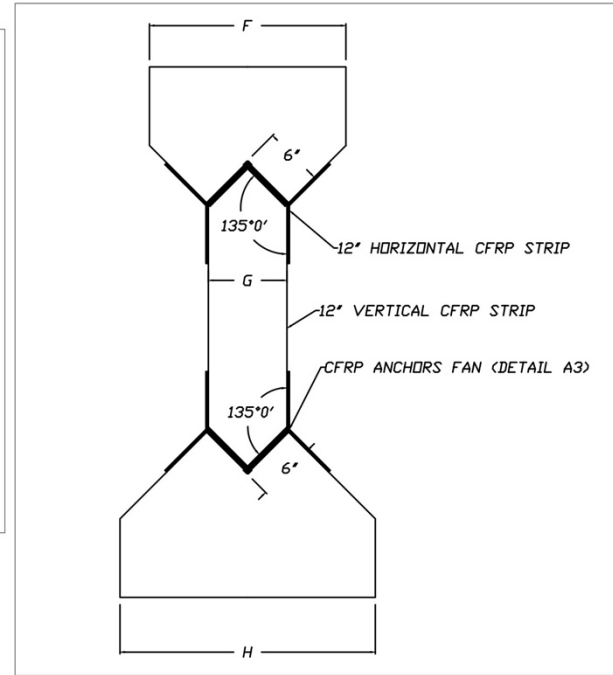
1. USE A NON-DESTRUCTIVE METHOD TO DETERMINE LOCATION OF REINFORCEMENT IN THE BEAMS. THE CONTRACTOR MAY ADJUST THE LOCATION OF THE CFRP ANCHORS UP TO 1" IN THE BOTH THE VERTICAL AND HORIZONTAL DIRECTIONS TO AVOID REINFORCEMENT. NOTIFY THE ENGINEER IF GREATER ADJUSTMENT IS REQUIRED.
2. THE ENGINEER MUST BE NOTIFIED IF ANCHOR HOLES MUST BE ANGLED.
3. DRILL A HOLE IN THE BEAM AT THE LOCATIONS AND DEPTH SHOWN IN THE PLANS.
4. ROUND THE EDGES AROUND THE LIP OF THE DRILLED HOLE. THE CHAMFER RADIUS SHALL NOT BE SMALLER THAN SPECIFIED.
5. CLEAN AND REMOVE ALL DEBRIS FROM THE ANCHORAGE HOLE USING NEGATIVE VACUUM PRESSURE.
6. INSTALL MAIN CFRP STRIPS IN ACCORDANCE WITH THESE PLANS AND TECHNICAL AND MANUFACTURER SPECIAL PROVISIONS.
7. MAIN CFRP STRIPS SHOULD COMPLETELY COVER THE ANCHOR HOLES. THE INDIVIDUAL FIBERS OF THE SATURATED CARBON FABRIC SHOULD BE SEPARATED TO ALLOW FOR INSTALLATION OF THE ANCHORS.
8. APPLY A COAT OF HIGH STRENGTH STRUCTURAL EPOXY TO THE INNER SURFACE OF THE ANCHOR HOLE.
9. FAN THE ENDS OF THE ANCHOR STRIPS TO ACHIEVE THE 60 DEG. FAN PROFILE.
10. COMPLETELY IMPREGNATE THE ANCHORS WITH THE HIGH STRENGTH STRUCTURAL EPOXY.
11. PUSH THE SATURATED ANCHORS INTO THE PRE-DRILLED HOLES.
12. SPREAD THE ANCHOR FAN AS SHOWN IN THE PLANS. THE FAN SHALL EXTEND  $\frac{1}{2}$ " BEYOND THE EDGES OF THE CFRP STRIPS.
13. APPLY THE UV PROTECTIVE COATING AT ALL ANCHOR LOCATIONS.

CARBON FIBER REINFORCED POLYMER SPIKE ANCHORS						
						
CLASSIFIED TYPE I THROUGH IV CFRP REINFORCEMENT DETAILS FLORIDA DEPARTMENT OF TRANSPORTATION						
<table border="1" style="width: 100%; border-collapse: collapse;"> <tr> <td style="width: 30%;">DOT-RFP 21-3033-04</td> <td style="width: 70%;">PJR</td> </tr> <tr> <td>1/31/22</td> <td>NS</td> </tr> <tr> <td>NOTED</td> <td>PJR</td> </tr> </table>	DOT-RFP 21-3033-04	PJR	1/31/22	NS	NOTED	PJR
DOT-RFP 21-3033-04	PJR					
1/31/22	NS					
NOTED	PJR					
A-1						

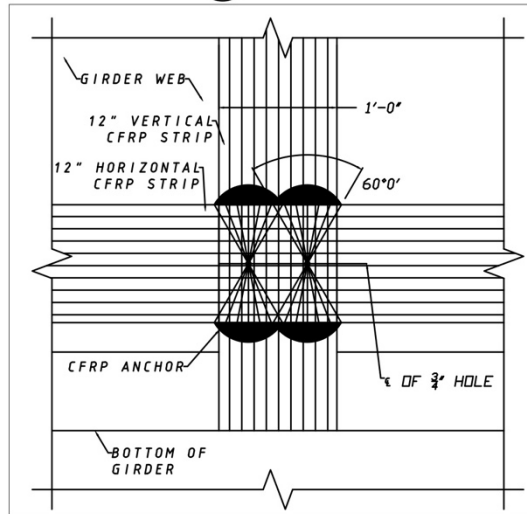




A1 AASHTO GIRDER I-IV SPIKE ANCHORS-ELEVATION



A2 AASHTO GIRDER I-IV SPIKE ANCHORS-SECTION



A3 AASHTO GIRDER I-IV SPIKE ANCHORS-DETAILS

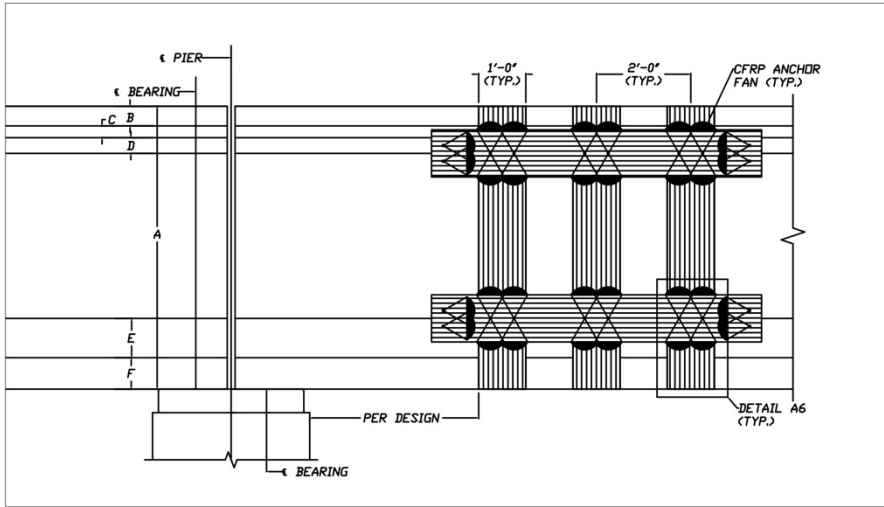
TABLE OF DIMENSIONS								
BEAM	A	B	C	D	E	F	G	H
AASHTO I	2'-4"	0'-4"	0'-3"	0'-5"	0'-5"	1'-0"	0'-6"	1'-4"
AASHTO II	3'-0"	0'-6"	0'-3"	0'-6"	0'-6"	1'-0"	0'-6"	1'-6"
AASHTO III	3'-9"	0'-7"	0'-5"	0'-8"	0'-7"	1'-4"	0'-7"	1'-10"
AASHTO IV	4'-6"	0'-8"	0'-6"	0'-9"	0'-8"	1'-8"	0'-8"	2'-2"

CARBON FIBER REINFORCED POLYMER SPIKE ANCHORS

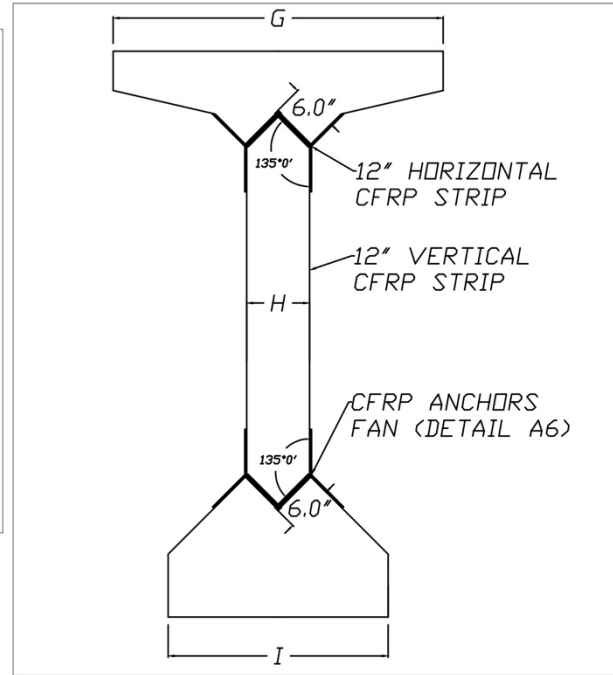


AASHTO TYPE I THROUGH IV CFRP REINFORCEMENT DETAILS  
FLORIDA DEPARTMENT OF TRANSPORTATION

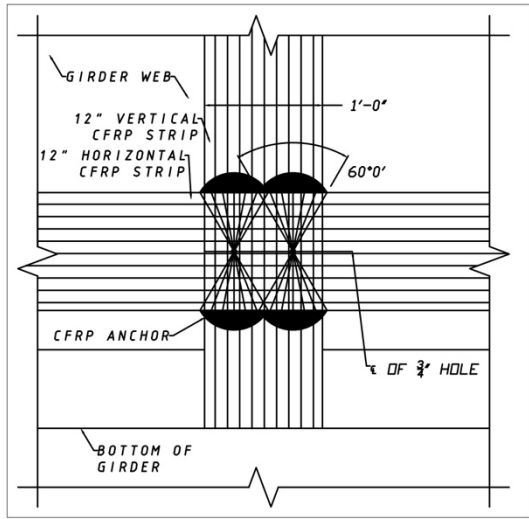
001-887 P.R.  
21-103-CA  
1/31/22 P.R.  
NOTED P.R.



A4 AASHTO GIRDER V-VI SPIKE ANCHORS-ELEVATION



A5 AASHTO GIRDER V-VI SPIKE ANCHORS-SECTION



A6 AASHTO GIRDER V-VI SPIKE ANCHORS-DETAILS

TABLE OF DIMENSIONS

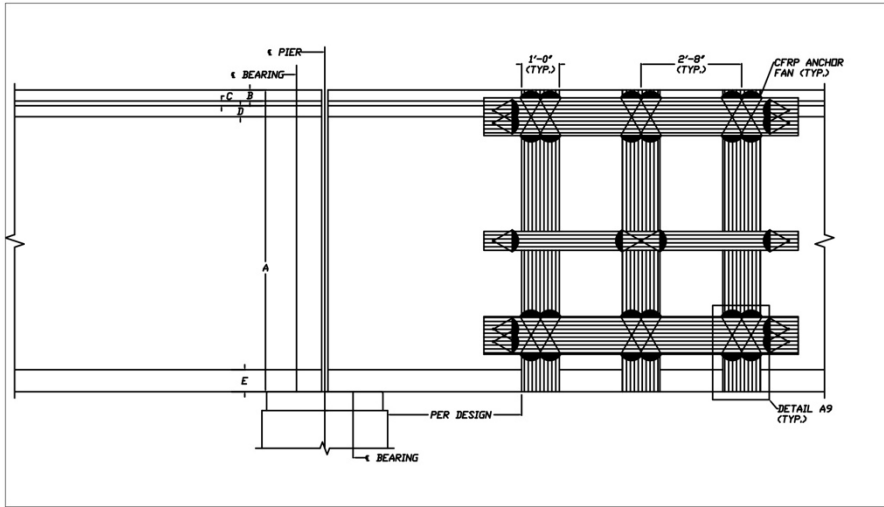
BEAM	A	B	C	D	E	F	G	H	I
AASHTO V	5'-3"	0'-5"	0'-3"	0'-4"	0'-10"	0'-8"	3'-6"	0'-8"	2'-4"
AASHTO VI	6'-0"	0'-5"	0'-3"	0'-4"	0'-10"	0'-8"	3'-6"	0'-8"	2'-4"

CARBON FIBER REINFORCED POLYMER SPIKE ANCHORS

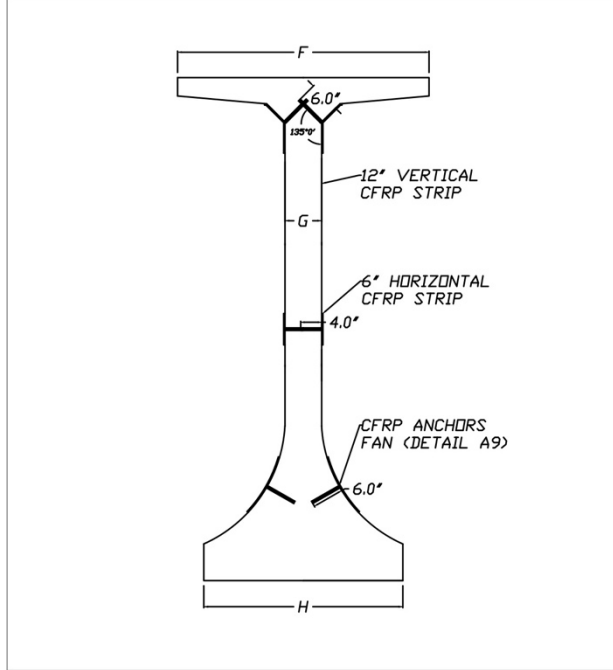


AASHTO TYPE V THROUGH VI CFRP REINFORCEMENT DETAILS  
FLORIDA DEPARTMENT OF TRANSPORTATION

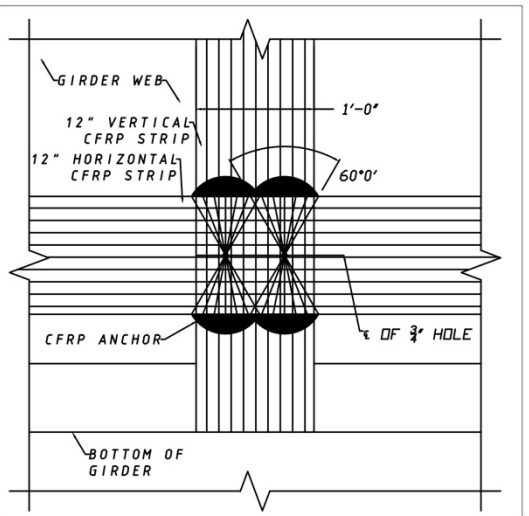
DOT-RP 21-2033-04	PJR
1/31/22	NS
NOTED	PJR



A7 FLORIDA I-BEAM SPIKE ANCHORS-ELEVATION



A8 FLORIDA I-BEAM SPIKE ANCHORS-SECTION



A9 FLORIDA I-BEAM SPIKE ANCHORS-DETAILS

TABLE OF DIMENSIONS

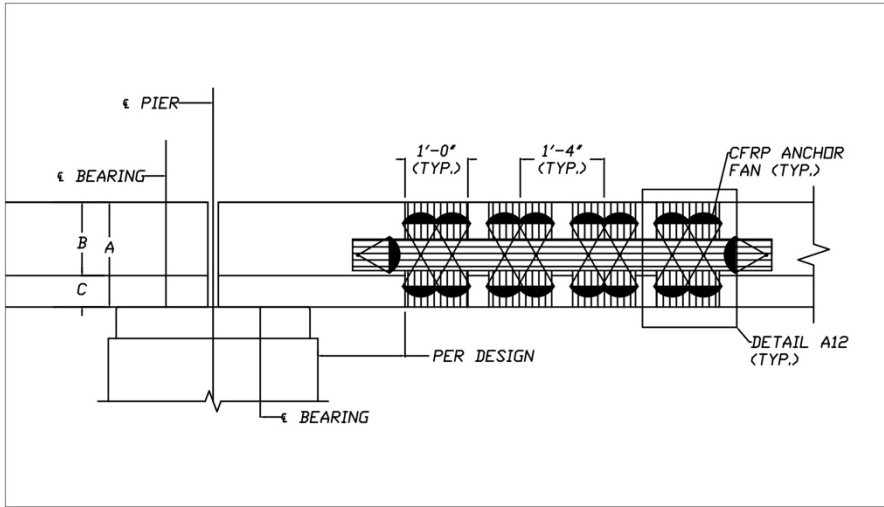
BEAM	A	B	C	D	E	F	G	H
BULB T-78	6'-6"	0'-3"	0'-4"	0'-3"	0'-8"	5'-0"	0'-7"	2'-4"
F I-96	8'-0"	0'-3 1/2"	0'-1 1/2"	0'-3 1/2"	0'-6"	4'-0"	0'-7"	3'-2"

CARBON FIBER REINFORCED POLYMER SPIKE ANCHORS

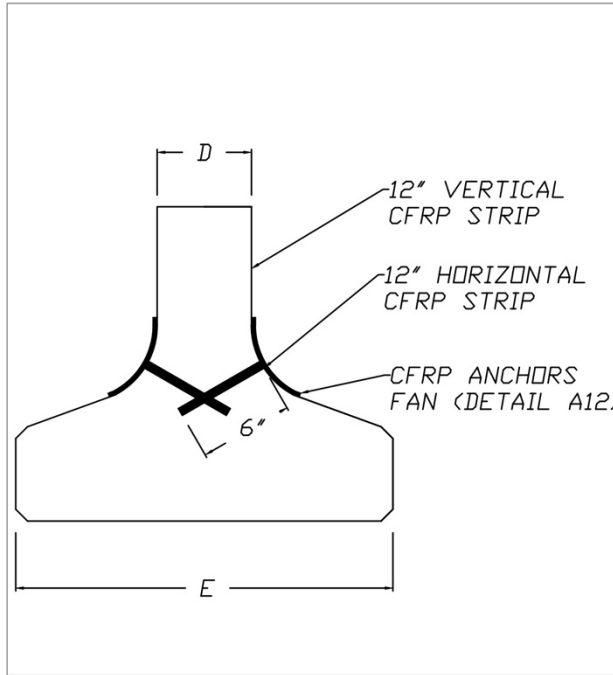


FLORIDA I-BEAM CFRP REINFORCEMENT DETAILS  
FLORIDA DEPARTMENT OF TRANSPORTATION

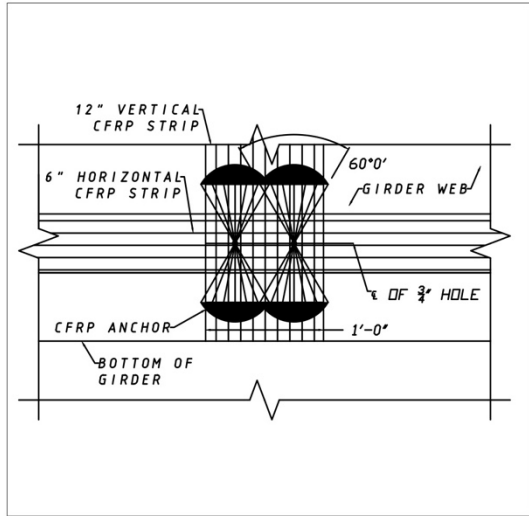
DOT-889 21-903-01	P.J.R.
1/31/22	NS
NOTED	P.J.R.



A10 INVERTED T-BEAM SPIKE ANCHORS—ELEVATION



A11 INVERTED T-BEAM SPIKE ANCHORS—SECTION



A12 INVERTED T-BEAM SPIKE ANCHORS—DETAILS

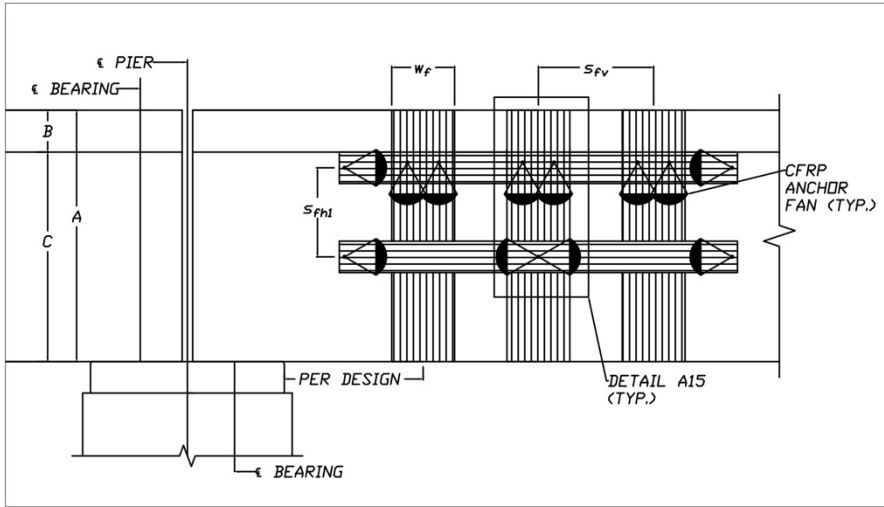
TABLE OF DIMENSIONS					
BEAM	A	B	C	D	E
INVERTED T-BEAM	1'-8"	1'-2"	0'-6"	0'-6"	2'-0"

CARBON FIBER REINFORCED POLYMER SPIKE ANCHORS

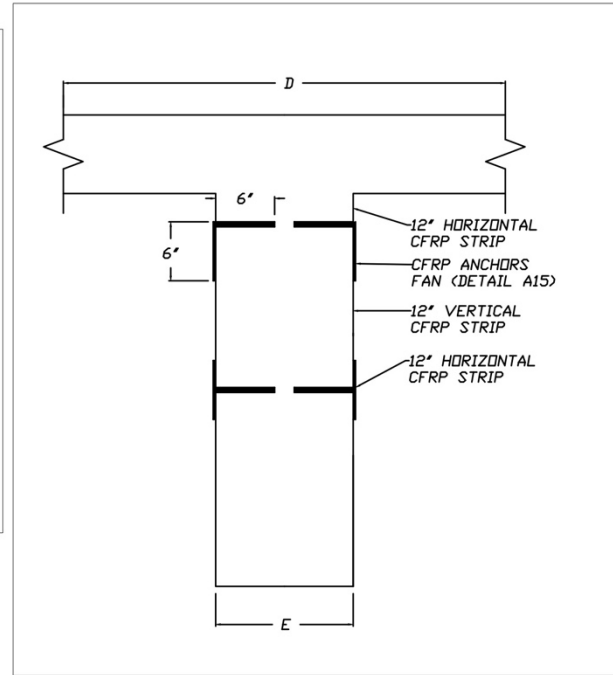


INVERTED T-BEAM CFRP REINFORCEMENT DETAILS  
FLORIDA DEPARTMENT OF TRANSPORTATION

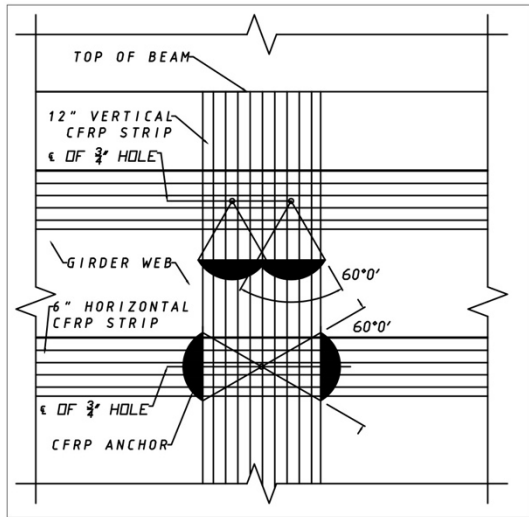
DOT-RFP 21-6033-0A	PJR
1/31/22	NS
NOTED	PJR



A13 RC BEAM (GENERIC) SPIKE ANCHORS-ELEVATION



A14 RC BEAM (GENERIC) SPIKE ANCHORS-SECTION



A15 RC BEAM (GENERIC) SPIKE ANCHORS-DETAILS

TABLE OF DIMENSIONS								
BEAM	A	B	C	D	E	F	Sfv	Sphi
RC T-BEAM	VARIABLES	VARIABLES	VARIABLES	VARIABLES	VARIABLES	VARIABLES	VARIABLES	VARIABLES

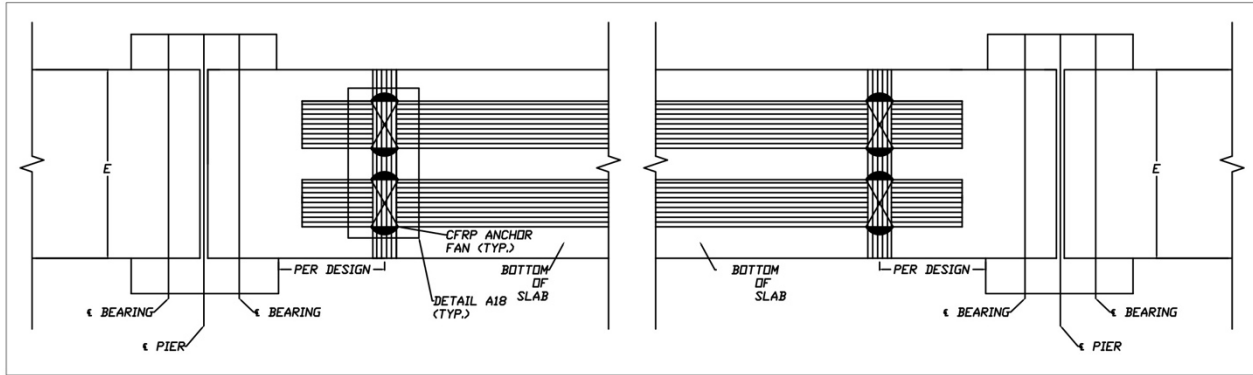
- NOTES
1. THE DETAILS SHOWN FOR THE "RC BEAM" ARE GENERIC AND WILL VARY BASED ON BEAM GEOMETRY.
  2. THE TOP FLANGE OF THE RC BEAM IS REPRESENTATIVE OF A SLAB AND SHOULD NOT BE WRAPPED OR ANCHORED.
  3. SPACING OF HORIZONTAL AND VERTICAL CFRP STRIPS SHALL BE DETERMINED BY BEAM DEPTH.
  4. SPACING OF VERTICAL STRIPS SHOULD BE UNIFORM ALONG THE ENTIRE LENGTH OF THE REPAIRED ZONE.

CARBON FIBER REINFORCED POLYMER SPIKE ANCHORS

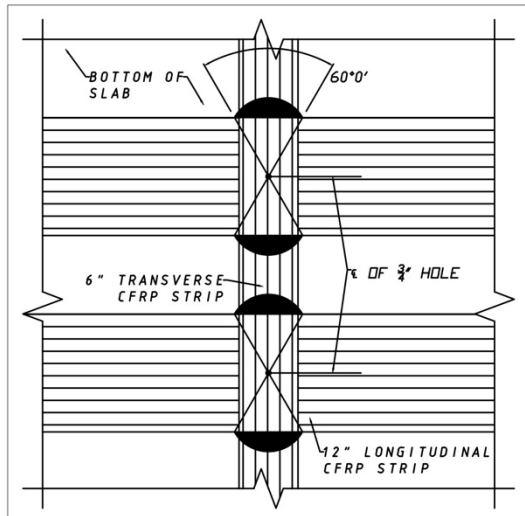


REINFORCED CONCRETE BEAM (GENERIC) DETAIL OF REINFORCEMENT DETAILS  
FLORIDA DEPARTMENT OF TRANSPORTATION

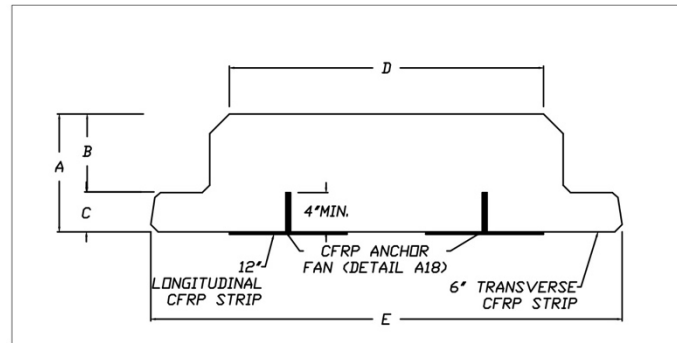
DOT-RFP 21-8033-04	PJR
1/31/22	NS
NOTED	PJR
A-6	



A16 SLAB BEAM SPIKE ANCHORS—BOTTOM VIEW



A18 SLAB BEAM SPIKE ANCHORS—DETAILS



A17 SLAB BEAM SPIKE ANCHORS—SECTION

TABLE OF DIMENSIONS

BEAM	A	B	C	D	E
12"	1'-0"	0'-8"	0'-4"	VARIES	VARIES
15"	1'-3"	0'-11"	0'-4"	VARIES	VARIES
18"	1'-6"	1'-2"	0'-4"	VARIES	VARIES

CARBON FIBER REINFORCED POLYMER SPIKE ANCHORS



SLAB BEAM CFRP REINFORCEMENT DETAILS  
FLORIDA DEPARTMENT OF TRANSPORTATION

DOT-RFP 21-8033-04	PJR
1/31/22	NS
NOTED	PJR

CARBON FIBER REINFORCED POLYMER REPAIR NOTES—MECHANICAL ANCHORS

1. NUMBER OF MECHANICAL ANCHORS AND AMOUNT OF CFRP LAMINATE DETERMINED BASED ON MOST CURRENT RESEARCH.
2. THE EXTENT OF REPAIR WILL DICTATE THE NUMBER OF VERTICAL STRIPS AND MECHANICAL ANCHORS USED.
3. VERTICAL STRIP WIDTH MAY VARY BASED ON MEMBER GEOMETRY AND ANCHOR TYPE.
4. NO HORIZONTAL STRIPS ARE NECESSARY IF MECHANICAL ANCHORS ARE UTILIZED.
5. ANCHORS SHOULD ALWAYS BE PLACED WITHIN THE VOLUME OF CONCRETE ENCLOSED BY THE TRANSVERSE REINFORCEMENT.
6. IF A STEEL BAR/REINFORCEMENT IS ENCOUNTERED DURING INSTALLATIONS, THE ENGINEER MUST BE CONSULTED TO DETERMINE PROPER MITIGATION TECHNIQUES.
7. SURFACE MUST BE CLEAN, SOUND AND DRY. REMOVE DUST, LAITANCE, GREASE, CURING COMPOUNDS, IMPREGNATIONS, WAXES, FOREIGN ARTICLES, DISINTEGRATED MATERIALS, AND OTHER BOND INHIBITING MATERIALS.
8. EXISTING UNEVEN SURFACES MUST BE FILLED WITH AN APPROPRIATE REPAIR MORTAR.
9. CRACKS WITH A WIDTH GREATER THAN OR EQUAL TO 0.008" MUST BE STABILIZED USING EPOXY INJECTION METHODS, PRIOR TO APPLICATION OF CFRP.
10. A UV PROTECTIVE COATING IS RECOMMENDED TO BE APPLIED TO ALL ANCHOR AREAS WITHIN 24 HOURS OF ANCHOR INSTALLATION.
11. THE RECOMMENDATIONS PROVIDED HEREIN SHOULD BE EVALUATED EXPERIMENTALLY PRIOR TO ADOPTION.

CFRP MECHANICAL ANCHOR INSTALLATION SEQUENCE

1. USE A NON-DESTRUCTIVE METHOD TO DETERMINE LOCATION OF REINFORCEMENT IN THE BEAMS. THE CONTRACTOR MUST NOTIFY THE ENGINEER IF ADJUSTMENT IS REQUIRED DUE TO CONFLICT WITH REINFORCEMENT.
2. DRILL A HOLE IN THE BEAM AT THE LOCATIONS AND DEPTH SHOWN IN THE PLANS.
3. CLEAN AND REMOVE ALL DEBRIS FROM THE ANCHORAGE HOLE USING NEGATIVE VACUUM PRESSURE.
4. INSTALL VERTICAL CFRP STRIPS IN ACCORDANCE WITH THESE PLANS AND TECHNICAL AND MANUFACTURER SPECIAL PROVISIONS.
5. APPLY A COAT OF HIGH STRENGTH STRUCTURAL EPOXY TO THE INNER SURFACE OF THE ANCHOR HOLE.
6. COMPLETELY IMPREGNATE THE ADHESIVE ANCHORS WITH THE HIGH STRENGTH STRUCTURAL EPOXY.
7. COMPLETELY IMPREGNATE MECHANICAL ANCHOR HARDWARE (STEEL PLATE) WITH THE HIGH STRENGTH STRUCTURAL EPOXY.
8. PUSH THE SATURATED PLATE ONTO THE VERTICAL STRIPS, ALIGNING THE ANCHOR HOLE IN THE PLATE TO THE DRILLED HOLE IN THE BEAM.
9. PUSH THE ANCHORS THROUGH THE HOLES IN THE ANCHOR PLATES AND INTO THE PRE-DRILLED HOLES IN THE BEAM.
10. APPLY THE UV PROTECTIVE COATING AT ALL ANCHOR LOCATIONS.

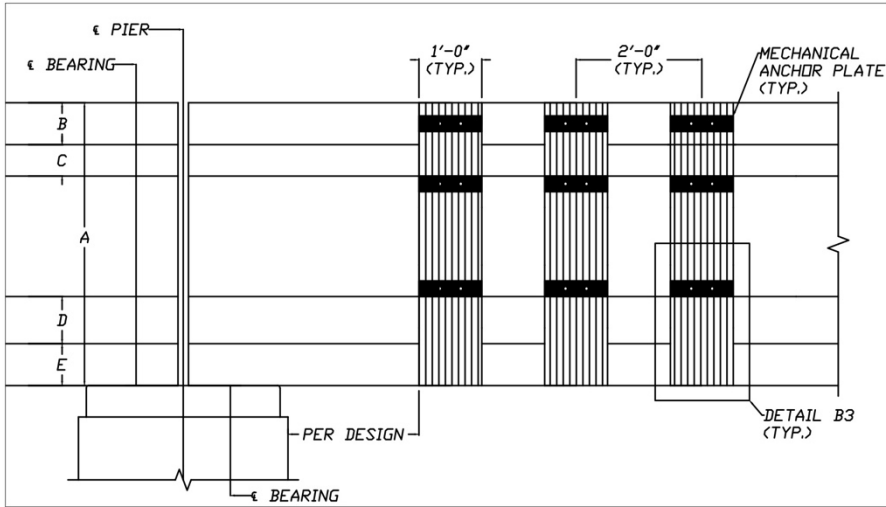
CARBON FIBER REINFORCED POLYMER  
MECHANICAL ANCHORS



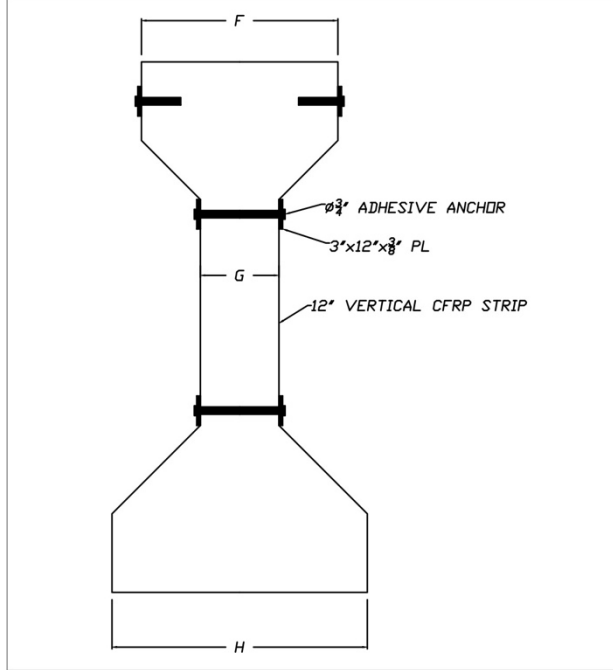
ASHTO TYPE I THROUGH IV CFRP  
REINFORCEMENT DETAILS  
FLORIDA DEPARTMENT OF  
TRANSPORTATION

DOT-REP FL-803-CA	PJR
1/31/22	NS
NOTED	PJR

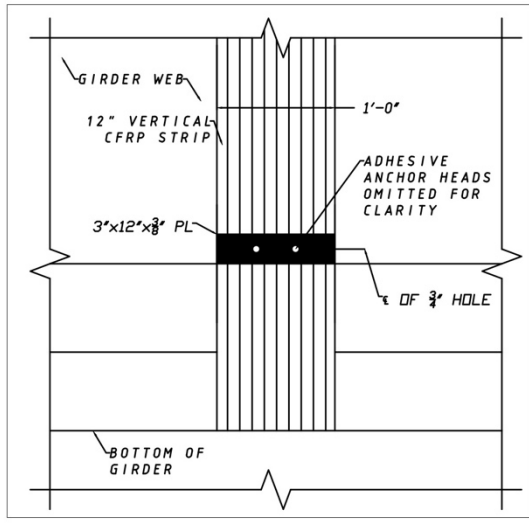




B1 AASHTO GIRDER I-IV MECHANICAL ANCHORS-ELEVATION



B2 AASHTO GIRDER I-IV MECHANICAL ANCHORS-SECTION



B1 AASHTO GIRDER I-IV MECHANICAL ANCHORS-DETAILS

TABLE OF DIMENSIONS								
BEAM	A	B	C	D	E	F	G	H
AASHTO I	2'-4"	0'-4"	0'-3"	0'-5"	0'-5"	1'-0"	0'-6"	1'-4"
AASHTO II	3'-0"	0'-6"	0'-3"	0'-6"	0'-6"	1'-0"	0'-6"	1'-6"
AASHTO III	3'-9"	0'-7"	0'-5"	0'-8"	0'-7"	1'-4"	0'-7"	1'-10"
AASHTO IV	4'-6"	0'-8"	0'-6"	0'-9"	0'-8"	1'-8"	0'-8"	2'-2"

CARBON FIBER REINFORCED POLYMER MECHANICAL ANCHORS

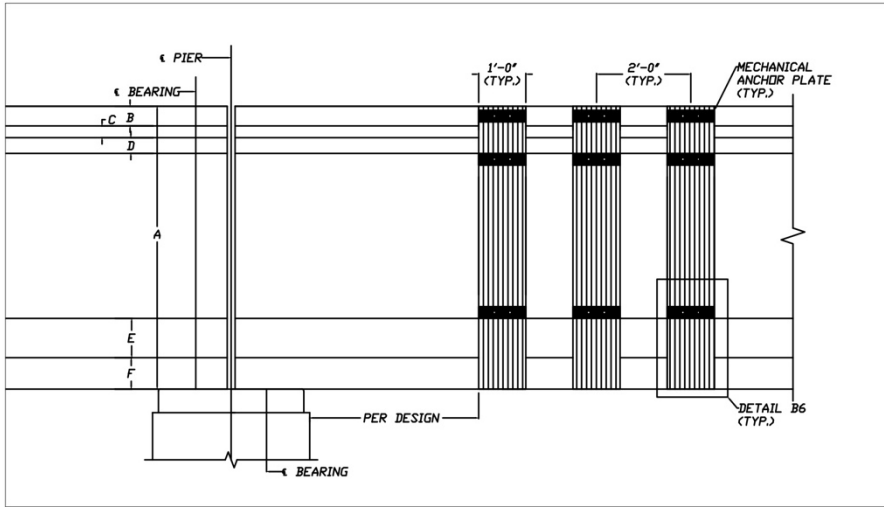
FLORIDA TECH

AASHTO TYPE I THROUGH IV CFRP REINFORCEMENT DETAILS  
FLORIDA DEPARTMENT OF TRANSPORTATION

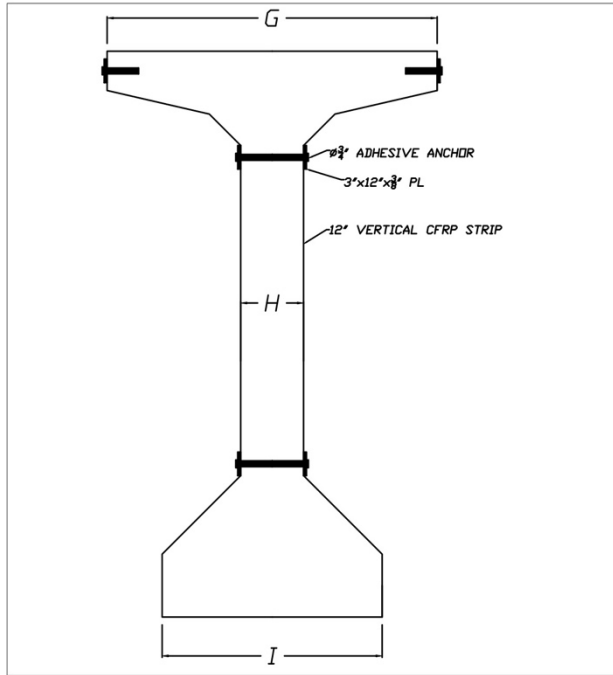
DOT-897	P.J.R.
21-893-0A	NS
1/31/22	NS
NOTED	P.J.R.

B-2

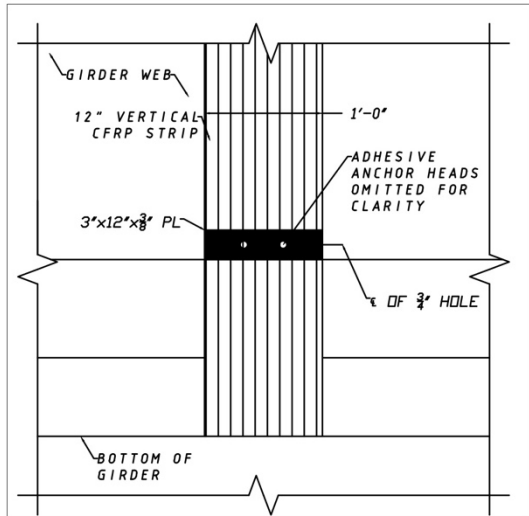




B4 AASHTO GIRDER V-VI MECHANICAL ANCHORS-ELEVATION



B5 AASHTO GIRDER V-VI MECHANICAL ANCHORS-SECTION



B6 AASHTO GIRDER V-VI MECHANICAL ANCHORS-DETAILS

TABLE OF DIMENSIONS

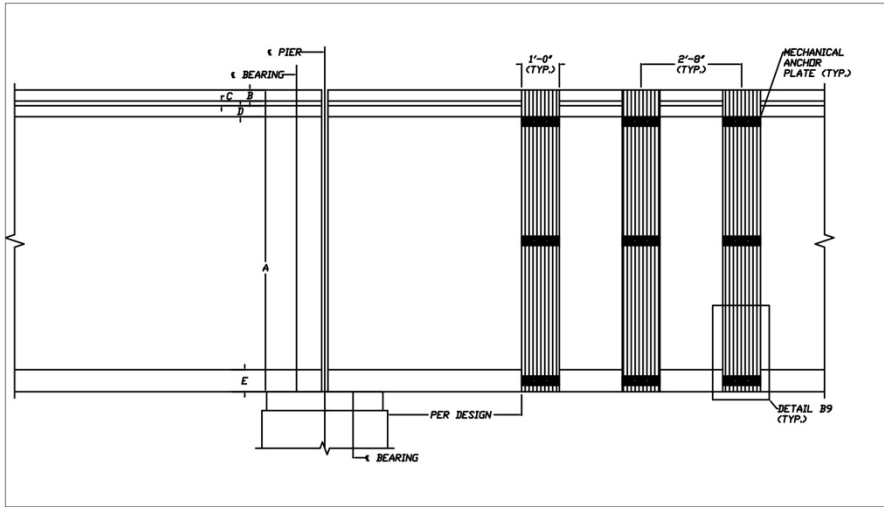
BEAM	A	B	C	D	E	F	G	H	I
AASHTO V	5'-3"	0'-5"	0'-3"	0'-4"	0'-10"	0'-8"	3'-6"	0'-8"	2'-4"
AASHTO VI	6'-0"	0'-5"	0'-3"	0'-4"	0'-10"	0'-8"	3'-6"	0'-8"	2'-4"

CARBON FIBER REINFORCED POLYMER MECHANICAL ANCHORS

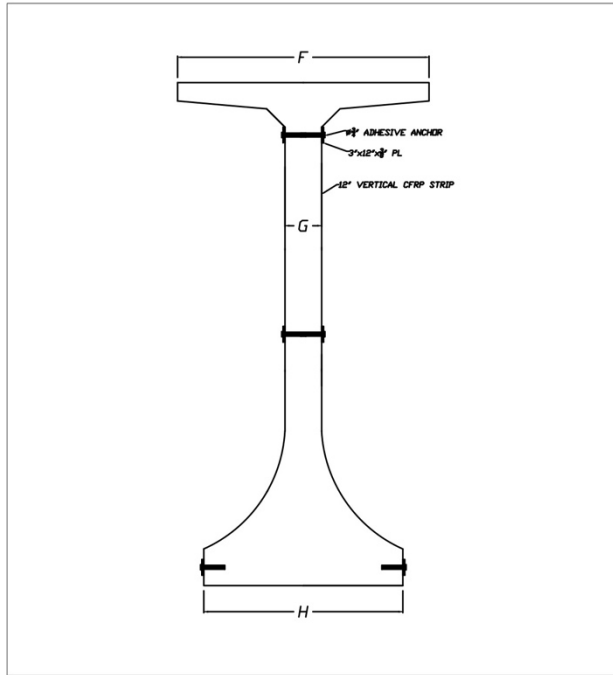


AASHTO TYPE V THROUGH VI CFRP REINFORCEMENT DETAILS  
FLORIDA DEPARTMENT OF TRANSPORTATION

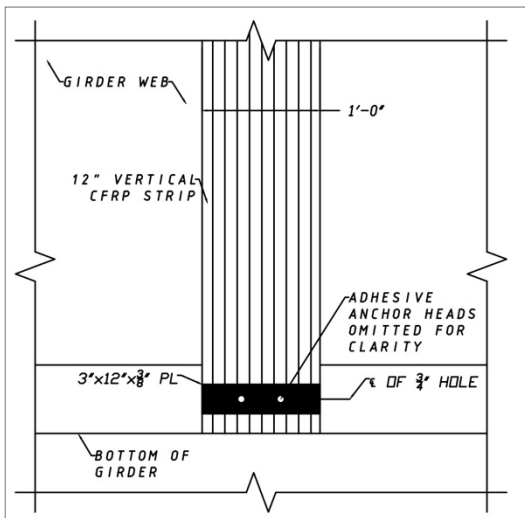
01-19	PJR
21-9933-01	NS
1/31/22	NS
NOTED	PJR



B7 FLORIDA I-BEAM MECHANICAL ANCHORS-ELEVATION



B8 FLORIDA I-BEAM MECHANICAL ANCHORS-SECTION



B9 FLORIDA I-BEAM MECHANICAL ANCHORS-DETAILS

TABLE OF DIMENSIONS

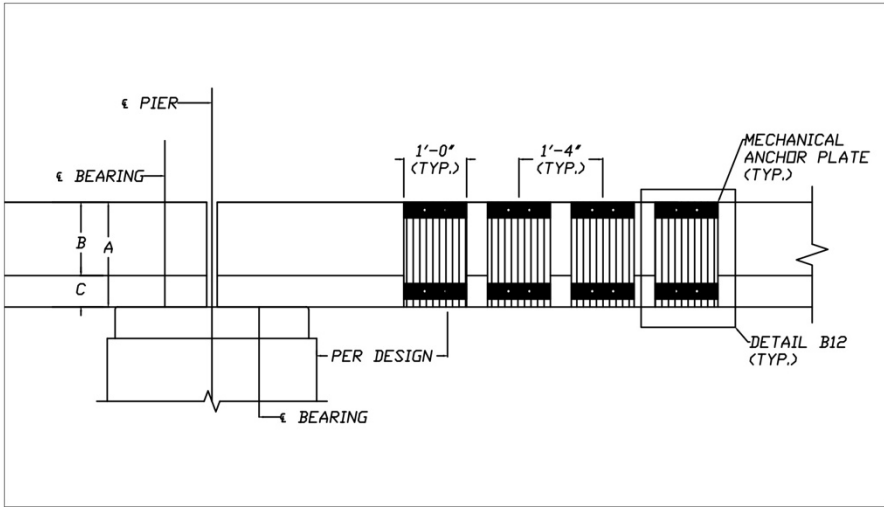
BEAM	A	B	C	D	E	F	G	H
BULB T-78	6'-6"	0'-3"	0'-4"	0'-3"	0'-8"	5'-0"	0'-7"	2'-4"
F I-96	8'-0"	0'-3 1/2"	0'-1 1/2"	0'-3 1/2"	0'-6"	4'-0"	0'-7"	3'-2"

CARBON FIBER REINFORCED POLYMER  
MECHANICAL ANCHORS

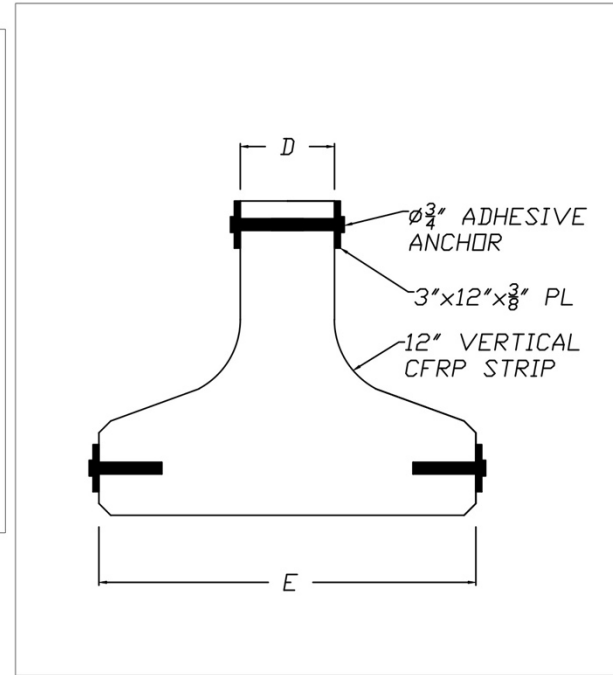
FLORIDA I-BEAM CFRP REINFORCEMENT DETAILS  
FLORIDA DEPARTMENT OF TRANSPORTATION

DOT-RFP 21-903-CA	P.J.R.
1/31/22	NS
NOTED	P.J.R.

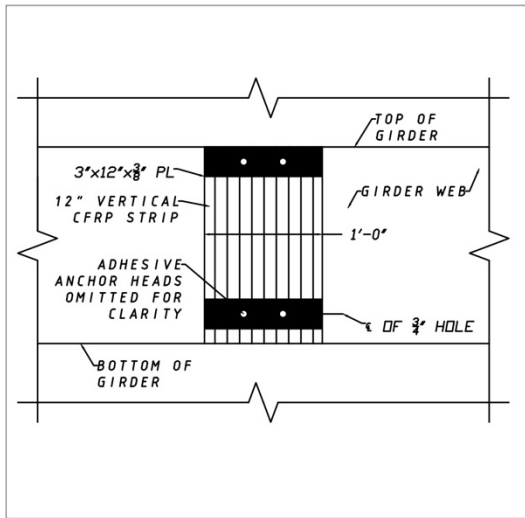
B-4



B10 INVERTED T-BEAM MECHANICAL ANCHORS-ELEVATION



B11 INVERTED T-BEAM MECHANICAL ANCHORS-SECTION



B12 INVERTED T-BEAM MECHANICAL ANCHORS-DETAILS

TABLE OF DIMENSIONS					
BEAM	A	B	C	D	E
INVERTED T-BEAM	1'-8"	1'-2"	0'-6"	0'-6"	2'-0"

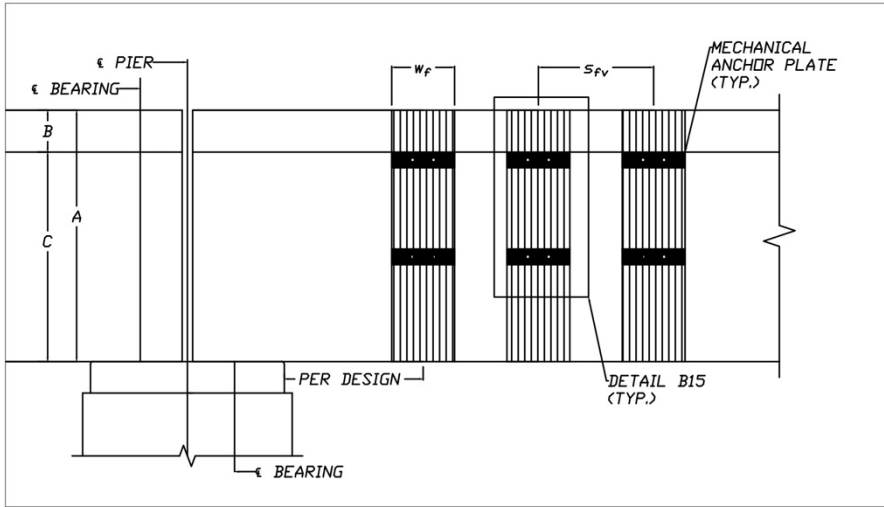
CARBON FIBER REINFORCED POLYMER MECHANICAL ANCHORS



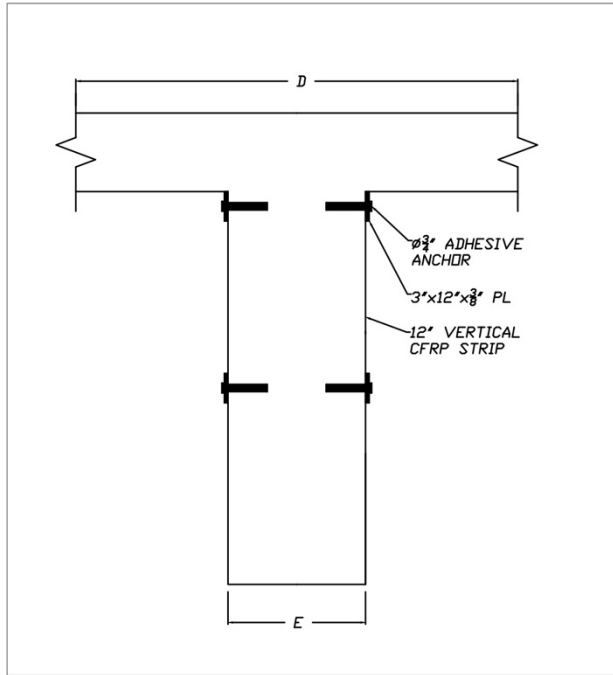
INVERTED T-BEAM CFRP REINFORCEMENT DETAILS  
FLORIDA DEPARTMENT OF TRANSPORTATION

DOT-HP  
21-1033-01 P.JR  
1/31/22 NS

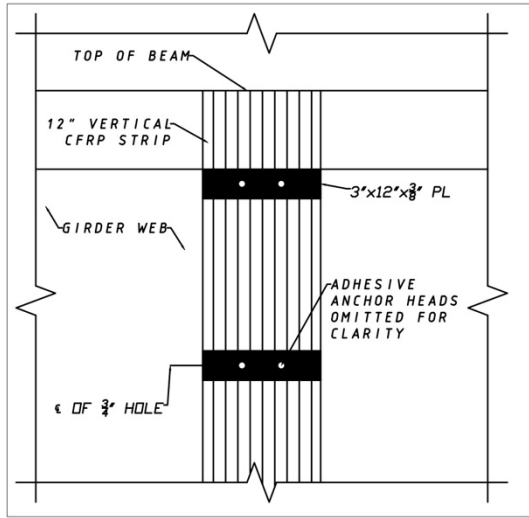
NOTED P.JR



B13 RC BEAM (GENERIC) MECHANICAL ANCHORS—ELEVATION



B14 RC BEAM (GENERIC) MECHANICAL ANCHORS—SECTION



B15 RC BEAM (GENERIC) MECHANICAL ANCHORS—DETAILS

TABLE OF DIMENSIONS

BEAM	A	B	C	D	E	F	S <sub>FV</sub>	S <sub>FH1</sub>
RC T-BEAM	VARIES	VARIES	VARIES	VARIES	VARIES	VARIES	VARIES	VARIES

NOTES

1. THE DETAILS SHOWN FOR THE "RC BEAM" ARE GENERIC AND WILL VARY BASED ON BEAM GEOMETRY.
2. THE TOP FLANGE OF THE RC BEAM IS REPRESENTATIVE OF A SLAB AND SHOULD NOT BE WRAPPED OR ANCHORED.
3. SPACING OF HORIZONTAL AND VERTICAL CFRP STRIPS SHALL BE DETERMINED BY BEAM DEPTH.
4. SPACING OF VERTICAL STRIPS SHOULD BE UNIFORM ALONG THE ENTIRE LENGTH OF THE REPAIRED ZONE.

CARBON FIBER REINFORCED POLYMER MECHANICAL ANCHORS



REINFORCED CONCRETE BEAM (GENERIC) CFRP REPAIR DETAILS  
FLORIDA DEPARTMENT OF TRANSPORTATION

DD-677 21-2033-04	PJR
1/31/22	NS
NOTED	PJR

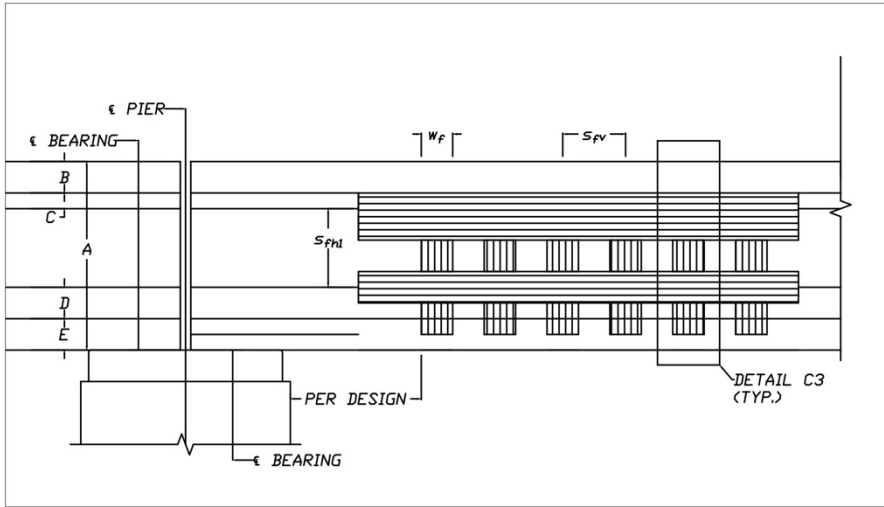
CARBON FIBER REINFORCED POLYMER REPAIR NOTES—LAMINATES ONLY

1. SPACED FRP STRIPS USED FOR SHEAR STRENGTHENING SHOULD BE INVESTIGATED TO EVALUATE THEIR CONTRIBUTION TO THE SHEAR STRENGTH.
2. SPACING SHOULD ADHERE TO THE LIMITS PRESCRIBED BY ACI 318 FOR INTERNAL STEEL SHEAR REINFORCEMENT.
3. THE RECOMMENDED CENTER-TO-CENTER SPACING OF TRANSVERSE CFRP STRIPS IS  $\frac{1}{2}$  TO  $\frac{2}{3}$  THE HEIGHT OF THE REINFORCED MEMBER.
4. THE SPACING OF FRP STRIPS IS DEFINED AS THE DISTANCE BETWEEN THE CENTERLINE OF THE STRIPS.
5. SURFACE MUST BE CLEAN, SOUND AND DRY. REMOVE DUST, LAITANCE, GREASE, CURING COMPOUNDS, IMPREGNATIONS, WAXES, FOREIGN ARTICLES, DISINTEGRATED MATERIALS, AND OTHER BOND INHIBITING MATERIALS.
6. EXISTING UNEVEN SURFACES MUST BE FILLED WITH AN APPROPRIATE REPAIR MORTAR.
7. CRACKS WITH A WIDTH GREATER THAN OR EQUAL TO 0.008" MUST BE STABILIZED USING EPOXY INJECTION METHODS, PRIOR TO APPLICATION OF CFRP.
8. A UV PROTECTIVE COATING IS RECOMMENDED TO BE APPLIED TO ALL ANCHOR AREAS WITHIN 24 HOURS OF ANCHOR INSTALLATION.
9. THE RECOMMENDATIONS PROVIDED HEREIN SHOULD BE EVALUATED EXPERIMENTALLY PRIOR TO ADOPTION.

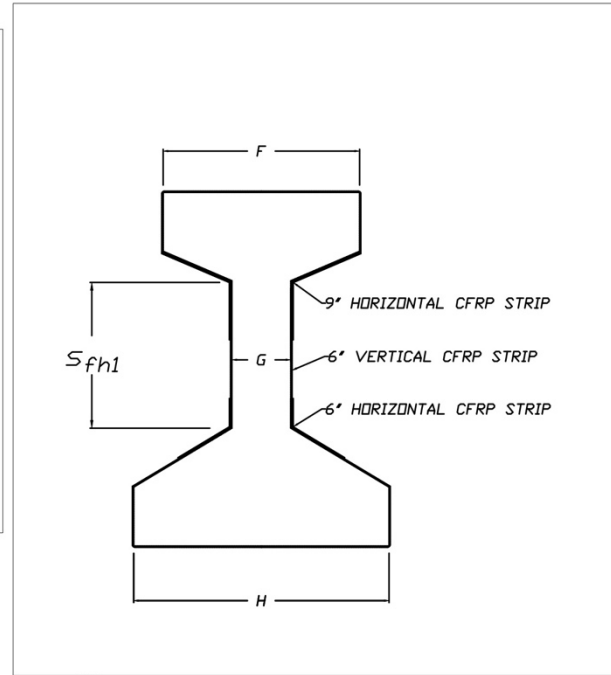
CFRP LAMINATES INSTALLATION SEQUENCE

1. THE ENGINEER MUST BE NOTIFIED IF SPACING AND/OR STRIP GEOMETRY MUST BE MODIFIED.
2. CLEAN AND REMOVE ALL DEBRIS FROM THE LAMINATE APPLICATION SITE.
3. INSTALL VERTICAL CFRP STRIPS IN ACCORDANCE WITH THESE PLANS AND TECHNICAL AND MANUFACTURER SPECIAL PROVISIONS.
3. INSTALL HORIZONTAL CFRP STRIPS IN ACCORDANCE WITH THESE PLANS AND TECHNICAL AND MANUFACTURER SPECIAL PROVISIONS.
4. APPLY A UV PROTECTIVE COATING AT ALL LAMINATE LOCATIONS.

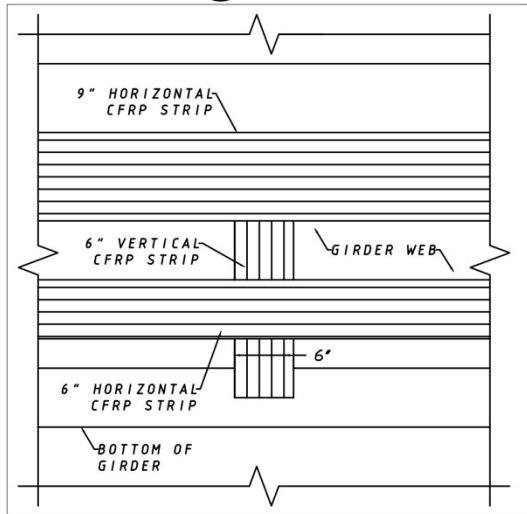
CARBON FIBER REINFORCED POLYMER LAMINATES ONLY	
	
GENERAL NOTES-CFRP REINFORCEMENT DETAILS FLORIDA DEPARTMENT OF TRANSPORTATION	
DOT-RP 21-5033-0A	PJR
10/26/21	NS
NOTED	PJR
C-1	



C1 AASHTO GIRDER I-II LAMINATES-ELEVATION



C2 AASHTO GIRDER I-II LAMINATES-SECTION



C3 AASHTO GIRDER I-II LAMINATES-DETAILS

TABLE OF DIMENSIONS

BEAM	A	B	C	D	E	F	G	H	Sfh1
AASHTO I	2'-4"	0'-4"	0'-3"	0'-5"	0'-5"	1'-0"	0'-6"	1'-4"	0'-11"
AASHTO II	3'-0"	0'-6"	0'-3"	0'-6"	0'-6"	1'-0"	0'-6"	1'-6"	1'-3"

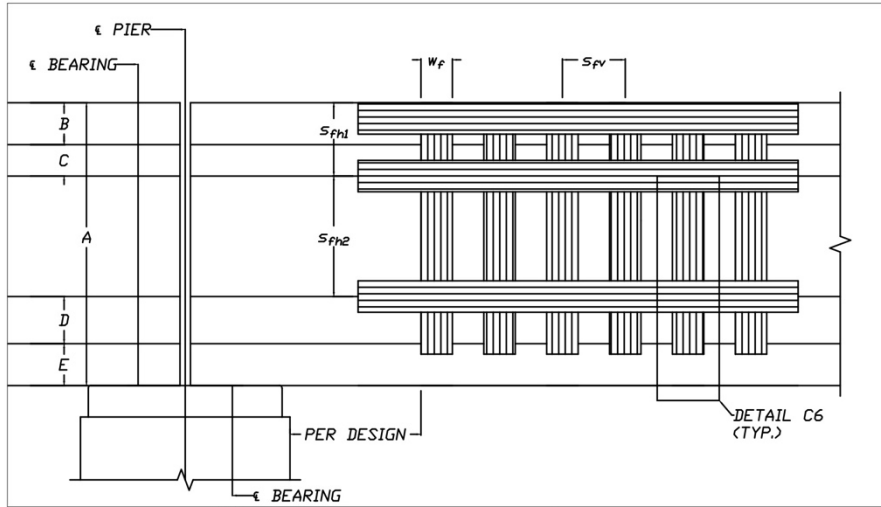
1. Sfh1 FOR AASHTO TYPE I AND TYPE II IS NOT THE O.C. DISTANCE BETWEEN HORIZONTAL STRIPS; IT IS THE WEB DEPTH OF THE BEAM, WHICH ALIGNS WITH 3" FROM THE TOP OF THE FIRST HORIZONTAL STRIP TO THE CENTER OF THE SECOND HORIZONTAL STRIP.

CARBON FIBER REINFORCED POLYMER LAMINATES ONLY

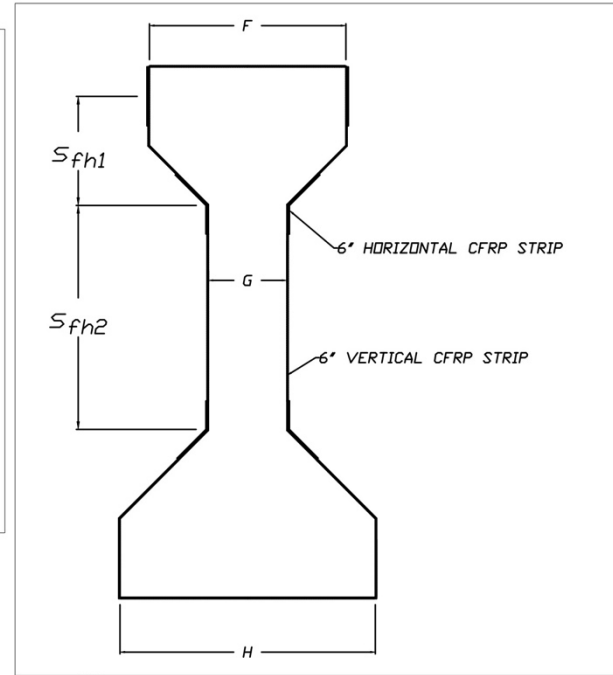


AASHTO TYPE I THROUGH II CFRP REINFORCEMENT DETAILS  
FLORIDA DEPARTMENT OF TRANSPORTATION

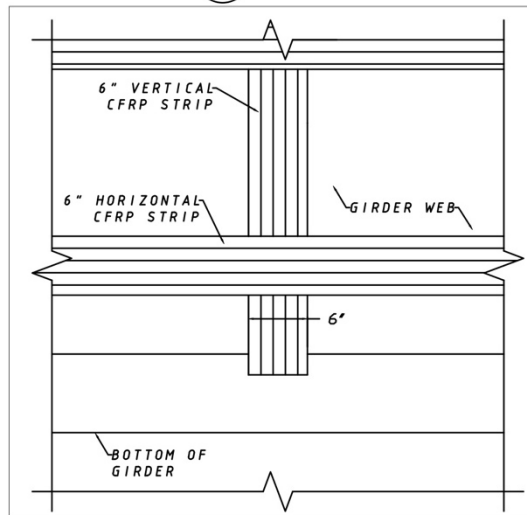
007-897	PJR
11-2003-04	NS
1/31/22	PJR
NOTED	PJR



C4 AASHTO GIRDER III-IV LAMINATES-ELEVATION



C5 AASHTO GIRDER III-IV LAMINATES-SECTION



C6 AASHTO GIRDER III-IV LAMINATES-DETAILS

TABLE OF DIMENSIONS

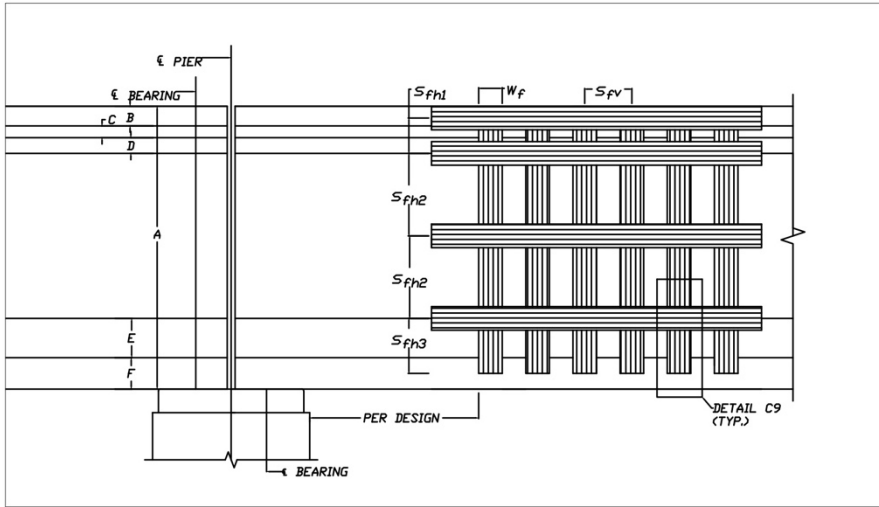
BEAM	A	B	C	D	E	F	G	H	Sfh1	Sfh2
AASHTO III	3'-9"	0'-7"	0'-5"	0'-8"	0'-7"	1'-4"	0'-7"	1'-10"	0'-9"	1'-6"
AASHTO IV	4'-6"	0'-8"	0'-6"	0'-9"	0'-8"	1'-8"	0'-8"	2'-2"	0'-11"	1'-11"

CARBON FIBER REINFORCED POLYMER LAMINATES ONLY

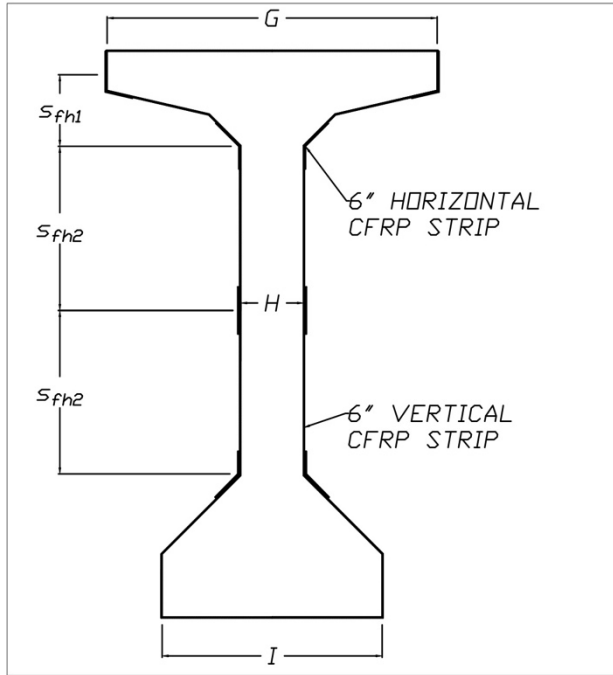


AASHTO TYPE III THROUGH IV CFRP REINFORCEMENT DETAILS  
FLORIDA DEPARTMENT OF TRANSPORTATION

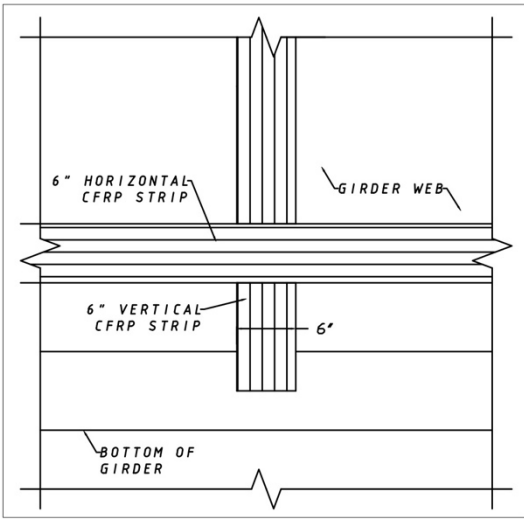
DOF-897	PJR
11-2003-04	NS
1/31/22	NS
NOTED	PJR



C7 AASHTO GIRDER V-VI LAMINATES-ELEVATION



C8 AASHTO GIRDER V-VI LAMINATES-SECTION



C9 AASHTO GIRDER V-VI LAMINATES-DETAILS

TABLE OF DIMENSIONS

BEAM	A	B	C	D	E	F	G	H	I	S <sub>fh1</sub>	S <sub>fh2</sub>
AASHTO V	5'-3"	0'-5"	0'-3"	0'-4"	0'-10"	0'-8"	3'-6"	0'-8"	2'-4"	0'-9"	1'-4 1/2"
AASHTO VI	6'-0"	0'-5"	0'-3"	0'-4"	0'-10"	0'-8"	3'-6"	0'-8"	2'-4"	0'-9"	1'-9"

- ALL MEASUREMENTS LISTED IN THE TABLE ABOVE REFLECT UNIFORM SPACING AND MAY BE ROUNDED TO THE NEAREST INCH.  
EXAMPLE: S<sub>fh2</sub> MAY BE TAKEN AS 1'-5" FOR EASE OF CONSTRUCTION.

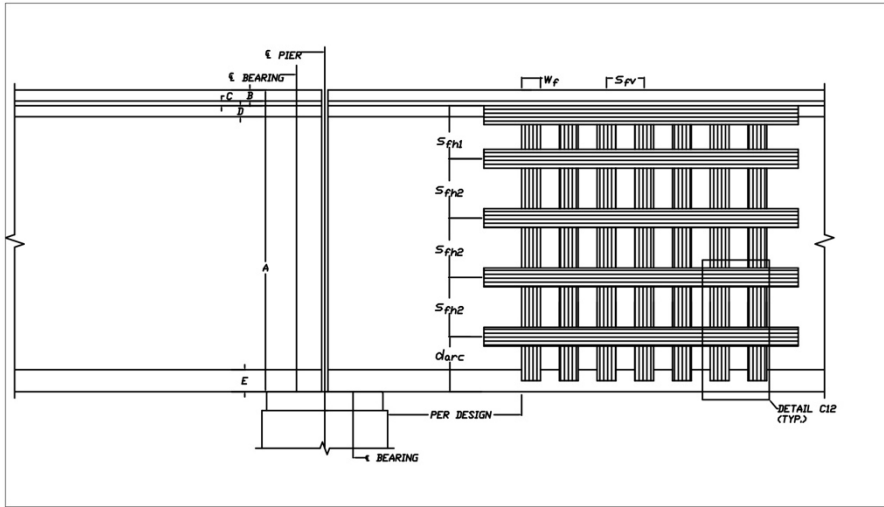
CARBON FIBER REINFORCED POLYMER LAMINATES ONLY



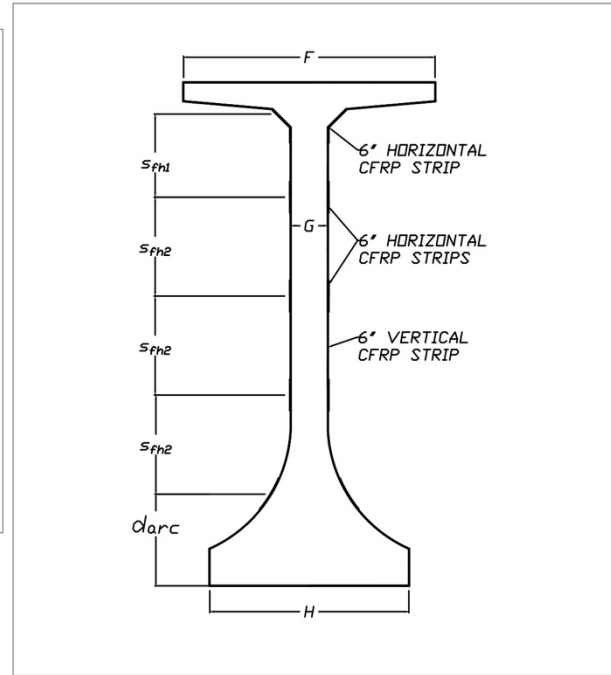
AASHTO TYPE V THROUGH VI CFRP REINFORCEMENT DETAILS  
FLORIDA DEPARTMENT OF TRANSPORTATION

DOI-119  
21-303-01  
1/31/22  
NOTED P.J.R.

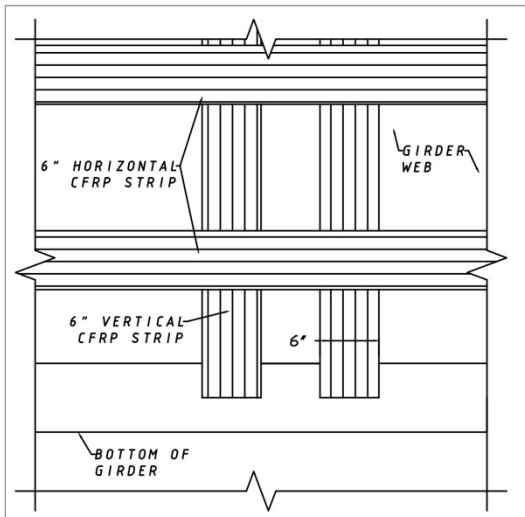




C10 FLORIDA I-BEAM LAMINATES—ELEVATION



C11 FLORIDA I-BEAM LAMINATES—SECTION



C12 FLORIDA I-BEAM LAMINATES—DETAILS

TABLE OF DIMENSIONS

BEAM	A	B	C	D	E	F	G	H	S <sub>fh1</sub>	S <sub>fh2</sub>
BULB T-78	6'-6"	0'-3"	0'-4"	0'-3"	0'-8"	5'-0"	0'-7"	2'-4"	2'-4 1/2"	2'-3 1/2"
F I-96	8'-0"	0'-3 1/2"	0'-1 1/2"	0'-3 1/2"	0'-6"	4'-0"	0'-7"	3'-2"	1'-4 3/8"	1'-6 7/8"

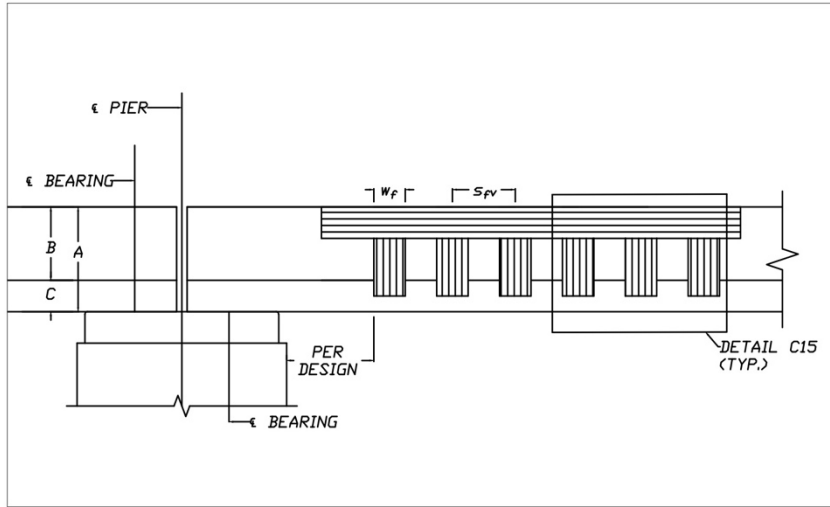
1. BULB T-78 CONTAINS 3 TRANSVERSE STRIPS; F I-96 CONTAINS 5 TRANSVERSE STRIPS.
2. clarc IS THE DISTANCE FROM THE BOTTOM OF THE BEAM TO THE APPROXIMATE CENTER OF THE CURVED PORTION OF THE BEAM (APPROXIMATELY EQUAL TO 19.5 IN.).
3. ALL MEASUREMENTS LISTED IN THE TABLE ABOVE REFLECT UNIFORM SPACING AND MAY BE ROUNDED TO THE NEAREST INCH.  
EXAMPLE: s<sub>fh1</sub> FOR BULB T-78 MAY BE TAKEN AS 2'-4" FOR EASE OF CONSTRUCTION.

CARBON FIBER REINFORCED POLYMER LAMINATES ONLY

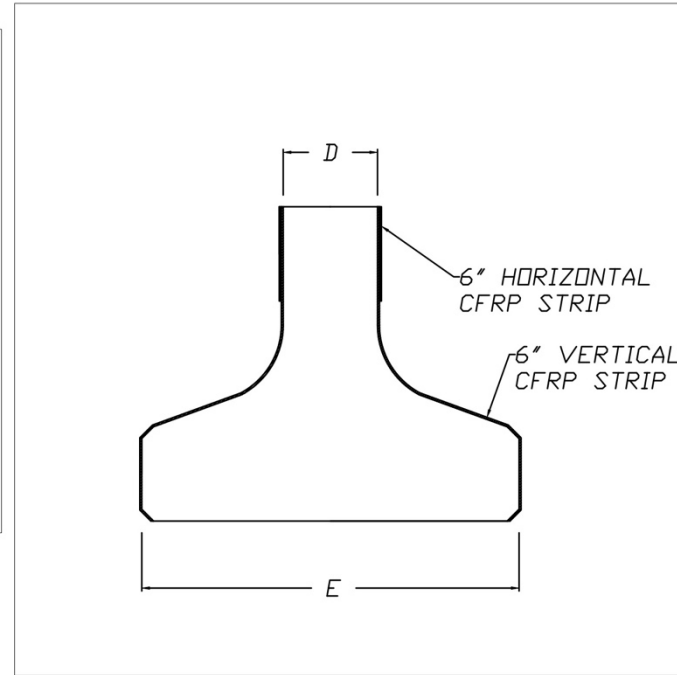


FLORIDA I-BEAM CFRP REINFORCEMENT DETAILS  
FLORIDA DEPARTMENT OF TRANSPORTATION

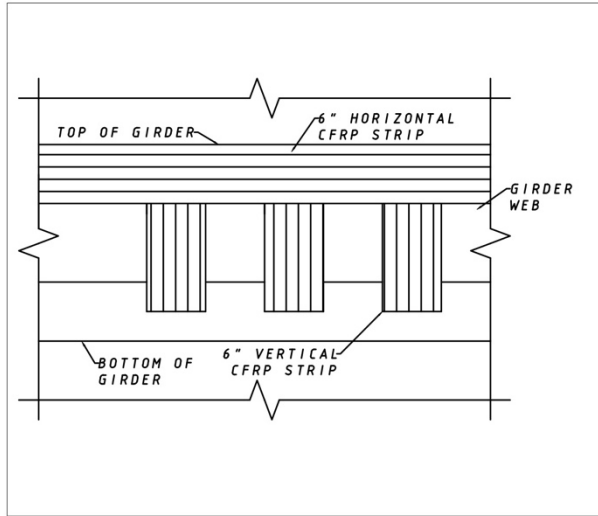
DOT-REP 21-6033-0A	PJR
1/31/22	NS
NOTED	PJR



C13 INVERTED T-BEAM LAMINATES—ELEVATION



C14 INVERTED T-BEAM LAMINATES—SECTION



C15 INVERTED T-BEAM LAMINATES—DETAILS

TABLE OF DIMENSIONS

BEAM	A	B	C	D	E
INVERTED T-BEAM	1'-8"	1'-2"	0'-6"	0'-6"	2'-0"

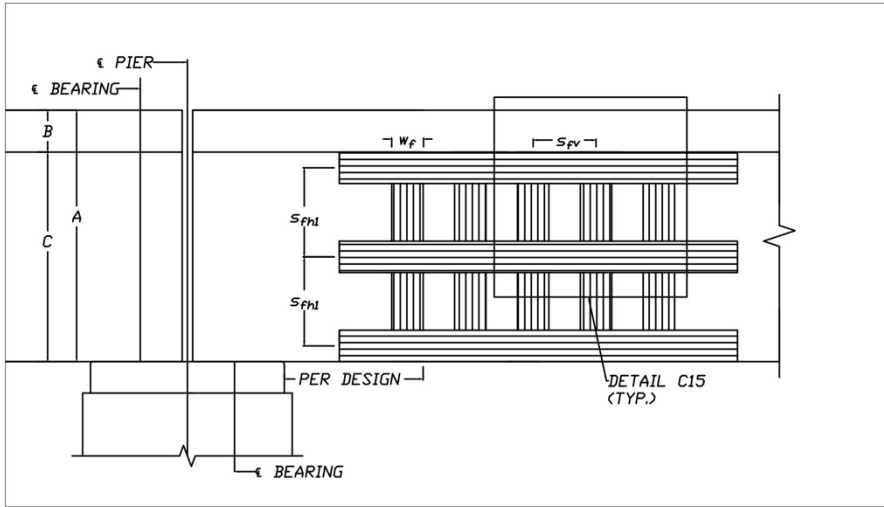
1. THE SMALL DEPTH OF THE INVERTED T-BEAM PERMITS THE USE OF ONE TRANSVERSE STRIP; THEREFORE, NO TRANSVERSE STRIP SPACING IS SPECIFIED.

CARBON FIBER REINFORCED POLYMER LAMINATES ONLY

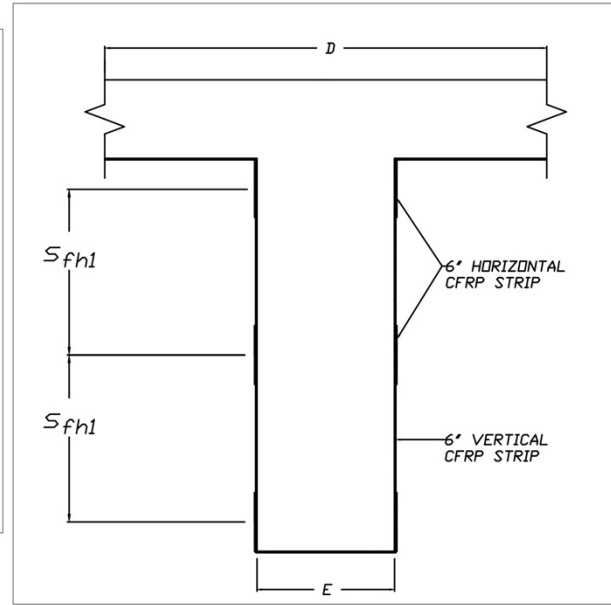


INVERTED T-BEAM CFRP REINFORCEMENT DETAILS  
FLORIDA DEPARTMENT OF TRANSPORTATION

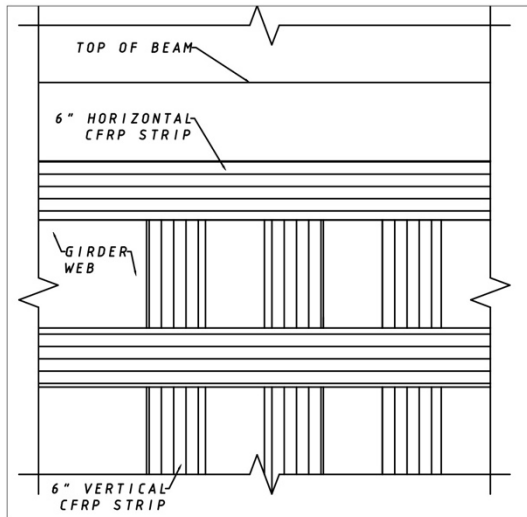
00-87	PJR
21-203-04	NS
1/31/22	NS
NOTED	PJR



C16 RC BEAM (GENERIC) LAMINATES-ELEVATION



C17 RC BEAM (GENERIC) LAMINATES-SECTION



C18 RC BEAM (GENERIC) LAMINATES-DETAILS

TABLE OF DIMENSIONS								
BEAM	A	B	C	D	E	F	$S_{fv}$	$S_{fh1}$
RC T-BEAM	VARIES	VARIES	VARIES	VARIES	VARIES	VARIES	VARIES	VARIES

NOTES

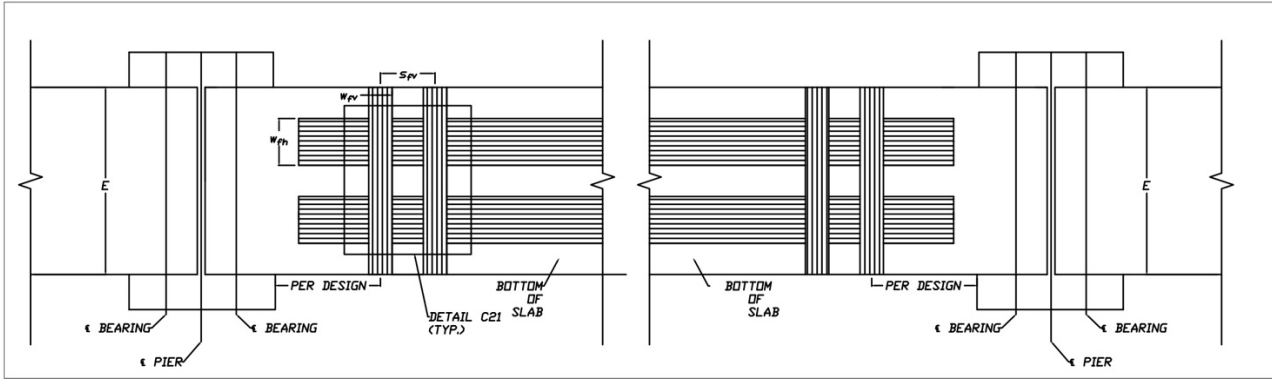
1. THE DETAILS SHOWN FOR THE "RC BEAM" ARE GENERIC AND WILL VARY BASED ON BEAM GEOMETRY.
2. THE TOP FLANGE OF THE RC BEAM IS REPRESENTATIVE OF A SLAB AND SHOULD NOT BE WRAPPED OR ANCHORED.
3. SPACING OF HORIZONTAL AND VERTICAL CFRP STRIPS SHALL BE DETERMINED BY BEAM DEPTH.
4. SPACING OF VERTICAL STRIPS SHOULD BE UNIFORM ALONG THE ENTIRE LENGTH OF THE REPAIRED ZONE.
5. SPACING OF HORIZONTAL STRIPS SHALL BE BETWEEN 12" AND 18".

CARBON FIBER REINFORCED POLYMER LAMINATES ONLY

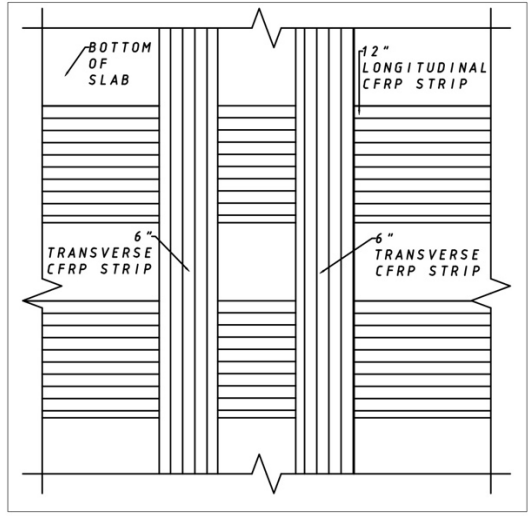


REINFORCED CONCRETE BEAM (GENERIC) CFRP REINFORCEMENT DETAILS  
FLORIDA DEPARTMENT OF TRANSPORTATION

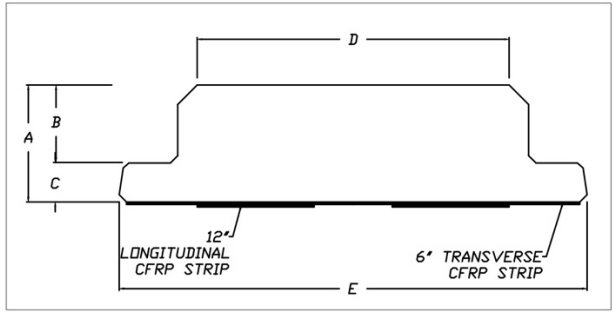
DOT-RFP 21-100-01	P.R.
1/31/22	NS
NOTED	P.R.



C19 SLAB BEAM LAMINATES—BOTTOM VIEW



C21 SLAB BEAM LAMINATES—DETAILS



C20 SLAB BEAM LAMINATES—SECTION

TABLE OF DIMENSIONS

BEAM	A	B	C	D	E	$W_{fv}$	$S_{fv}$	$W_{fh}$
12"	1'-0"	0'-8"	0'-4"	VARIES	VARIES	0'-6"	1'-2"	1'-0"
15"	1'-3"	0'-11"	0'-4"	VARIES	VARIES	0'-6"	1'-4"	1'-0"
18"	1'-6"	1'-2"	0'-4"	VARIES	VARIES	0'-6"	1'-6"	1'-0"

CARBON FIBER REINFORCED POLYMER LAMINATES ONLY



SLAB BEAM CFRP REINFORCEMENT DETAILS  
FLORIDA DEPARTMENT OF TRANSPORTATION

DOT-RFP 21-8033-0A	PJR
1/31/22	NS
NOTED	PJR
C-8	